SwelFlo User Manual
Version 2.02

Dr. Mark J. McGuinness
Marsan Consulting Ltd
Wellington, NZ

December 2015

Abstract

This is a User Manual for the geothermal wellbore simulator SwelFlo. The graphical user interface to the simulator is compiled to run under Windows XP, Vista, and Windows 7, and is designed to give easy and fast setup and to allow quick plotting of data together with simulated results, while retaining functionality. It is intended as a tool to model flow in a geothermal well, to be used by reservoir engineers and modellers who wish to run simulations predicting the effects of changing the setup and operability of a geothermal well, or the effects of changes in reservoir properties over time on production from a geothermal well. Both production and injection flows may be modelled. Flow of vapor and liquid phases of water, together or alone, together with carbon dioxide, is modelled. Simulations may proceed from the bottom up, or from the top down, with corresponding differences in which boundary condition is important. Downhole values of variables may be examined for a simulation, or multiple bottom up runs may be combined to produce an output curve. Multiple feedpoints are allowed, with variable wellbore geometry, heat flow between wellbore and the surrounding country, and production or injection.

Contents

1 Version notes — current version

Version 2.02 provides for the display of saturation pressure of pure water (dashed line) on the same graph as pressure (solid line). This gives an indication of how far above the bubble point of pure water the fluid is, which echoes the temperature profile and the carbon dioxide concentration.

Known Bugs: When the user was allowed to direct the simulator to open and read from a saved Feedpoints comma-separated file into the Feedpoints Grid window, it crashed. Hence Open and New have been removed from the File menu for this grid window for the time being. In a future release an Open command will be added separately to its menu.

2 Introduction

The geothermal wellbore simulator SwelFlo is intended as a tool for geothermal reservoir engineers and modellers, and for academics investigating two-phase upflow in pipes, to allow them to rapidly set up and solve a model of a geothermal wellbore, and to test that model against data from production tests, injection tests, and output tests. The governing equations are as described in Appendix (C). They solve coupled steady-state mass, momentum and energy conservation equations, for liquid, vapour or two-phase water with carbon dioxide gas present in both phases. The flow correlations available to determine the relative velocities of vapour and liquid phases are the Armand correlation, the Orkizewski correlation, the Hadgu correlation [19], the Duns and Ros correlation [14, 36], and the Hagedorn and Brown correlation [36, 7]. Dissolved solids like NaCl are not accounted for. Noncondensable gases are modelled as carbon dioxide.

The thermodynamic subroutines require that some carbon dioxide is present in the fluid, in order to compute fluid properties. Specifying pressure, temperature and a nonzero carbon dioxide concentration fixes the in-place dryness and enthalpy. Alternatively, specifying pressure, nonzero carbon dioxide, and an in-place dryness fixes the temperature and in-place enthalpy. Specifying any three of the properties pressure, temperature, nonzero carbon dioxide concentration, static dryness that is between one and zero, or in-place two-phase enthalpy then sets required consistent values for the other two properties. As a consequence the simulator internally sets a minimum mass fraction of XCO2=0.001. Note that this is a

little less than the equilibrium value for water in contact with air at one atmosphere and at room temperature, so is not an unreasonable minimum value.

Multiple feeds of four different types are allowed, drawdown (linear or nonlinear), productivity index (linear or nonlinear), fixed flowrate or dry steam. The user may specify multiple variations in casing geometry — radius, roughness, inclination, or a casing section may be chosen from an editable database file of casing types.

2.1 System Requirements

Presently Swelflo is designed to run under Windows XP/Vista/7, and the exe file is about 10MB in size. SwelFlo may run under other Windows operating systems, but is not intended to. It is recommended to run it on a computer or laptop with at least 1Gb of RAM. Topdown simulations are almost instantaneous, while output curves, and bottomup runs (which use an output curve to help match wellhead pressure) take about 10–15 seconds to run under Parallels on a 2010 MacBook (2.26 GHz Intel Core 2 Duo).

3 First Steps

SwelFlo is usually installed in its own directory, at the installer's choice. When SwelFlo is first started, it will ask the user for a project directory to work in. This directory will be used to save input and output files. Subsequent startups of SwelFlo will open the last project directory that was used on that computer.

Once SwelFlo is installed, start it by double-clicking on the exe file icon, or on the desktop shortcut. If necessary, ensure you are starting it as administrator. In Windows 7, this is done by selecting the exe file, then choosing Organise, then Properties, then Compatibility, then tick the "run as administrator" box. Or you can right-click the exe file, and choose the "run as administrator" option. You will be prompted to choose a folder to work in, which should be somewhere in your documents folder. You can create subfolders as part of the selection process.

If SwelFlo has not been run in the working folder before, it will automatically create a basic simulation from the built-in template. Then the setup can be modified, or another setup can be imported from another folder to replace the current setup, if there is another one available.

An important file in the SwelFlo project folder is the file called SWFinput.txt. It saves all of the latest details of the wellbore simulation, and is the file that the simulator looks for when it is directed to a project folder. More information on this main input file may be found later in this manual.

Fig. (1) shows the resulting windows that should be visible at this stage. The main window contains tabs for STARTUP, DATA INPUT, RESULTS display, and GRAPHS display. The smaller Progress window is to provide information to the user. The resizable Error Reporting region at the bottom of the main window is to report more serious errors found in the setup or encountered while running.

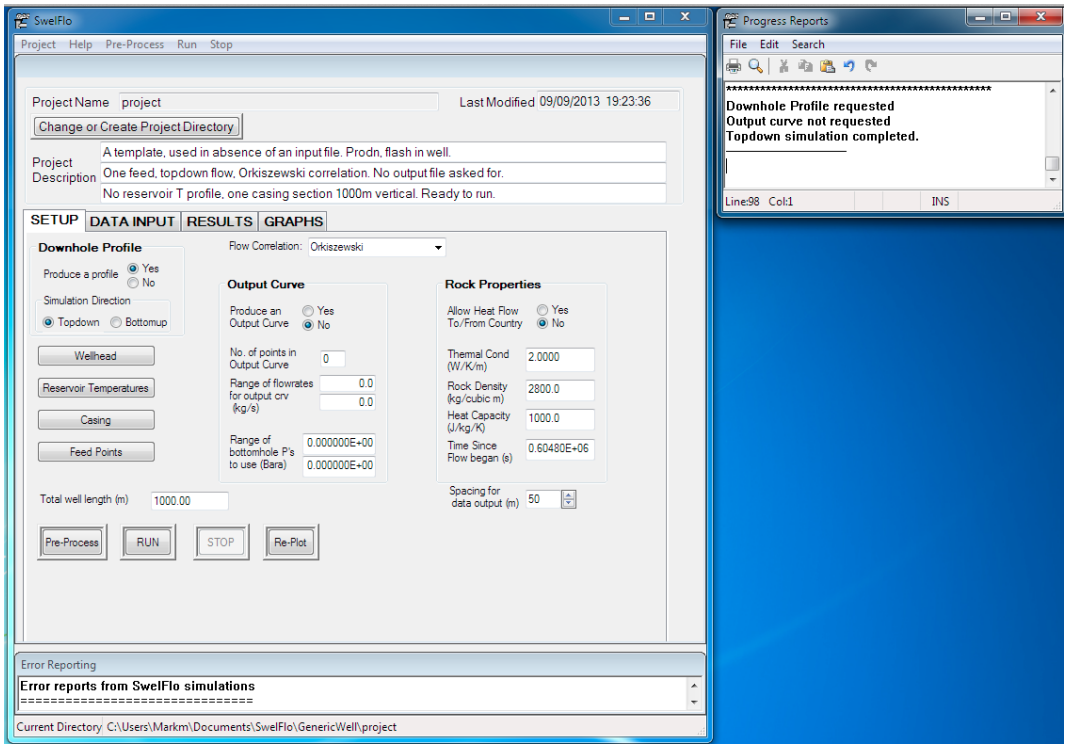

Figure 1: SwelFlo windows visible on a first startup.

3.1 A Topdown Run

The built-in template is for a topdown simulation of the downhole profile of a producing vertical well of length 1000m, with wellhead pressure P 8 bara, flowrate Q 20 kg/s, temperature T 169.75 °C, and mass fraction of carbon dioxide XCO_2 0.001. **Press the Run button** hear the bottom of the main window, or the Run command in the menu of that window, to perform a topdown simulation starting at the wellhead values specified. It should run very quickly, and show the resulting pressure versus depth in the well. The downhole pressure profile should look like that portrayed in Fig. (2). Clicking on the T and V tabs reveals temperature and mass-weighted velocity (spinner velocity) profiles, as depicted in Fig. (3).

To change the wellhead conditions click the SETUP tab, and then click the Wellhead button. The Wellhead Conditions grid window will open, with two rows, one row for each desired

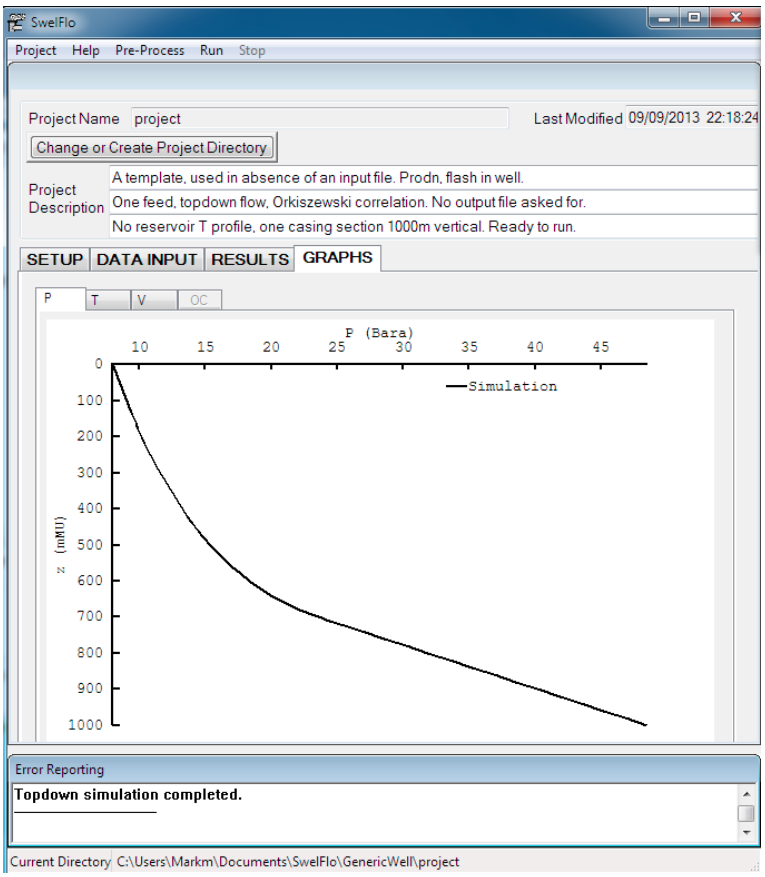

Figure 2: SwelFlo first steps, after running, showing simulated pressure versus depth profile.

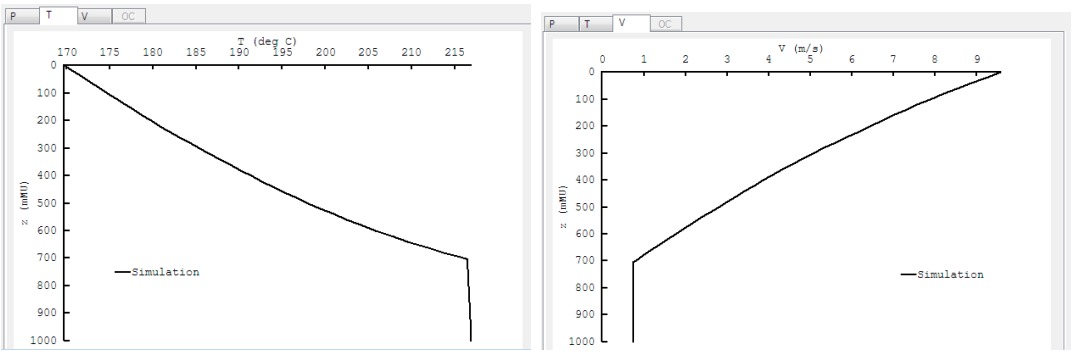

Figure 3: SwelFlo first steps, showing simulated temperature and spinner velocity profiles.

simulation. Typically the simulator is run with just the first row active - a pressure value less than one bar in a row will cause the simulator to ignore it. For example you can change the wellhead pressure to 7 bara and Run again.

There is no need to Save any changes - they are automatically saved every time the simulator is Pre-Processed or Run. The Save commands on the grid windows are really to allow the user to save for example the wellbore geometry, to a file that can be opened later by the same kind of grid window in a different project.

To check that correct conditions are set at the wellhead (and at feedpoints) and that the simulator is ready to run, click the Pre-Process button in the SETUP tab window. Clicking the Run button also performs a Pre-Process to check that the simulator is ready to run, before running it.

Besides the quick plots of simulation results, text values of simulated variables versus distance down the well are available under the RESULTS tab. A summary of wellhead values, flash depth and feedpoint values is presented, plus a button to browse the latest output file produced by SwelFlo. The first parts of that file describe the input setup used, so that this output file provides a complete summary of the simulation performed. This output file is read by SwelFlo to produce the RESULTS summary and the plots displayed, so that if a user edits the latest output file, it is likely that SwelFlo will be unable to show RESULTS and plots unless it is Run again. New output files do not overwrite old ones, due to the numbering system used for the filenames (see below).

A number of properties of the flow may be set at wellhead — the pressure and XCO_2 are considered fundamental, while temperature T, enthalpy H and steam mass fraction X are considered interdependent. Note that a distinction is also drawn between static and flowing values of enthalpy and steam mass fraction, which coincide for a single-phase flow or for homogeneous two-phase flow. Any one of these five variables is sufficient to determine the other four, given P and XCO_2.

3.1.1 Consistent Wellhead Values

There is a hierarchy in the case that more than one of (T, H, H_{flo}, X, X_{flo}) are set by the user at the wellhead, to ensure that the values are consistent. The hierarchy is that X_{flo} is most dominant — a value between 0 and 1 will override any value that is set for T, H, X, or H_{flo}. Next is H_{flo}, which will override any value that is set for T, H, or X. Next is X, which will override any value that is set for T or H. Next is H, which will override any value that is set for T. Hence the T value that is set will only have effect if none of (H, H_{flo}, X, X_{flo}) are set. To clear a cell in a grid window, use the menu item Clear current cell, or Clear current selection after selecting the cells you wish emptied.

An exceptional case is when X or X_{flo} is set to zero or one, AND the other values T, H, and H_{flo} are empty. This is taken as a signal that the user wants to set the fluid to the bubble point (zero) or liquidus (one), but only if all of the other values T, H, and H_{flo} are all empty.

If both X and X_{flo} are set to zero, this means the same thing. If there is a conflict, X_{flo} wins.

A simple way to ensure the desired value is being set, from the list (T, H, H_{flo}, X, X_{flo}), is to clear the other four values. Then Run. Clicking Pre-Process will populate the remaining four with consistent values.

3.2 SETUP

Other settings in this tab include:

Produce a downhole profile, or not — turning this off will ensure no downhole values of P, T etc are produced or presented. Simulation Direction can be Topdown or Bottomup. Wellhead values determine the starting point for a topdown simulation, and fluid properties at the lowest feed (which is also taken to be the bottom of the simulated wellbore) follow from the simulation results. Bottomhole values (reservoir values of P, T, etc) are used in a bottom-up simulation, with the exception of bottomhole pressure, which is varied in an attempt to match wellhead pressure, and to a lesser extent to match flowrate. Reservoir properties as well as feed properties at a feedpoint, including bottomhole, may be set using the Feed Points button and entering values into the grid window that appears.

An output curve may be requested, and the number of points desired in it. The actual number achieved will often be less than the number requested, but will not usually be less than half. A range of flowrates may be specified if it is desired to tidy up the appearance of the output curve. A range of bottomhole pressures may be specified, and often needs to be specified to obtain a reasonable number of points in the output curve. The detailed RESULTS file will indicate the bottomhole pressures that were successful in producing steady state solutions and hence points on the output curve. If just one or two points are achieved, narrowing the range of bottomhole pressures to nearby values will improve the simulator's chances of producing a good-looking output curve. The order does not matter, for the range of flowrates or bottomhole pressures.

Heat flow to or from the country may be turned off or on, and rock properties set. The time since flow began box reflects the use of a transient solution to the diffusive temperature equation, and should relate to the time that the well has been constantly discharging (stabilization time), if comparing with measured downhole data.

It is possible to STOP a simulation if desired, during a simulation while a progress bar is showing, if computation of an output curve or a bottomup match to wellhead values is taking too long.

It is possible to change the total length of the well (arc length), which should match the total casing length. An incorrect length entered here will be over-written by the sum of the casing lengths, on preprocessing.

The three lines of Project Description text may be used as desired, to describe the current project. They appear in the output files generated for each simulation.

Error information is offered in the bottom section of the main window, while progress reports appear in the small resizable window in the top right part of the screen.

To illustrate some of the features of the simulator, the next section shows how to compute a bottomup simulation that matches a topdown simulation, and how to compute an output curve.

3.3 Bottomup Match

To start from a common baseline, click Project - Load Template, and agree to the subsequent over-writing of the current project. Click RUN (button or menu).

We will now set up a plot of the results just obtained from this Topdown run, for later comparison with a bottomup simulation. We will treat them as data. Click DATA INPUT - existing Pressure. Choose the latest PDataSim*** file offered. Similarly choose T and V files, generated by the most recent simulation performed in the previous paragraph.

Re-Plot (top right in current window, or bottom of SETUP window). Note the plots now also have symbols from the most recent simulation, spaced apart every 50m. This spacing can be altered using the box in the bottom right corner of the SETUP window (then RUN and reload the data files and rep lot as above). The symbols will trivially lie exactly on the lines, since they came from the same simulation.

Now set up the feed at bottomhole for a bottomup simulation: The best feed type for an output curve is Productivity Index. Set this by clicking on the Feed Points button. To get a match with the Topdown simulation, it is necessary to set up the correct (flowing) enthalpy for fluid entering from bottomhole, and the correct productivity index value. These may be read from the RESULTS tab, but should already match the values that have been read in from the template. That is, sigma should already be set to the value computed from the topdown run, 0.45052E-1, and reservoir enthalpy should already match the value resulting from the topdown simulation, 929.86 kJ/kg.

To obtain a single bottomup simulation, set the range of bottomhole pressures in the Output Curve section of the SETUP tab, both to the single value obtained from the topdown simulation, 48.505 bara.

Click RUN. The graphs should show that the bottomup run matches the symbols from the previous topdown run, as in Fig. (4). If not, check the work you have just done for mistakes.

It is a good test of numerical accuracy that topdown matches bottomup. That is, solving the differential equations describing conservation of momentum and energy in one direction, then

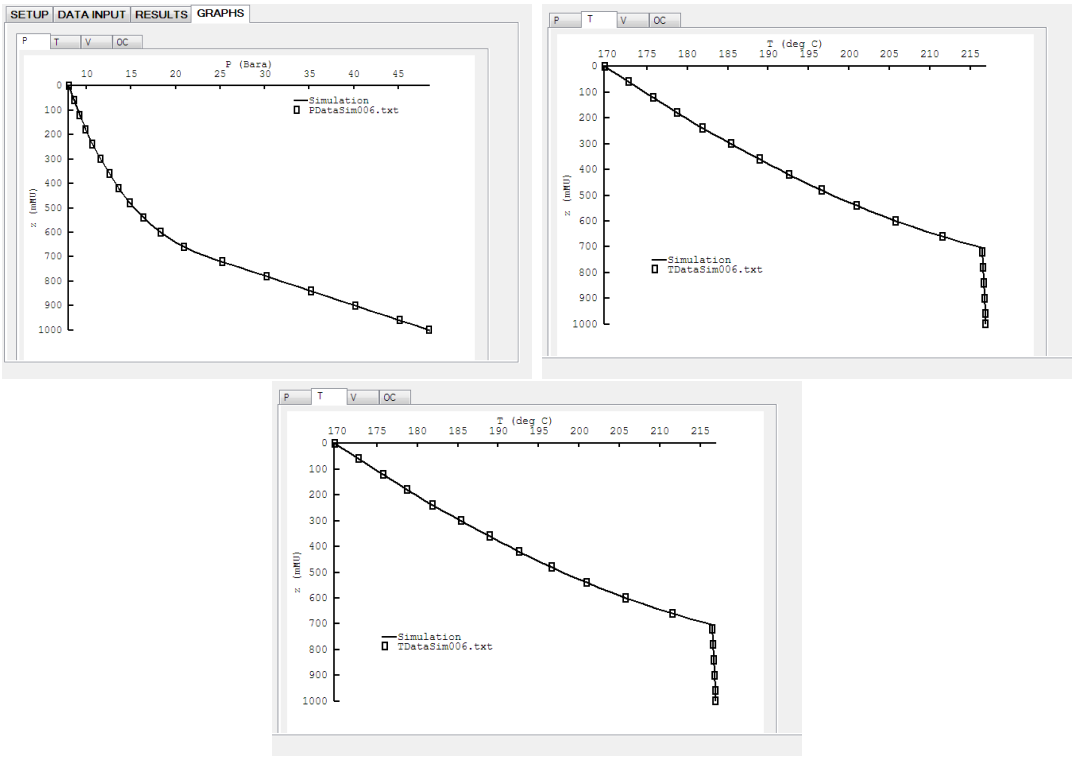

Figure 4: SwelFlo first steps, showing simulated pressure, temperature and spinner velocity profiles from a bottom-up run, matching values saved from a topdown run.

using the resulting values to solve back in the other direction, and seeing that the numerical solutions match to within graphical accuracy, provides direct evidence of that accuracy.

More commonly, the correct bottomhole pressure that matches wellhead values may not be known a priori. In this case, the user can set a range of bottomhole pressures to be automatically searched upon, or let the simulator choose a range by setting the bottomhole P range values both to 0.0. Try this - set both to zero, and RUN.

Note that the search for the correct bottomhole pressure takes a lot more time - many simulations are run, until a match is found to the wellhead values provided. The resulting best bottomup run should be indistinguishable from the previous one.

Note also that if the feed enthalpies are not carefully chosen, there may not be an ideal bottomhole pressure that gives a match to wellhead values. The process this tutorial has just gone through, of performing a topdown run using wellhead values to infer bottomhole properties, then performing a bottomup run using inferred values, is an excellent process for setting up wellbore properties given wellhead values. It also sets up feedpoints for computation of an output curve, which does require bottomup runs with varying bottomhole pressures.

3.4 Output Curve

Since a productivity index is known for the feedpoint, an output curve may be computed. Turn off the Downhole Profile option (this is just for better speed here — it is generally possible to compute both a profile and an output curve in the same run), and click Yes for the Produce an Output Curve option, in the SETUP tab. Now RUN causes the simulator to compute only an output curve, with just 12 successful points if bottomhole P range is the default of zero, as illustrated in Fig. (5).

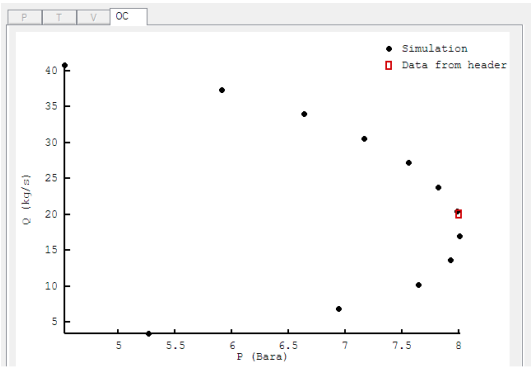

Figure 5: SwelFlo first steps, showing the output curve computed from the template setup with no bottomhole pressure range specified.

The number of points in the output curve may be refined by looking at RESULTS - Show Detailed Output, and noting the range of bottomhole pressures, near the end of the output

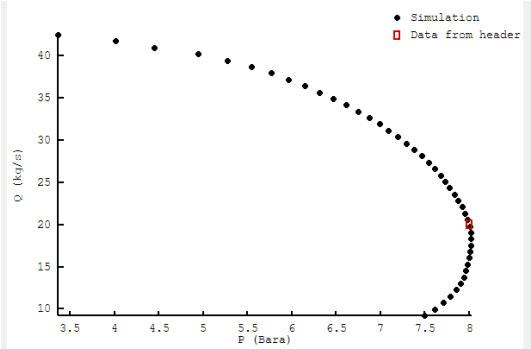

Figure 6: SwelFlo first steps, showing the improved output curve computed from the template setup with refined bottomhole pressure range.

file, that gave successful output points. Then, for example, setting a range of 40 to 52 bara here for bottomhole pressures and running again gives a much faster computation and many more points on the output curve, as illustrated in Fig. (6). Similarly, setting a range like this also affects bottomup computation of a downhole profile, and gives a much faster bottomup match to wellhead values if a downhole profile is requested.

If the user wants to examine the full downhole profile at any point on the output curve, they can specify the corresponding wellhead values for that point, and request a Downhole profile, to see graphs of P, T and V versus depth giving those wellhead values.

4 The SETUP Tab

This section contains more detailed information about the working of the SETUP tab.

4.1 Simulating Downhole Profiles

This section gives more detail about the ways to simulate and obtain a downhole profile, that is, values of pressure, temperature, saturation, enthalpy, density and flowrates versus depth in the well. In the SETUP tab, the user chooses Yes for Produce a profile, chooses a Flow correlation and a Simulation Direction. Then the four buttons labelled Wellhead, Reservoir Temperature, Casing and Feed Points may be used to set up the simulation. This requires setting wellhead values, a reservoir temperature profile if heat transfer between wellbore and country is to be included, casing geometry, and feed point properties. These four buttons are discussed in more detail in later subsections.

The ranges that are allowed for the simulation variables are listed in Table (1), and the maximum dimensions of variables are listed in Table (2).

Variable	min value	max value	units
pressure	1.0	1000	Bara
temperature	1	374	°C
well length	1	5000	m
casing section length	1	5000	m
wellbore radius	0	10	m
roughness	-1	10	m
subdivision length	0.01	1000	m
casing deviation angle	0	90	°
vertical extent of casing section	-1	5000	m
feed depth	0	5000	m
vertical depth to reservoir T	-1	5000	m
reservoir T for profile	1	374	°C
reservoir pressure at feed	-230.0	1000.0	Bara
reservoir H at feed	4.3	3000	kJ/kg
A, n or d at feed	0.0	3×10^{37}	
XCO_2 at feed or wellhead	0.001	1.0	
X (static dryness) at feed or wellhead	-2.0	1.0	
wellhead pressure	1.0	230	Bara
wellhead flowrate	-500.0	500.0	kg/s
wellhead or feed H	4.3	3000	kJ/kg
bottomhole pressure range	0.0	1000	Bara
thermal conductivity	0	10	W/K/m
rock density	0	4000	kg/m^3
heat capacity	0	4000	J/kg/K
time since discharge began, for			
heat transport to country calcs	0	10^9	s
spacing for data plot output from simulation	5	1000	m
relative tolerance for matching WHP	10^{-6}	0.5	
max and min wellhead flowrates for o/curve plot	0.0	2000.0	kg/s

Table 1: Ranges imposed by the simulator on input values of parameters. Input values outside these ranges will not be accepted by the input windows. The user can avoid entering a valid value once started, by clearing the value using the window menu.

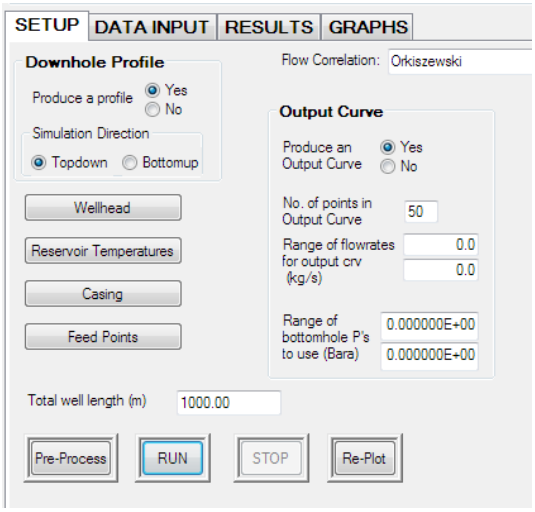

Figure 7: Screen snap of the SETUP tab in the main SwelFlo window

Item	Max Number
Separately defined sections of wellbore	500
Number of subdivisions of the wellbore	5000
Feedpoints	10
Points where reservoir temperature is specified	20
Data files	20
Data in each file	10000
length of file names	50
Points in simulated output curve	400

Table 2: List of maximum dimensions for variables in SwelFlo.

4.2 Topdown and Bottomup modes

The simulator will run either in topdown or in bottom-up mode, chosen in the Downhole Profile section of the SETUP tab. Either production (positive total flowrates) or injection (negative total flowrates) may be simulated in either mode.

Topdown means that the wellhead fluid flow properties are used to initiate the solution of the steady-state conservation equations, and the simulator steps from the wellhead down the wellbore, adding or subtracting fluid at intermediate feeds on the way down, until at bottomhole there is a final set of values of flowrate, enthalpy, carbon dioxide, and pressure computed for the fluid flow there.

Each bottom-up simulation begins with some value for wellbore pressure at bottomhole, as well as other properties like flowrate, mass fraction of carbon dioxide, and temperature or enthalpy or dryness, and iterates upwards to solve the conservation equations, adding or subtracting fluid at feeds on the way. Then the simulation arrives at the wellhead with values for flowrate, enthalpy, mass fraction of carbon dioxide and pressure that are determined by the computation. Many such simulations are performed in bottomup mode, and the value of bottomhole wellbore pressure is varied in an attempt to match the wellhead pressure.

To perform a bottomup simulation of a downhole profile, and to compute an output curve, the user must provide reservoir pressure, feed properties, and either temperature, enthalpy or vapor mass fraction, at bottomhole (and at any other feeds).

The range of bottomhole pressures that are used to perform this search for a match to wellhead values defaults to a maximum of the reservoir pressure at bottomhole, and a minimum of 1 bara. The user may help the simulator by refining the pressure range to be searched on at bottomhole, by entering two different pressure values into the boxes labelled "Range of bottomhole P's to use", at the lower end of the Output Curve section of the main SwelFlow window. This range serves two purposes, one to help the downhole profile to match wellhead values, and the other to set the range used to compute an output curve.

The two modes have different uses. Bottom-up is useful for predicting the flowrate for a target wellhead pressure, given feed and reservoir properties. Output curves (wellhead flowrate versus wellhead pressure) require a series of bottom up simulations. Topdown mode solves the same equations but starts with the given wellhead setup, in particular with a known flowrate and wellhead pressure, and predicts the resulting flow and pressure at bottomhole. Injection of single-phase fluid is handled correctly. For two-phase production, the rise velocity of vapour bubbles imposes a minimum upwards mass flow velocity in the correlations, typically about 1 kg/s.

4.2.1 A single bottom-up simulation

If a negative reservoir pressure is provided at the bottom of the well for a bottom-up simulation, this is taken to be a signal that the absolute value of this pressure is to be used as

a single bottomhole flowing pressure (wellbore pressure) for a single bottom-up simulation. There is no attempt to match whp in this case. Feedpoint flowrate must be specified if this option is used.

An alternative way to ensure this is to enter the same value of bottom hole maximum pressure and minimum pressure in the Input Setup tab (then reservoir pressure can also be separately specified, and the bottom feed can be of any type). This can be a useful option for comparing bottomup and topdown simulations — a topdown simulation can give bottomhole flowrate, enthalpy, and wellbore pressure. Setting these and running a bottomup simulation should give the same downhole profile. The advantage of this over the alternative option of setting a negative reservoir pressure at bottom hole, is that here a different (positive) reservoir pressure may be set, so that the bottom feed may be of any type — productivity index, fixed flowrate, dry steam, or drawdown.

4.3 Total well length

There is a place to enter the total well length (arc length along the casing centerline) just above the button for Pre-Process, Run, Stop and Re-Plot. The reason for this is to provide a check on the casing geometry setup. If the sum of the casing sections provided by the user in the Casing grid window is different, that sum over-rides the value entered by the user, and is displayed there.

In the event that a top-down simulation has no feed information provided, the total well length is used as the default location of the bottomhole feed. A bottom-up simulation requires at least one feed to be provided in the Feed Points grid window.

4.4 Correlations

The conservation equations that are solved in the simulator are simplifications of the conservation equations for the individual phases (liquid and vapor phases of water), obtained by adding them together to simplify interfacial interaction terms in the original equations. As a result extra empirical conditions are needed, to determine the relative velocities of liquid and vapor phases, depending on saturations. They form a correlation between static steam saturation and flowing steam quality, or equivalently between static steam saturation and the flowrate of one of the phases of water.

A number of these conditions are in the literature, and the ones currently on offer in SwelFlo are Orkiszewski, Armand, Hadgu with just the phase velocities affected, full Hadgu with momentum conservation also affected, Duns and Ros with just the phase velocities affected, Duns and Ros with momentum conservation also affected, and the Hagedorn and Brown correlation. These correlations were originally developed for the petroleum industry rather than the geothermal industry. More details on these correlations and how they have been modified for this simulator appear in the appendices to this manual.

It is unclear which correlation is preferable, despite a number of studies comparing them. The Hadgu correlation is likely to be the basis for the WELLSIM simulator, and is based on Hadgu's thesis results [19], and also draws on the GWELL code [1, 5] that was available in the early 1990's. The Orkiszewski correlation is quite popular in geothermal wellbore simulation.

4.5 Wellhead Conditions

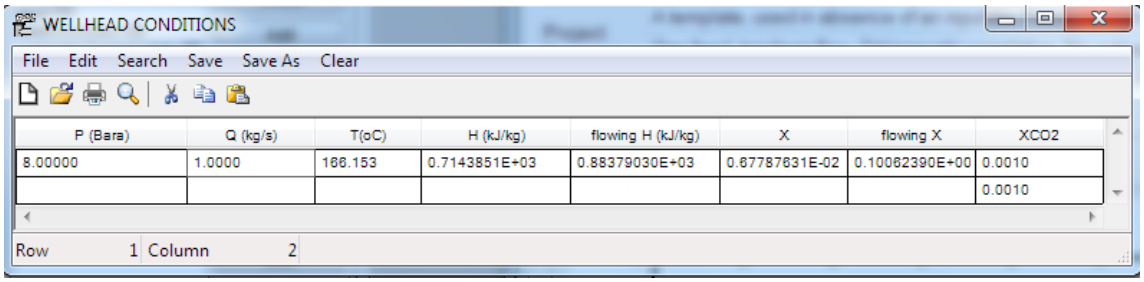

Figure 8: The Wellhead Conditions grid window in SwelFlo.

Fig. (8) shows the Wellhead Conditions grid window that appears when the Wellhead button is clicked. It is important to set the wellhead pressure, flowrate, XCO2, and one of (T, H, H_{flo}, X, X_{flo}). The simplest way to set one is to ensure the other four are cleared using the Clear menu item in this window. There is a hierarchy, used in the event that more than one of temperature, enthalpy or steam mass fraction are specified, and the most important term in the hierarchy is used to determine consistent values of all of the others, and replace them with the consistent values if they are present, otherwise show the consistent values, when the user clicks the Pre-Process or Run button.

4.5.1 Wellhead Thermodynamic Setup Priorities

Note that a distinction is drawn between static and flowing values of enthalpy and steam mass fraction, which coincide for a single-phase flow or for homogeneous two-phase flow. Any one of the five variables (T, H, H_{flo}, X, X_{flo}) is sufficient to determine the other four, given P and XCO_2. The hierarchy is that

1. X_{flo} is most dominant — a value between 0 and 1 will override any value that is set for T, H, X, or H_{flo}.
2. Next is H_{flo}, which will override any value that is set for T, H, or X.
3. Next is X, which will override any value that is set for T or H.
4. Next is H, which will override any value that is set for T.
5. The T value that is set will only have effect if none of (H, H_{flo}, X, X_{flo}) are set.

An exceptional case is when X or X_{flo} is set to zero or one, and there are no values set for T, H, and H_{flo}. This is taken as a signal that the user wants to set the fluid to the bubble point (zero) or liquidus (one), but only if all of the other values T, H, and H_{flo} are Cleared. If both X and X_{flo} are set to zero, this means the same thing. If there is a conflict, X_{flo} wins.

It is never necessary to Save the Wellhead Conditions grid window, or any of the other grid windows in SwelFlo. All simulation settings are automatically saved to the current project folder, each time Pre-Process or Run or Save in the main window menu is clicked, and if a user tries to exit after altering a simulation setting, SwelFlo will prompt for an overall Save before exiting. The overall save writes to the file SWFinput.txt, over-writing any previous setup, in the current project directory. This file is the main place that a simulation setup is saved. Since it is over-written each time the user modifies the project, it is useful to copy the SWFinput.txt file to another name using the Windows environment, if a user wishes to preserve that setup, say as a template for other simulations. Such a template may be imported to any (current) project, over-writing it after a warning, using the menu in the main SwelFlow window "Project- Import Existing SwelFlo setup".

It is possible to Save the Wellhead Conditions setup, from the Wellhead grid window menu. Then a csv file is created, with a default name SWFWHcon.csv, that can be Opened by another Wellhead Conditions grid window, providing the user with a way to share parts of the simulator setup between several different projects.

Copying and pasting between cells of a grid window and/or text files is supported.

4.6 Reservoir Temperatures

Reservoir temperatures versus depth may optionally be entered into this grid window. Either the distance along the wellbore, or the true vertical depth, of a reservoir temperature may be entered. The simulator expects one or the other of these columns to be used, but not bits of both. If both are used, then either the column with more values is used, or if both columns have the same number of values, the true vertical depth column is used.

The reservoir temperature profile entered here, if any, is used to calculate transient heat loss or gain between casing and country. The mathematics of that calculation may be found in the Appendices.

The Edit Row menu item in this grid window allows the user to insert or delete entire rows, or clear their contents. A maximum of twenty rows is currently allowed. The Clear menu item allows the user to clear the contents of the current cell, the selected cells, or the current row.

It is possible to Save the Reservoir Temperature profile to a file that may be Opened by another project from its Reservoir Properties grid window, over-riding any pre-existing reservoir temperature profile, just as for the Wellhead grid window. The default name for this file is SWFTres.csv.

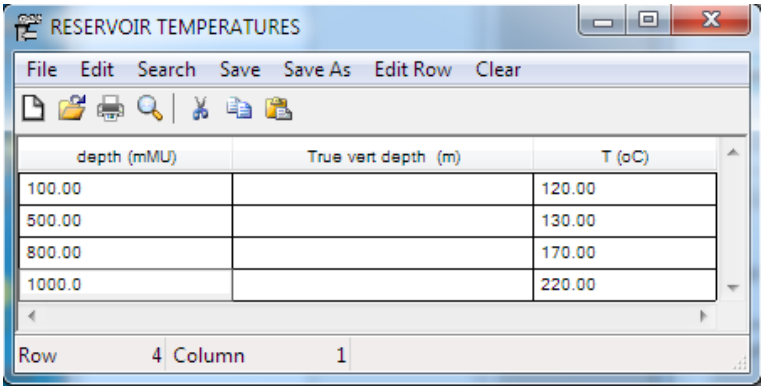

Figure 9: An example of the Reservoir Temperatures grid window in SwelFlo.

4.7 Casing Geometry

The Casing button opens a *CASING GEOMETRY* window, which is essential to the simulation, and the user enters the details of one or more, up to 500 sections of casing — length (measured depth MD) of the section, an optional Casing Identifier selection, radius, roughness, and angle to the horizontal (in degrees, so that 90.0 is vertical) or alternatively the vertical extent of the section. If vertical extent and length (measured depth MD along the casing) are provided and are nonzero, the simulator will calculate the angle and override any angle values given. The newly calculated angles will be displayed if the Preprocess button is pressed. If vertical extent is set to zero or less, it is ignored.

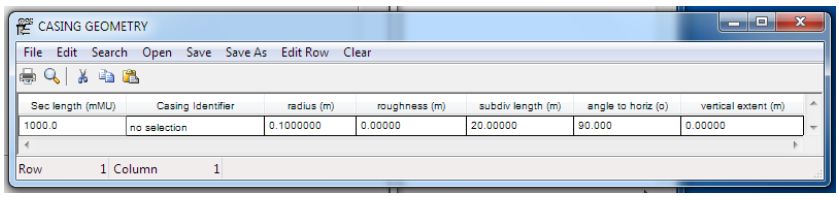

Figure 10: Screen snap of the Casing Geometry grid window

The user also specifies the size of subdivisions of a section, which is the mesh used for imposing conservation laws in the simulator. If subdivisions are set to too large a size, the conservation equations may fail to hold within the desired accuracy. The simulator will attempt to further subdivide a subsection where there is no convergence of solution to the conservation equations, down to a size of about two centimetres. This happens particularly if a flash point is encountered. It is recommended that the user set sizes of the order of five to twenty metres for subdivision lengths (mesh size).

Casing Identifier values will override any radius values entered, and any roughness values entered. Preprocessing will cause the over-riding values to appear in the *CASING GEOMETRY* window — radius, roughness and angle. If radius is set to zero, or roughness to a negative value, they are over-written by the default values radius=0.1m and

roughness=0m.

The Casing Identifier drop-down menu is read from the file called Casing_Liner_Database.csv in the directory that the exe file is stored in. A user may add lines to this database as desired, using a text editor in the Winows environment. The format of this csv file is that the first line is ignored, so can be a header, and the following lines take the form Casing ID (text, which can include the " character), inner diameter (inches), outer diameter (inches), and roughness (inches). All of these should be separated only by a comma. Quote characters should not be used to surround each entry, the commas are sufficient to separate values. Here is a sample from the first four lines of this file:

```
CASINGLIN ,INNERDIAM, OUTERDIAM, ROUGHNESS
CASING BASIC , 0.1, 0.15, 0.0018
CASING 4"1/2 M 9.5 ,4.1, 4.5, 0.0018
CASING 6"5/8 B 28.0 ,5.8, 6.6, 0.0018
```

Changes or additions to the Casing_Liner_Database.csv file will not show up in the simulator unless it is (re)started after the changes are made, since the simulator reads this file only on startup.

The Edit Row menu item in this grid window allows the user to insert or delete entire rows, or clear their contents. A maximum of 500 rows is currently allowed. The Clear menu item allows the user to clear the contents of the current cell, the selected cells, or the current row.

There is no need to Save this window before closing. There is no prompt when the user closes, since setup data is not lost. However, there is a Save and a Save As menu item on this window, which allows the user to either save to the current Project directory the default wellhead conditions csv file SWFCasing.csv, or to save the setup as a SWFCasing***.csv, where *** could be digits, or to save the csv file with any other name if desired. This is to give some flexibility in saving casing geometry setups, for example if the user wishes to import (read/open) them from another project, from within the corresponding Casing grid window. Depths and radii are saved as scaled variables, using the scaling currently chosen by the user. These saved csv files are what may be opened by the *CASING GEOMETRY* window menu File $->$ Open. Trying to Open an incorrectly shaped csv file may result in the exe file crashing.

4.8 Feed Points

The *FEEDPOINTS* window allows the user to set or modify the measured depth of up to ten feedpoints, the type (see below), the reservoir pressure, the reservoir temperature or enthalpy, XCO2 in the reservoir, and optionally the dryness of the reservoir fluid near the feedpoint. Other parameters are also set depending on the feed type or code. Dryness (steam mass fraction) is optional, and if entered and nonnegative it will cause the enthalpy or temperature to be overridden to be consistent with the desired dryness at the given reservoir pressure. The

resulting enthalpy is then taken to be the flowing enthalpy of any reservoir fluid that enters the feed.

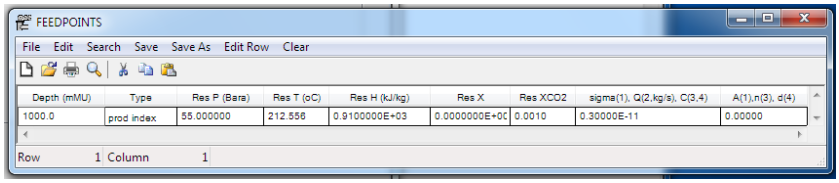

Figure 11: A view of the Feedpoints grid window

Any value of enthalpy entered for a feed point is interpreted as flowing enthalpy, since it is flowing enthalpy that is required for applying energy conservation laws. If a temperature is set for the reservoir at a feed point, and no enthalpy or dryness values are set, then this temperature is used to determine a static enthalpy, and this is then taken to be the flowing enthalpy of any fluid entering from the reservoir. If a dryness is set at a feed point, it is used to compute a static enthalpy, which over-rides any temperature or enthalpy value entered for this feed, and is then taken to be the flowing enthalpy at this feed.

The effective two-phase viscosity at a feedpoint is computed as an average, by averaging the inverse viscosity

$$\frac{1}{\nu} = \frac{k_{rl}}{\nu_l} + \frac{k_{rv}}{\nu_v} \ ,$$

over values taken between the reservoir pressure and the wellbore pressure, where $k_{rl} = 1 - S$ and $k_{rv} = S$ are relative permeabilities for liquid and steam, respectively, S is vapor saturation, and ν_l and ν_v are kinematic viscosities for liquid and vapor phases respectively. The computation of this viscosity is discussed in Appendix (J). It essentially assumes sub-horizontal flow from the reservoir to the feed.

For a bottom-up simulation, there must be at least one feedpoint, at a depth corresponding to the well length. For topdown simulation a feed is not required to be specified at bottom-hole (or anywhere else), since flow there is already predetermined by the rest of the well above it.

The Edit Row menu item in this grid window allows the user to insert or delete entire rows, or clear their contents. A maximum of ten rows or feeds is currently allowed. The Clear menu item allows the user to clear the contents of the current cell, the selected cells, or the current row.

Feed depths are not required to match a subsection depth on input. It they do not, the simulator inserts a new node at the feed depth, to make this so. Feeds must be in depth order, with the shallowest at the top. The following checks are made:

1. if DELZ does not divide evenly within 1E-07 into SECL, it is altered so that with the nearest integer number of sections, it does.

2. if LENGTH does not match the sum of section lengths, it is reset to equal the sum of section lengths, the user is warned in the error and progress windows, and the new value of LENGTH is displayed in the main input window.

3. If bottom feed depth does not match LENGTH of well within 0.01, length is set to bottom feed depth. However, for a topdown simulation, the bottom feed is allowed to be absent from the input information. If so, it is assumed to be at the well bottom, a distance LENGTH from the wellhead, and information about this bottom feed (flowrate, enthalpy, wellbore pressure, etc) is available in the detailed output file (*Show Detailed Output*) but only those feeds whose information is provided as input to the simulator have their information summarised in the main RESULTS tab.

4. If bottom feed depth does not match sum of section lengths within 0.01, simulation stops with detailed warnings.

5. If any feed depth does not match up with a subsection DELZ within 0.1, simulator inserts a new node to match the feed depth. This mismatch might be caused by previous adjustments, and is best fixed by altering the input file.

Feedpoints must be one of four possible types, with the codes

1. specified productivity index together with a quadratic Forcheimer term A which may be zero, or

2. specified flowrates, or

3. dry steam power law parameters, or

4. linear and/or quadratic drawdown parameters.

Productivity Index Feeds The extra parameters that must be provided in columns eight and nine of the FEEDPOINTS grid window for this type of feed are the productivity index Σ (m^3) of the feedpoint, and the nonlinear term A (floating point) in Forcheimer's equation for drawdown at a feedpoint, which should be set to zero for linear drawdown.

This case means that the following Forcheimer equation relating pressure drop (Pa) at a feed to flowrate Q (kg/s) is used:

$$P_{\text{res}} - P_{\text{well}} = \frac{1}{P_1} Q + \frac{A}{\sqrt{P_1}} Q|Q|$$

where $P_1 = \Sigma/\nu$ is the usual productivity (converted from t/hr/bar to kg/s/Pa) if A is zero, Σ is the *productivity index* which is needed if drawdown information is to be independent of viscosity changes at a feedpoint for output curve simulations, ν (m^2/s) is the effective kinematic viscosity for flow between the feed and the reservoir, and A is a nonlinear Forcheimer term. If A is set to zero, this equation is just Darcy's law for linear drawdown at a feed. Forcheimer's equation is an extension of Darcy's law to

situations where turbulent flow near the wellbore leads to lower flowrates and nonlinear dependence on pressure drop [28].

Please see Appendix (J) for details about effective viscosity and productivity index, and for a discussion on their relationship to the more usual productivity in t/hr/bar. Note that the usual productivity (in kg/s/Pa) is the productivity index divided by effective viscosity.

The productivity index (and perhaps also A for quadratic drawdown) is needed for correct output curve calculations, since the effective viscosity changes with pressure and especially also if flashing occurs at a feedpoint at higher flowrates, and this changes the flowrate.

Note that if the feed is specified to be a fixed flowrate feed, or a drawdown feed, and if an output curve is requested and a positive reservoir pressure is provided at the feed depth, then a productivity index is computed from the topdown or bottomup run that produces a downhole profile. This productivity index is then used in computing the output curve, and the feed is temporarily treated as a productivity index feed for the purpose of computing the output curve.

Fixed Flowrate Feeds The only extra parameter required here is the fixed flowrate desired at the feedpoint, set in column eight. Positive flow is for production, that is, flow from the reservoir towards the wellbore. Reservoir pressure is only required for this feed type if the user wants a productivity index calculated.

Dry Steam Feeds The extra parameters to be provided for dry steam feedpoints are C and n, in columns eight and nine, the power law parameters in the dry steam power law

$$Q = C(P^2_{\text{reservoir}} - P^2_{\text{well}})^n \ .$$

Usually $n = 0.75$, and C ranges from 0.4 for typical producers, to 0.75 for good producers, to 1.5 for the very best producers. Note that in this formula, however, pressure in the reservoir and in the well are first converted to bars, before squaring etc, and the calculated flowrate is taken to be in t/hr (and is then converted to kg/s internally afterwards). So C and n must be chosen accordingly (for pressure in bars and flowrate in t/hr). Dryness may be specified, but this does not really make sense for a dry steam feed.

Drawdown Feeds The extra parameters to be provided are c, the linear drawdown in bars/(t/hr), which is in fact one over the usual productivity (in t/hr/bar), and d, the nonlinear drawdown term for flowrate in t/hr and pressures in bara, in the drawdown equation

$$P_{\text{reservoir}} - P_{\text{well}} = cQ + dQ|Q| \ .$$

To get just linear drawdown, you can set $d = 0$ in the input file in column nine. Note that here, as for dry steam, pressures are first converted to bara, and the calculated Q is assumed to be t/hr, so is then converted to kg/s afterwards.

As noted above, there is no need to Save this window before closing. There is no prompt when the user closes, since setup data is not lost. However, there is a Save and a Save As menu item on this window, which allows the user to either save to the current Project directory the default wellhead conditions csv file SWFFeeds.csv, or to save the setup as a SWFFeeds***.csv, where *** could be digits, or to save the csv file with any other name if desired. This is to give some flexibility in saving wellhead setups, for example if the user wishes to import (read/open) them from another project, from within the corresponding grid window. These saved csv files are what may be opened by the *Feeds* window menu File $->$ Open. Trying to Open an incorrectly shaped csv file usually results in the exe file crashing.

4.9 Pre-Process, Run, Stop, Re-Plot

The first three of these buttons at the bottom of the INPUT SETUP Tab have the same effect as the corresponding menu items. **Pre-Process** saves input values from the input windows to internal arrays, does some checking of the setup to ensure it is ready to run, and if it is ready to run then the input file SWFinput.txt is saved to the current project folder. **RUN** will run the simulation; it will also Preprocess if necessary, first. Note that hence it is always possible to ONLY press Run, without first pressing Preprocess. Bottomup runs and/or output curves requested will cause a progress bar to appear; the *simulation* progress bar show progress during a bottomup search for a match to whp, and the *output curve* progress bar monitors progress during the generation of an output curve. The **STOP** button (and stop menu) will be active during simulation, and cause an immediate but non-catastrophic stop in the middle of simulation if pressed, returning simulator control to the user. The **Re-Plot** button allows the user to re-plot any existing graphs of simulator results and data files, taking into account any changes recently made since the last simulation run to the ranges of flowrates desired in the output curve, and taking into account any changes made to the data files the user wants displayed with the simulation results, or any new data files added to the list the user wants displayed alongside the simulated results. Re-plot uses the most recently generated output file for simulated values — hence if the user has changed units without re-running the simulation, plots will show incorrect units upon replotting.

4.10 Output Curves

An output curve is produced if "Yes" is selected in the radio buttons under the Output Curve label in the SETUP tab of the main SwelFlo window (see Fig. 7).

The number of points desired may be set, just below these radio buttons. This number is

indicative only. If it was zero, and the user selects "Yes" for an output curve, this number defaults to 50. It may be adjusted by the user.

The range of flowrates desired at the wellhead is used, if nonzero, to restrict the plotted points presented in the output curve.

The range of bottomhole pressures set by the user are to help the simulator find those bottomhole pressures that give steady state solutions for the current setup. If these pressures are set to zero, the simulator defaults to searching between one bara and the reservoir pressure at bottomhole. This range is usually much too large, and many of the simulations fail to complete since there is no steady state solution. Refining this range speeds up the computations, and helps provide a good selection of output curve points to be plotted. If a range of flowrates is specified, only those results lying in this range will be plotted in the output curve.

In topdown mode, if feed information is provided at bottomhole (optionally), the reservoir pressure may be used to determine a productivity index, given the calculated flow, calculated wellbore pressure, and effective viscosity at bottomhole. Then, if an output curve is requested together with a topdown run, a series of bottomup simulations are run to produce an output curve, using this productivity index, over-riding any nonzero value that the user has previously set at bottomhole. The value of bottomhole productivity index (and enthalpy) shown in the input window is as set by the user; the values of feedpoint enthalpy and productivity index displayed under the RESULTS tab are the values computed in the topdown run, and used to get the output curve; values detailed under the output button in the RESULTS tab (that is, in the main output file) corresponding to the output curve results are also the actual values used (as computed from the topdown run). A productivity index is also calculated for any other types of feedpoints for which

1. one is not already provided, and
2. it is not a dry steam power law case, and
3. reservoir pressure is provided and is positive.

The productivity index is important for reliable output curves, since it provides a measure of feed productivity that takes proper account of changes in the viscosity of the fluid at the feed as the enthalpy, pressure and saturation of the fluid change at different flowrates. Simply using linear or quadratic drawdown parameters is only accurate near the flow conditions that produced them; they should vary with viscosity (but don't), while the productivity index is independent of viscosity. Using a constant productivity index gives more accurate and reliable output curves, since it allows for the effects on flowrate of any changes in viscosity at feedpoints, as operating conditions change.

In bottomup mode, if an output curve is requested, if a productivity index is provided then that is used at a feed. If flowrate is specified, or linear drawdown, at a feed, then a productivity index is calculated from the downhole profile, and used to produce the output curve. If quadratic drawdown is specified, the Forcheimer term A is computed as well as the

productivity index, and both are used to compute the output curve. Otherwise A is set to zero, giving linear drawdown at that feed. If a dry steam power law is specified at a feed, no attempt is made to compute a productivity index there; an output curve is still generated. Dry steam accounts explicitly for variations in steam density, so the productivity index approach is not appropriate.

Hence, in both topdown and bottomup cases, a simulation that attempts to match a given well-head pressure is used (except for the dry steam power law case) to produce a productivity index at feeds where required, especially at bottomhole, and these indices are used to generate an output curve. Generation of an output curve requires that a reservoir pressure be provided at least at bottomhole.

If a fixed flowrate is specified at a feedpoint, and a positive reservoir pressure is provided there, the output curve will use the internally computed productivity index to calculate flowrates there, not the fixed flowrate. The matched bottom up simulation, however, will use the fixed flowrate. This can lead to differences between output curve and simulation run, if the reservoir pressure is inconsistent with the sign of the fixed flowrate specified, for example, if reservoir pressure is below wellbore pressure and a positive flowrate is specified. If the user wishes to retain the fixed flowrate at a feedpoint during computation of the output curve, they can impose this by setting the reservoir pressure to a negative value at that feed.

4.11 Rock Properties

Heat flow between casing and country may be turned on and off by selecting "Yes" or "No" in the "Allow Heat Flow To/From Country" radio buttons in the Rock Properties section of the SETUP tab in the main SwelFlo window. Values for thermal conductivity, density, heat capacity and time since flow began may be set or altered here also. The choice of time since flow began reflects the transient heat flow model that is used to compute heat flow. It would usually be the time in seconds since well discharge commenced, starting from an equilibrated zero heat flow initial state with the temperature in the wellbore assumed equal to the temperature in the country, at each depth value. A typical value is one week, or 604800 s.

4.12 Depth Spacing for data output

In the SETUP tab, in the bottom right-hand corner is a box labelled *Spacing for data output (m)*. This allows the user to choose the depth spacing between simulated results output to text files in the project directory, for pressure, temperature and velocity. These files are in the correct format for input as data files to SwelFlo, say from later runs in the same project folder. The files have names that include the project folder name, together with a three-digit generation number that matches the number on the main output file, and this allows the user to compare the results of simulations in different projects or between different simulations in

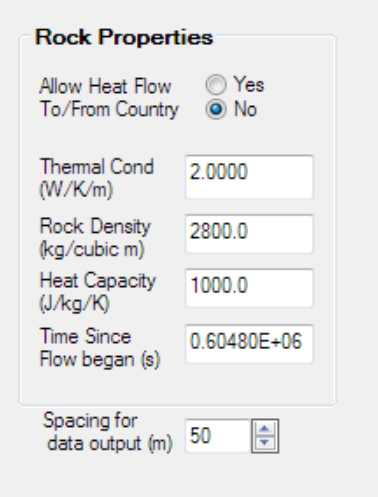

Figure 12: A view of the Rock Properties section of the SETUP tab in the main SwelFlo window

the same project, for example, different correlations or different feed parameters used. The units used when saving are the currently chosen units set by the user (for pressure and depth and flowrate).

5 Data Input Tab

The DATA INPUT tab, pictured in Fig. 13, allows the user to add data files for display on the same plots as the simulated P, T, V versus depth profiles, and the output curve, if asked for. It allows the user to choose files generated by previous simulations, in the same folder or elsewhere, or to create and then edit completely new data files from scratch.

Up to twenty data files may be read, edited, saved or created to go into the well folder, containing either pressure, temperature or mass-averaged fluid velocity values versus depth downhole, or output curve values (wellhead pressure vs flowrate). The format that these files must have is summarised in the Data Input tab, and is described in detail here:

Downhole profile data files for P, T or V have either pressure, temperature or velocity data versus depth (MD), and the first line should be:

Mass flowrate at wellhead, wellhead pressure, flowing enthalpy
and the remaining lines (up to 10,000 of them) should each contain:

depth (MD), data value

The mass-weighted velocity is the combination $Xu_v + (1 - X)u_l$ [17], where X is static steam dryness, u_v is vapor phase velocity, and u_l is liquid phase velocity.

The units for pressure and depth in data files are assumed to be the same as the units the

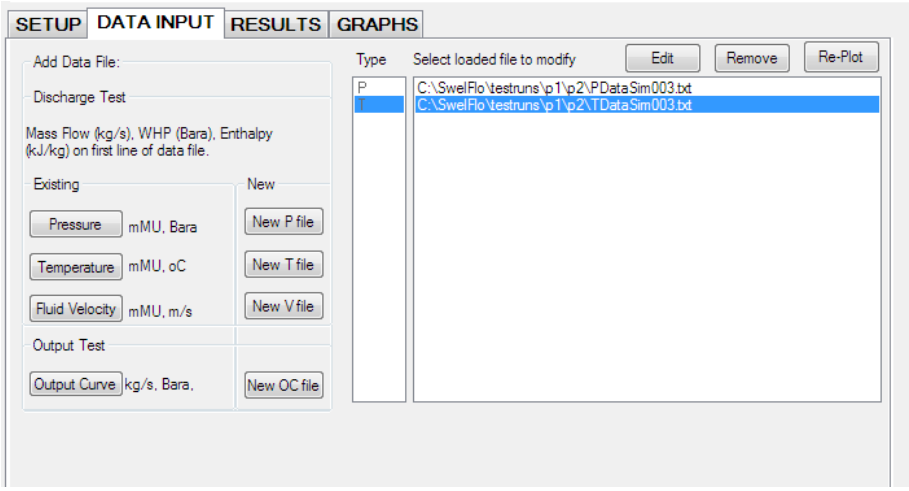

Figure 13: Screen snap of the DATA INPUT tab in the main SwelFlo window

user has most recently chosen in the menu item *Change Units*, and they default to Pa and m. For the output curve, the default flowrate units are kg/s. Note that if the user changes units in a project, the simulator makes no attempt to change the units in the data files in the project directory. The data files are always assumed to contain data that is in the units currently chosen by the user for the current well. Hence the user needs to ensure that data units match their chosen set of units, by directly editing data files from inside the simulator, or by using an editor like Notepad, from outside the simulator.

Enthalpy data at the wellhead is simply passed through to csv files if provided in P, T or V data files, so the units are up to the user. Enthalpy is simply passed through to csv files, not plotted or used. Temperature is always in degrees C, and fluid velocity is m/s.

Any output test data provided may have up to 3000 lines, each of which must take the form:
Mass flowrate at wellhead, wellhead pressure, flowing enthalpy

Inclusion of enthalpy can be avoided by ending the line with a /, or in fact it can simply be omitted and there can be just two values per line, flowrate and whp, in the units currently chosen by the user.

Note that the csv output curve files written by simulations are compatible with being read in as data files for other simulations without alteration. The first line gives a read error, but such lines are ignored by the simulator, which just tries to read the next line.

The wellhead information (flowrate, wh pressure) given in the first line from each of the downhole profile data files is also added to output test data for display in the GRAPH of the output curve, if an output curve is requested by the user.

The Re-Plot commands found on the DATA INPUT tab and on the INPUT tab will read in any data files added, before re-plotting the most recent simulation.

6 Results Tab

A text view of the results of the last simulation run in a folder is presented in the RESULTS tab, showing wellhead values, flash depth if any, and feedpoint flow properties, either imposed as boundary conditions or obtained as simulation results, depending on whether the simulation was topdown or bottomup. A button in this tab also allows the user to view the latest output file generated in the current folder.

The depth, if any, at which liquid flashes to two-phase is displayed just below the wellhead values.

In both topdown and bottom-up modes, the simulator detects changes in phase, between liquid flow, two-phase flow, and vapour flow. In particular, the depth at which a change from up-flowing liquid to up-flowing two-phase fluid occurs (the flashpoint) is located to within the minimum mesh size accuracy (of 2 cm), by subdividing nodes when such a change is detected until the minimum node size is reached. This helps to reduce the discretization effects of coarse meshing on output curve computations.

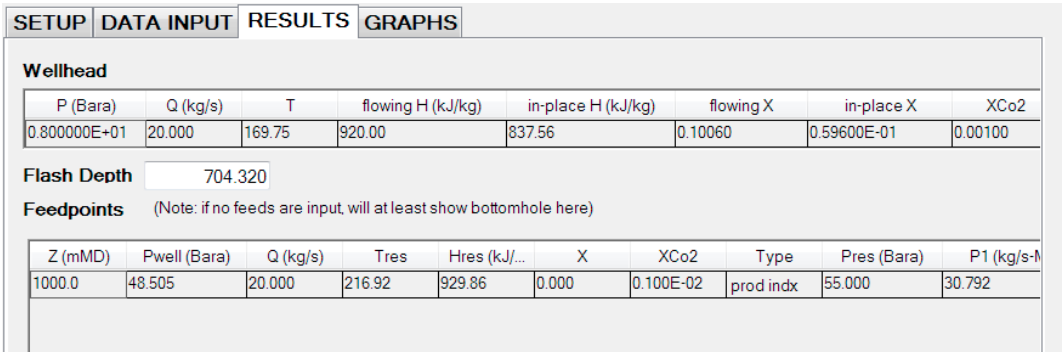

Figure 14: A view of the RESULTS tab in the main SwelFlo window

In the detailed output file are any downhole values computed (depth, pressure, temperature, static dryness, enthalpies of liquid and vapour phases, velocities of liquid and vapour phases, densities of liquid and vapour phases, total static fluid enthalpy, wellbore radius, flow regime, mass concentration of CO2, total mass flowrate, flowing enthalpy, flowing steam quality) that match most closely the wellhead pressure and flowrate given, depth of flash point if a transition from liquid to two-phase occurs in the wellbore, and a summary of feed and wellhead values for successful output curve simulations.

7 Graphs Tab

Plots may be viewed under the *GRAPHS* tab. Plots of simulated results are produced combined with any data provided for immediate feedback on how closely the simulated

wellbore setup matches available data. Presently, pressure, temperature, velocity and (if requested) output curve plots are presented.

The pressure plot shows total pressure (solid line), and saturation pressure of pure water (P_{sat}, dashed line), together with any pressure data provided.

The temperature plot shows the fluid temperature versus depth, together with any temperature data provided.

The velocity plot shows the simulated mass-weighted velocity, together with any spinner velocity data provided. The mass-weighted velocity is the combination $Xu_v + (1 - X)u_l$ [17], where X is static steam dryness, u_v is vapor phase velocity, and u_l is liquid phase velocity.

These plots are only intended to provide quick feedback, so cannot be altered or adjusted. Separate csv files are output to the project folder that allow the user to tailor plots for presentation purposes using an application like Grapher or Excel. The units for the plots are as chosen by the user for depth, pressure and flowrate. Otherwise, temperature is in °C, and velocity is the mass-weighted velocity expected to be obtained from a spinner in m/s.

Note that the data files provided by the user are assumed to use the units chosen by the user, for that well.

Simulated results are converted from the internally used SI units to the user units, before displaying together with any data provided.

8 Menu Items

The menu in the main window has five major items, Project, Help, Pre-process, Run and Stop.

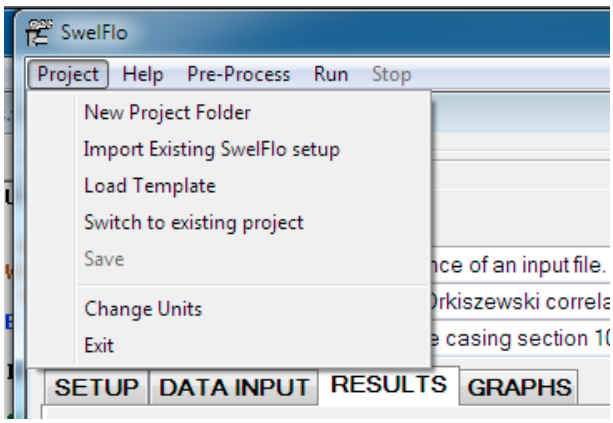

Figure 15: The Project menu in the main SwelFlo window

8.1 Project

This menu item has five submenus, New Project Folder, Import Existing SwelFlo setup, Load Template, Switch to existing project, Save, Change Units and Exit.

8.1.1 New Project Folder

This menu item has the same action as the "Change or Create Project Directory" button at the top of the main window. They allow the selection of different existing parent directories to work within, or the creation of new ones. Selection of a different existing Project directory with a SWFinput file already present results in that file being read by the simulator and loaded to internal arrays, and the simulator is now based in the newly chosen Project directory. The user can select a new path involving multiple new folders, and the simulator will create each new folder as required to create the new path.

8.1.2 Import Existing SwelFlo setup

This item allows the user to select and import the setup from another (existing) SwelFlo directory, by reading its SWFinput file, without changing the current working directory (Project folder). The new setup is written to the current (and unchanged) Project directory, over-writing any previously set up simulation state in the current directory. Hence the user is warned before any action is taken here.

8.1.3 Load Template

This menu item loads the internal template (detailed in Section 3.1), for a topdown simulation of the downhole profile of a producing vertical well of length 1000m, with wellhead pressure P 8 bara, flowrate Q 20 kg/s, temperature T 169.75 °C, and mass fraction of carbon dioxide XCO_2 0.001, providing a simple ready to run simulation that may be used as a starting point for modification.

8.1.4 Switch to Existing Project

Selecting *Switch to Existing Project* also changes the current working project directory to the one containing the selected input file, effectively switching to another existing project. Usually the user will select the file named SWFinput.txt, which is the file used by SwelFlo to store the current setup, and is the file read by default when SwelFlo visits a folder. When the user makes changes to a simulation setup, these changes are written to SWFinput.txt whenever a Pre-Process, Run or Save is performed.

The user is only prompted if there are unsaved changes in the original Project directory, which will be lost when switching to the other directory. The input file selected in the newly chosen pre-existing directory is then read into internal arrays, and any graphical data is also read in and displayed.

8.1.5 Save

This item causes the simulator to save the current setup to the default input file SWFinput.txt, essentially saving the project ready to be read in again if the simulator is restarted or switches to this Project directory at a later time. If there are preprocessing errors, the user is prompted before the input file is written to. There is no Save As menu item; each input file is uniquely identified with a project folder, so that output files etc are uniquely identified with the input file that generates them. Of course, the user may choose to duplicate by Importing a SWFinput.txt file from another project. And in the Windows environment, a user may save a SWFinput.txt file under another name, to preserve it for use as a template, ready to be imported by using the menu item "Import Existing SwelFlo setup". But a Project folder has only one working input file associated with it (and saved inside it), and it is called SWFinput.txt.

The Save button is greyed out and unresponsive if everything in the simulation setup has already been saved to SWFinput.txt.

8.1.6 Change Units

This allows the user to choose different units for displaying results, in the RESULTS and GRAPHS tabs, and in the main output file. These units are saved in the text file SWFunitsChoices.txt in the project directory, so applying only to the current project. The chosen units are also the units that are assumed to apply to any data files used by the project, and are also used in all saved csv files and output files in the project directory. Internal units are SI units; these are also the units saved to the project file SWFinput.txt when writing pressures and flowrates etc. Changing units after setting up data files may lead to incorrect display of data files, since they are assumed to use the current unit system. If plots are re-displayed by using the Re-Plot button immediately after changing units, they will also show incorrect units, since the output file being used to generate the plot is still in the previously chosen units. A rerun will fix this. It is up to the user to ensure that data files use the same units as the simulator.

8.2 Help

This menu option offers the option to display a simple pdf help file, that contains this Manual. It also gives access to an About menu item, which will display the version number

and a brief message about the simulator.

8.3 Pre-Process, Run, Stop

These have the same effect as the corresponding buttons at the bottom of the INPUT SETUP tab. Preprocess saves input values from the input windows to internal arrays, does some checking of the setup to ensure it is ready to run, and if it is ready to run then the input file SWFinput.txt is saved to the current project directory, as displayed in the Status Bar at the bottom of the main SwelFlo window. Run will run the simulation; it will also Preprocess if necessary, first. Note that hence it is always possible to ONLY press Run, without first pressing Preprocess. Bottomup runs and/or output curves requested will cause a progress bar to appear; the *simulation* progress bar show progress during a bottomup search for a match to whp, and the *output curve* progress bar monitors progress during the generation of an output curve by running bottomup with various bottomhole pressures as starting points. The stop menu and stop button will be active during simulation, and cause an immediate stop in the middle of simulation if pressed, returning simulator control to the user.

Note that there is no need for a *Close* menu item or button — opening an input file is really just an import process, which reads in the setup then closes the input file. If it is desired to wipe clean all existing input values, the user should select (mouse drag or shift click) and Clear values inside each grid window using the grid window menu Clear. An alternative is to import the setup from another project, or from an input file that the user has saved especially with a different name, so that it serves as a template. Or simply change the project directory to a new one for a clean slate start with the template. These changes are then written to the input file if the user presses Save, Preprocess or Run.

9 Output Files Generated

Output files generated by SwelFlo are

1. The text file *SWFoutput001.dat* is the main output file, always created in the current project folder. It contains
   (a) a record of the input used to create it, and
   (b) a summary of flowrates and properties at the wellhead and at the feedpoints, the depth of the flash point, and
   (c) detailed downhole simulated properties of the flow if a downhole profile was requested, and
   (d) a summary of wellhead and feedpoint pressures and flowrates and properties, and flash depth, for each successful output curve point calculated, if an output curve

was requested.

If SWFoutput001.dat already exists in the project folder, then the name SWFoutput002.dat will be tried, and so on up to SWFoutput999.dat before giving up and prompting for a filename from the keyboard. This file is displayed if the user presses the *Show Detailed Output* button in the RESULTS tab in the main simulator window.

Columns output in part (c) of this output file are, in order:

measured depth along the wellstring centreline,
vertical depth, pressure, temperature, flowing steam quality,
the enthalpy of the liquid phase (water plus carbon dioxide),
the enthalpy of the vapor phase (water plus carbon dioxide),
the velocity of the liquid phase and of the vapor phase,
the density of the liquid phase and of the vapor phase (water plus carbon dioxide),
total (static) enthalpy of the fluid,
radius, flow regime name, the total mass fraction of carbon dioxide,
the total mass flowrate, the flowing enthalpy of the mixture,
the enthalpy of the water component in the vapor phase (the steam),
the enthalpy of the water in the liquid phase,
the enthalpy of the carbon dioxide component in the vapor phase,
the enthalpy of solution of the carbon dioxide dissolved in the liquid phase,
the partial pressure of carbon dioxide,
the saturation pressure of pure water at the current temperature, and
the word "CHOKED" if the flow is choked in this section.

2. the comma-separated file *SWFplot001.csv* is created in the working folder if a downhole profile was requested, with numbering in the name being the same number as that currently applying to SWFoutput***.dat. It contains comma-separated simulated results (depth (MD), downhole P, T (°C) and mass-weighted velocity (m/s), positive for production, each in its own column) versus depth (MD), plus any data provided in data files. This file is intended for graphing when the user wants total control over the appearance of the graphs, and is ready to be used as input to the Grapher package, or opens very nicely in Excel. Each column has a header describing what it is (depth, P, T, V). Since a run always generated an output file, but does not always generate a downhole profile, there may be gaps in the numbering of the plot files, so that they always have the same number as the corresponding output file.

3. The text file *SWFoutcrv001.csv* is created in the current or working folder if an output curve is requested and obtained, containing an output curve ready for Grapher input, with flowrate in column 1, wellhead pressure in column 2, flowing enthapy in column 3, then any flowrates and WHPs and flowing enthalpies in columns 4, 5 and 6, that may have been provided in data files. Units used for user provided flowrates, pressures and enthalpies depend on what the user has chosen for this project. Numbering is chosen to match that for the corresponding SWFoutput file. This file is also in the correct format

to be added to the Data files that SwelFlo reads and displays in graphs along with simulated results. In that case SwelFlo will only read the first two columns, to extract simulated flowrates and WHPs. This allows a user to compare output curves from different projects, on the same graph. Or from different runs in the same working folder, differentiated by number.

4. Three files are created summarising simulation results if a downhole profile is requested, suitable for immediate input as data files, say for comparing two different projects under the same well directory. There is a pressure file, a temperature file and a velocity file, generated in the current project folder. The names are set to *PDataSim001.txt*, *TDataSim001.txt*, and *VDataSim001.txt*, with numbers that match the corresponding SWFoutput file. The format of these files is the same as the required format for data input files, a first line with Q, *whp* and H (flowing enthalpy at wellhead), subsequent lines with two columns, the first being depth and the second being the variable, all in units chosen by the user. Then a simulation that is subsequently run in another project folder, or in the same project folder, can use these data files and display them for comparison against (perhaps differently set up) simulated results. The spacing (in m) between depth values chosen for sampling the simulated results may be set by the user, under the INPUT SETUP tab, in the box labelled *Spacing for data output (m)*.

5. *ProgressReport.txt* in the project folder holds the text that was most recently displayed in SwelFlo's Progress grid window. Each time the simulator is restarted, or visits a project folder from elsewhere, this file is overwritten.

6. *SGWlog.txt* which is a general purpose text file for logging purposes, and is stored in the same directory as the exe file. It is overwritten whenever SwelFlo starts.

7. *ErrorReports.txt* is the file where error reports are kept, in the same directory as the SwelFlo exe file. It is overwritten whenever the simulator exe is started up.

10 Command Line Execution

SwelFlo can now be called with command line arguments, from a Windows command window. The arguments that have effect are:

command	followed by	effect
-s		silent mode, no windows
-f	"full path and filename"	input file, required for silent mode
-p	"path name"	a path for directory output is to go to, if different to directory containing input file

Note that silent mode requires an input file to be provided. The name of the input file must contain the full path. If spaces are desired in this name, enclose the whole thing in double

quotes. There must be a gap between the -f and the name, and between the -p and the path name if a separate path for the output directory is provided.

For example, the command

```
>swelflo.exe -s -f c:\swelflo\testruns\p1\SWFinput.txt
```

will run SwelFlo silently, on the input file SWFinput.txt, in the folder

```
c:\swelflo\testruns\p1
```

and output will go to the same folder.

The command

```
>swelflo.exe -s -f "c:\swelflo\testruns\project one\SWFinput.txt"
-p c:\swelflo\testruns\out1
```

will run an input file in the directory

```
c:\swelflo\testruns\project one
```

but output will go to the folder

```
c:\swelflo\testruns\out1
```

Note that the directory that output is to go to, must exist before running SwelFlo.

If an input file is provided, but silent mode is not invoked, SwelFlo will run in full interactive windows mode, using that input file, and running in the same folder as the input file, ignoring any output path provided. It is recommended that the user chooses the default input filename "SWFinput.txt".

If no input file is provided in silent mode, a warning is sent to the log file, and the simulator attempts to run on the last saved state in PrevSimState.txt in the execution folder, if any. If an output path is provided, it is ignored in this case.

References

[1] Aunzo, Z.P., 1990. GWELL : a multi-component multi-feedzone geothermal wellbore simulator. M.S. Thesis, University of California, Berkeley. 250 pp.

[2] Battistelli, A., Calore, C., & Pruess, K. (1993) A Fluid Property Module for the TOUGH2 Simulator for Saline Brines with Non-Condensible Gas, in Proceedings, Eighteenth Workshop on Geothermal Reservoir Engineering, Stanford University, Stanford, California, Jan 26–28, 1993. SGP-TR-145. pp. 249–259.

[3] Bilicki, Z., & Kestin, J. (1980) FLOW IN GEOTHERMAL WELLS: PART IV., Transition Criteria For Two-Phase Flow Patterns, Report GEOFLO/6, DOE/ET/27225-9, Division of Engineering, Brown University, Providence, R.I., 26 pages.

[4] Bilicki, Z., & Kestin, J. (1983) Two-phase flow in a vertical pipe and the phenomenon of choking: Homogeneous diffusion model -I. Homogeneous flow models, *Int. J. Multiphase Flow* **Vol 9**, Issue 3, pp. 269–288.

[5] Aunzo, Z.P., Bjornsson, G., Bodvarsson, G., 1991. Wellbore models GWELL, GWNACL, and HOLA User's Guide. Lawrence Berkeley Lab, University of California, Earth Sciences Division Report LBL-31428, UC-251. 103 pp.

[6] Barnea, D., A unified model for predicting flow pattern transitions for the whole range of pipe inclinations, *Int. J. Multiphase Flow*, **Vol 13**, No. 1 (1987) pp. 1–12.

[7] Brill, J.P., and Beggs, H.D. (1991) *Two Phase Flow in Pipes*, University of Tulsa, sixth edition.

[8] Carslaw, H.S., and Jaeger, J.C. (1959) Conduction of Heat in Solids, Oxford University Press, 2nd edition.

[9] Colebrook, C. F. and White, C. M. (1937). Experiments with Fluid Friction in Roughened Pipes. *Proceedings of the Royal Society of London. Series A, Mathematical and Physical Sciences* **161** (906): 367–381. Bibcode 1937RSPSA.161..367C. doi:10.1098/rspa.1937.0150

[10] Chisholm, D., *Two-phase flow in pipelines and heat exchangers*, Pitman Press Ltd, Bath, 1983.

[11] DeGance, A.E., and Atherton, R.W. (1970) Chemical Engineering aspects of two-phase flow: Part 6 – Vertical and inclined-flow correlations. *Chem. Eng.* **77** pp. 87–94, October 1970.

[12] Drew, D.A., & Wood, R.T., Overview and taxonomy of models and methods for workshop on two-phase flow fundamentals, in *Proc. 1st Int. Worshop on Two-Phase Flow Fundamentals* (National Bureau of Standards, Gaithersburg, Maryland, Sep 22-27,1985) pp. 1–88.

[13] Dukler, A.E., Moye Wicks, III, & Cleveland, R.G., Frictional pressure drop in two-phase flow: B. An approach through similarity analysis, *AIChE Journal*, Vol 10, No. 1 (1964) pp. 44–51.

[14] Duns, H. Jr., & Ros, N.C.J., Vertical flow of gas and liquid mixtures in wells. *Proc. 6th World Pet. Congress*, Frankfurt, Section II, Paper 22-PD6, pp.451–465 (1963) June 19–26.

[15] Ellis, A.J., & Golding, R.M., The Solubility of Carbon Dioxide Above 100°C in Water and in Sodium Chloride Solutions", American Journal of Science, **Vol. 261** (1963) pp. 47–60.

[16] Fernandes, R.C., Semiat, R., & Dukler, A.E., Hydrodynamic Model for Gas-Liquid Slug Flow in Vertical Tubes, *AIChE Journal*, Vol 29, No. 6 (1983) pp. 981–989.

[17] Garg, S.K., Pritchett, J.W., & Alexander, J.H. A new liquid hold-up correlation for geothermal wells, *Geothermics* **33** (2004) pp.795–817.

[18] Grant, M.A., Donaldson, I.G., and Bixley, P.F., *Geothermal Reservoir Engineering*, Academic Press, 1982.

[19] Hadgu, T., Vertical Two-Phase Flow Studies and the Modelling of Flow in Geothermal Wells, PhD thesis, University of Auckland, 1989.

[20] Hadgu, T., & Freeson, D.H., A Multipurpose Wellbore Simulator, GRC Transactions, Vol 14, Part II, pp. 1279–1286,Aug 1990.

[21] Hagedorn, A.R., & Brown, K.E. (1965). Experimental Study of Pressure Gradients Occurring During Continuous Two-Phase Flow in Small Diameter Vertical Conduit. J. Pet. Tech., Volume 17, Number 4, pp. 475–484.

[22] Kjaran, S.P., and Eliasson, J. (1983): Geothermal reservoir engineering, lecture notes, University of Iceland. UNU Geothermal Training Programme, Iceland, Report/983-2. `http://www.os.is/gogn/unu-gtp-report/UNU-GTP-1983-02.pdf`

[23] C.T. Kelley, *Iterative Methods for Linear and Nonlinear Equations*, SIAM, 1995.

[24] Malanin, S.D. (1959): The system water-carbon dioxide at high temperatures and pressures. Geochemistry No. 3, pp. 292–306.

[25] M.J. McGuinness, The impact of varying wellbore area on flow simulation, in the Proceedings of the Thirty-Eighth Workshop on Geothermal Reservoir Engineering, Stanford University, Stanford, California, February 11-13, 2013. SGP-TR-198. Six pages.

[26] M.J. McGuinness, *Feedpoint viscosity in geothermal wellbore simulation*, Geothermics, **50** (April 2014) 24–29.
DOI: 10.1016/j.geothermics.2013.07.007
`http://www.sciencedirect.com/science/article/pii/S0375650513000552`

[27] McGuinness, M.J. (2013). Correct Energy Conservation in Geothermal Wellbore Simulation. Submitted to Geothermics, 2013, minor revisions requested.

[28] Nield, D.A. & Bejan, A., *Convection in Porous Media*, Springer-Verlag, NY, 1999.

[29] Orkiszewski, J., Predicting Two-phase Pressure Drops in Vertical Pipe, J. Petroleum Tech. (June, 1967) pp. 829–838.

[30] Pritchett, J.W., Rice, M.H., & Riney, T.D., Equation-of-state for water-carbon dioxide mixtures: implications for Baca Reservoir. DOE/ET.27163-8, 1981.

[31] Serghides, T.K., Estimate Friction Factor Accurately, *Chem. Eng.* (March 5, 1984) **91** pp. 63–64.

[32] Sutton, F.M., Pressure-temperature curves for a two-phase mixture of water and carbon dioxide. N.Z. Journal of Science (1976) **19**, pp. 297–301.

[33] Takenouchi, S., & Kennedy, G.C., The binary system H_2O–CO_2 at high temperatures and pressures, AM. J. Sci. **Vol 262** (1964) p. 1055–1074.

[34] Taitel, Y., Advances in Two-Phase Flow Modeling, SPE27959, 1994, presented at the Tulsa Centennial Petroleum Engineering Symposium held in Tulsa, OK, USA, 29–31 August 1994.

[35] Todheide, K., & Franck, E.U. (1963): Das Zweiphasengebeit und die Kritische Kurve im System Kohlendioxid-Wasser bis zu Drucken von 3500 bar. Zeitschrift fur Physikalische Chemie (Neue Folge) **37** pp. 387–401.

[36] Torrens, T.S., *Vertically upward two phase flow in an annulus*, a thesis submitted in 1993 for the degree of Master of Engineering, Dept of Mechanical Engineering, University of Auckland, New Zealand.

[37] Yadigaroglu, G., & Lahey, R.T. Jr. On the various forms of the conservation equations in two-phase flow. Int. J. Multiphase Flow, Vol. **2** (1976) pp. 477–494.

A Input File Format

Here is a full description of the file SWFinput.txt. It can be generated directly by SwelFlo, so that the user does not need to create an input file. It contains all of the wellbore parameters and simulation settings that SwelFlo needs to determine a simulation, and is the main file read in by SwelFlo when it first enters a project directory. It is where SwelFlo saves its current setup. It is a text file, so can be modified directly, using a text editor if desired. The advantage of using the simulator to change the input file is that the format is then guaranteed correct.

The simulator can also read (import) input files from other SwelFlo projects or directories. When the Save or Preprocess or Run buttons or menus are pressed, the simulator saves the current simulation setup to the default input file.

The default name for the input file is *SWFinput.txt* . The Save command in the main menu creates this file, in the project directory, containing the input setup ready for reading if the simulator is directed to this project at another time. The simulator can be directed to read any text file as an input file if desired. The default name *SWFinput.txt* is where all changes made are saved to. The project structure associates each such input file uniquely with the Project folder it is inside.

There is no Save As command in the main menu. If the user desires to save the current setup in the correct format to a different file name which will not be automatically overwritten, they may copy that file within the main Windows desktop environment. Having another file name

for an original input file is one way to protect that input file against changes being written to it by the simulator, or to set up what is effectively a template, since the simulator will not overwrite such a file unless it is called SWFinput.txt.

Here is a line-by-line review of what is in the input file. The line number is also indicated, but should not appear in the actual file:

line 1. **TEXT1**
line 2. **TEXT2**
line 3. **TEXT3**

these lines of text are echoed in output files, and are designed to help identify a particular simulation. Each line may be up to 80 characters long.

line 4. **ANS, VELT, NSIMVALS, WANTOUTC, DOUBLESIM, GWELLFLAG, SIMRANOK, GOTOUTC, READYTOPLOT, GETPROFILE, ALLOWHFLO, QMAXOC, QMINOC,NSIMOUTCPTS,SPACNG**

These variables should be separated by blanks. This line is read in as a large character, max length 300 characters, then parsed by looking for the blanks.

ANS is I1, VELT is I1, and NSIMVALS and WANTOUTC are I of any size. They are integers.
DOUBLESIM is a real, F3.1. GWELLFLAG is an integer, and SIMRANOK, GOTOUTC, READYTOPLOT, GETPROFILE, ALLOWHFLO are logicals (T or F).
QMAXOC and QMINOC are real numbers, read in free format. NSIMOUTCPTS is an integer, and SPACNG is an integer, read in free format.

ANS determines whether simulation is topdown (ANS<=1) or bottomup (ANS>1, say 2).
VELT determines which 2-phase flow correlation will be used. Currently VELT=0 gives Armand; VELT=1 gives Orkiszewski; VELT=2 gives Hadgu for phase velocities only; VELT=3 gives a full Hadgu correlation, with Hadgu's choice of momentum terms as well as phase velocities; VELT=4 gives the Duns and Ros correlation for phase velocities only; VELT=5 gives the full Duns and Ros correlation including its treatment of momentum conservation; and VELT=6 gives the Hagedorn and Brown correlation.
NSIMVALS is the number of points desired to be computed in the output curve.
DOUBLESIM is redundant.
GWELLFLAG is redundant.
SIMRANOK (the most recent simulation ran OK) is used to decide whether to display graphs and results (display if true);
GOTOUTC (computed an output curve OK) is used to decide whether to display an output curve;
READYTOPLOT is set to true if there are data points and/or simulation points ready to be plotted.
GETPROFILE is true if the user wants a downhole profile computed.

ALLOWHFLO is true if the user want to allow heat to flow between the casing and the country.
QMAXOC and QMINOC set the upper and lower limits for wellhead flowrate, in the plot of the output curve, in the current units chosen for flowrates (kg/s or t/hr).
NSIMOUTCPTS records the number of output curve points that have been successfully simulated in the latest simulation.
SPACNG is the number of metres depth spacing (MD) desired between points output to files, after simulation, for future simulations to easily read in and plot as data alongside simulated results. For P, T and V versus depth. Files are called PDataSim***.txt, TDataSim***.txt, and VDataSim***.txt, where the asterisks stand for numbers 001 to 999 corresponding to the simulation number.

line 5. **NDATAF** (integer)

The number of data file names to be read from this input file, up to a maximum of 20 files. Each data file may contain up to 10,000 data points.

line 6. **data file name1** (character) , type of file (integer)

The name of the first data file to be read. Currently up to 256 characters. This must be just the FULL filename, with full path information.

The file type is an integer, 1 for pressures, 2 for temperatures, 3 for velocities interpreted from spinner data, 4 for output curve data. There can be only one type of data in a single data file, but there can be many pressure data files, for example.

The units for depths, pressures and flowrates in all data files are taken to be as set by the user in the simulator menu, and data files are assumed to contain data in the currently chosen units.

line 7. **data file name2** (character), type of file (integer)

The name of the next data file to be read, and type.
.
.
.

line (5 + NDATAF). **data file name*** (character), type of file (integer)

The name of the next data file to be read, and type.

line (6 + NDATAF). **NOTOPS** (integer)

The number of lines of wellhead values provided next. Exactly 2 lines are assumed present, and the second one is ignored if important terms are out of range.

line (7+NDATAF). **P, Q, T, H, Hflo, X, Xflo, XCO2** (floating point)

P is wellhead pressure (Pa)
Q is flow at the wellhead, positive for production, negative for injection (kg/s)

T is temperature, H is static enthalpy, and Hflo is the flowing enthalpy of the fluid at the wellhead.
X is the static steam mass fraction (dryness) , Xflo is the flowing steam quality, and XCO2 is the mass fraction in the total fluid of CO2, at the wellhead.

These values determine the starting conditions for topdown simulations.

line (8+NDATAF). **P, Q, T, H, Hflo, X, Xflo, XCO2** (floating point)

The second line of wellhead values, if another simulation is wanted.

line (7+NDATAF+NOTOPS). **WHPTOLERANCE,PMINSET,PMAXSET** (floating point values)

WHPTOLERANCE is the desired relative tolerance, used to decide when wellhead pressure is matched for bottom-up simulations. Recommended: 10^{-3}. If this is set too small, the simulation will still find a nearby WHP as best it can.
PMINSET,PMAXSET are the maximum and minimum allowed values for bottom hole pressures, to use when computing an output curve, or to restrict the range when searching for a bottomup match to desired wellhead conditions.

line 8+NDATAF+NOTOPS. **LENGTH**

a floating-point number, the total length of the well, mMD (metres measured depth, not vertical depth, but is distance down the casing). If it does not match the depth of the bottom feed, it is reset internally to that depth. Then if it does not match the result of adding up all of the section lengths, the program stops. It is used exclusively (together with angles to the vertical) to calculate the changes in potential energy of the flow.

line 9+NDATAF+NOTOPS. **THCON**

floating point number, the thermal conductivity of rock, usually 2.0 W/m/deg C.

line 10+NDATAF+NOTOPS. **RHOR**

floating point number, the density of rock, usually 2800.0 kg/ cubic m

line 11+NDATAF+NOTOPS. **HCAP**

floating point number, the heat capacity of rock, usually 1000.0 J/kg.

line 12+NDATAF+NOTOPS. **TIME**

floating point number, the time in seconds since started discharging (for transient heat flow calculations between well and adjacent country rock/reservoir), suggested is one week, 6.048E05 seconds

line 13+NDATAF+NOTOPS. **NUSEC**

integer, number of wellbore casing sections that follow. NUSEC must not be more than 500, and must be at least one.

lines 14+NDATAF+NOTOPS to 13+NDATAF+NOTOPS + NUSEC:
SECL RAD EPS DELZ DEV TRUEV CASINGCHOICE

section length (MD), radius of this section of casing, roughness, subdivision length desired for computations (MD), deviation angle from horizontal in degrees (vertical is 90.0), the true vertical extent of this section, casing choice. All numbers are floating point, separated by space(s), except Casing Choice which is an integer. There should be NUSEC of these lines. The units for lengths and pipe roughness in the input file are m, whereas in the displayed grid windows these depend on the user's choices for units. If a positive value is entered for true vertical extent, this is used together with the measured length (arclength, along the wellstring) to calculate and override the deviation angle. If a value for CASINGCHOICE (integer) greater than one is entered, the values on this line for radius and roughness are over-ridden by values read in from the database file *CasingLinerDatabase.csv* in the main SwelFlo directory. The number for Casing Choice is taken to be the line number in the csv file. The number one is *no choice* (the header line).

The subdivision length DELZ should divide exactly into the section length, and determines the distance between computational nodes. If it does not divide exactly, SwelFlo calculates a subdivision length that does, with the nearest integer number of subdivisions. It is unusual to go much less than 4m in subdivision length, except internally at the flash point. The total number of all of the subdivisions in the well cannot exceed 5000 in total.

Any feed points listed later in the input file should be exactly at the join between two subdivisions. If they do not, SwelFlo ensures that a subdivision is split into two at the feed depth. The total well length should match exactly the sum of section lengths. The deepest feedpoint should appear exactly at the bottom of the well, but if it does not the simulator tries to place it there. The maximum total number of subdivisions overall is 5000. There are a number of built-in checks and fixes of subsection lengths that do not exactly divide into section lengths, and fixes for overall LENGTH.

Checks have been added, in the following order:

1. if DELZ does not divide evenly within 1E-07 into SECL, it is altered so that with the nearest integer number of sections, it does.
2. If bottom feed depth does not match LENGTH of well within 0.01, length is set to bottom feed depth.
3. If sum of section lengths does not match LENGTH within 0.01, LENGTH is adjusted to match the sum of section lengths.
4. If bottom feed depth does not match sum of section lengths within 0.01, simulator stops with detailed warnings.
5. If any feed depth does not match up with a subsection DELZ within 0.01, the subsection is split at the feed depth.

line 14+NDATAF+NOTOPS + NUSEC: **NUPO**

integer, the number of points in the reservoir at which temperatures will be provided, to calculate heat loss or gain through the casing to/from the country. No more than 20. Can be zero.

lines 15+NDATAF+NOTOPS+NUSEC to 14+NUSEC + NUPO:
T_DEPTH TEMP

floating point numbers, separated by space(s), depth and reservoir temperature at that depth. There should be NUPO of these lines. Note that "depth" here, as elsewhere in the input file, is distance along the wellbore (MD), not the vertical depth in the reservoir. If the bottom value is recorded as a negative value, this is interpreted to mean that the absolute values of all entered depths here are in fact true vertical depths rather than distance along the wellbore.

next line: **NUFEED**

integer, the number of feedpoints that will be modelled. No more than 10 can be handled. This is the last set of lines read in from the input file.

next NUFEED lines: **F_DEPTH(I) FICODE(I) other values**

The program first reads the depth (floating point) and the code (integer). Then it backspaces, and what it then tries to read again from the same line depends on the value of FICODE it just read.

F_DEPTH(I): feed depth (m MD); (floating point)
Note that all "depths" in the simulation are actually distances along the casing, that is, "measured depth", not true depths. The casing angles are used to find true depth changes when needed. Feeds should be listed in order from shallowest to deepest.

The **other values** depend on what number is entered for FICODE(I) (an integer). They can be different for each feedpoint.

If FICODE is 1: Forcheimers equation:
the whole line should contain

F_DEPTH(I), FICODE(I), RESV(1,I), RESV(3,I), RESV(12,I), FDRY(I), RESV(6,I), RESV(4,I), RESV(7,I)

where RESV(1,I) is reservoir pressure (Pa) (floating point); RESV(3,I) is reservoir temperature (°C), RESV(12,I) is flowing fluid enthalpy (J/kg) in the reservoir; FDRY(I) is the floating point flowing dryness of the reservoir fluid at this feed, RESV(6,I) is the mass fraction of CO_2 in the reservoir fluid, RESV(4,I) is the productivity index Σ (m^3) of the feedpoint (floating point); RESV(7,I) is the nonlinear term A (floating point) in Forcheimer's equation for drawdown at a feedpoint, which should be set to zero for linear drawdown. Note that enthalpy is interpreted as a flowing enthalpy from reservoir to well, if provided.

This case means that the following Forcheimer equation relating pressure drop (Pa) at a feed to flowrate Q (kg/s) is used:

$$P_{\text{res}} - P_{\text{well}} = \frac{1}{P_1} Q + \frac{A}{\sqrt{P_1}} Q|Q|$$

where $P_1 = \Sigma/\nu$ is the usual productivity (converted from t/hr/bar to kg/s/Pa) if A is zero, Σ is the *productivity index* which is needed if drawdown information is to be independent of viscosity changes at a feedpoint for output curve simulations, ν (m^2/s) is the effective kinematic viscosity for flow between the feed and the reservoir, and A is a nonlinear Forcheimer term. If A is set to zero, this equation is just Darcy's law for linear drawdown at a feed. Forcheimer's equation is an extension of Darcy's law to situations where turbulent flow near the wellbore leads to lower flowrates and nonlinear dependence on pressure drop [28].

Please see Appendix (J) for details about effective viscosity and productivity index, and for a discussion on their relationship to the more usual productivity in t/hr/bar.

The productivity index (and perhaps also A for quadratic drawdown) is needed for correct output curve calculations, since the effective viscosity changes with pressure and especially also if flashing occurs at a feedpoint at higher flowrates, and this changes the flowrate.

If FICODE is 2: flowrate fixed
the whole line should contain

F_DEPTH(I), FICODE(I), RESV(1,I), RESV(3,I), RESV(12,I), FDRY(I),RESV(6,I), FLOW(I)

where the new variable is FLOW(I), the fixed flowrate desired at the feedpoint in kg/s (floating point). Positive flow is for production.

If FICODE is 3: dry steam power law
the whole line should contain

F_DEPTH(I), FICODE(I), RESV(1,I), RESV(3,I), RESV(12,I), FDRY(I), RESV(6,I), RESV(10,I), RESV(11,I)

The new variables are RESV(10,I) = C, and RESV(11,I)=n, both floating point, where C and n are the power law parameters in the dry steam power law

$$Q = C(P^2_{\text{reservoir}} - P^2_{\text{well}})^n$$

and usually $n = 0.75$, and C ranges from 0.4 for typical producers, to 0.75 for good producers, to 1.5 for the very best producers. Note that in this formula, however, pressure in the reservoir and in the well are first converted to bars, before squaring etc, and flowrate is taken to be in t/hr (so is then converted to kg/s afterwards). So C and n must be chosen accordingly (for pressure in bars and flowrate in t/hr). Dryness may be specified not equal to one, but this is not very appropriate for a dry steam feed.

If FICODE is 4: linear or quadratic drawdown
the whole line should contain

F_DEPTH(I), FICODE(I), RESV(1,I), RESV(3,I), RESV(12,I), FDRY(I), RESV(6,I), RESV(8,I), RESV(9,I)

The new variables are RESV(8,I) = c, the floating-point linear drawdown in bars/(t/hr), which is in fact one over the usual productivity (in t/hr/bar), and RESV(9,I) = d, the nonlinear drawdown term for flowrate in t/hr and pressures in bara, in the drawdown equation

$$P_{\text{reservoir}} - P_{\text{well}} = cQ + dQ|Q| \ .$$

To get just linear drawdown, you can set $d = 0$ in the input file. Note that here, as for dry steam, pressures are first converted to bara, and Q is assumed to be t/hr, so is then converted to kg/s afterwards.

THE END: The input file is read until end-of-file, looking for all feeds provided. Nothing further is sought in the input file.

B Nomenclature

A	wellbore cross-section area	m
c	thermal capacity of rock	J/kg/ °C
C_A	Armand coefficient	
D	diameter of wellbore	m
D_r	thermal diffusivity of rock	m^2/s
f_D	Darcy friction factor	
f_H	Fanning friction factor $f_D/4$	
g	gravitational acceleration	$m.s^{-2}$
G	mass flux	$kg/s/m^2$
h	specific enthalpy	J/kg
k	thermal conductivity	J/(m.s.°C)
K	ratio of phase velocities	
M	mass flow rate of a phase	kg/s
N_{lv}	dimensionless liquid velocity	
N_{gv}	dimensionless gas velocity	
N_d	dimensionless casing diam	
N_l	dimensionless liquid viscosity	
P	pressure	Pa
Q	total mass flow rate	kg/s
Q_t	heat flow, rock to casing	J/m
r	radius of casing	m
Re	Reynolds number	
S	vapor saturation	
T	temperature	°C
u	velocity	m/s
U_{SG}	superficial gas velocity	m/s
U_{SL}	superficial liquid velocity	m/s
v	specific volume	m^3/kg
$< v >$	average flowing velocity	m/s
X	steam dryness (static mass fr)	
X_{flow}	steam quality (flowing mass fr)	

Subscripts

H	homogeneous
l	liquid phase
res	reservoir
v	vapor phase
w	well

α	vapor saturation	
β	vol. gas flow ratio	
ϵ	roughness	m
ρ	density	kg/m^3
$< \rho >$	ave two-phase density	kg/m^3
ρ_m	ave two-phase density	kg/m^3
σ	surface tension - water	N/m
μ	dynamic viscosity	Pa.s

C Governing Equations

The steady-state equations that SwelFlo solves in sections of the well between feedpoints are outlined here.

C.1 Two-Phase Flow Terminology

The notation introduced here follows [10], and is also broadly consistent with the GWELL manual and Hadgu's thesis.

Note that the two-phase correlations discussed in this manual have all been developed only for upflow of both phases, and are incorrect for counterflow or downflow.

M_v is the mass flow rate (kg/s) of vapour phase up the well, M_l is the liquid mass flow rate. u_v is the actual speed (m/s) of vapour up the well,

$$u_v = \frac{M_v}{\alpha A \rho_v} \ , \tag{1}$$

with a similar eqn for liquid, where $\alpha = A_v/A$ is the (static) void fraction or saturation, A_v is the cross-section area occupied by vapour, ρ_v is vapour phase density, and A is the total cross-section area of the well.

$$X_{\text{flow}} = \frac{M_v}{Q} \tag{2}$$

where $Q = M_v + M_l$ is the total mass flow rate. The velocity ratio is

$$K = \frac{u_v}{u_l} \ .$$

Slip velocity is $u_v - u_l$, and drift velocity is $u_v - u_H$, where u_H is the homogeneous velocity, which both phase velocities are equal to if $K = 1$,

$$u_H = G\left(\frac{X_{\text{flow}}}{\rho_v} + \frac{1 - X_{\text{flow}}}{\rho_l}\right) \ .$$

$$u_v = G\left(\frac{X_{\text{flow}}}{\rho_v} + \frac{K(1 - X_{\text{flow}})}{\rho_l}\right) \ ,$$

where $G = \frac{Q}{A}$.

Superficial gas velocity (in m/s) is saturation times gas velocity, and is

$$U_{SG} = \frac{M_v}{\rho_v A} = S u_v \ .$$

This is the steam velocity in the absence of the liquid phase. Similarly, superficial liquid velocity (m/s) is

$$U_{SL} = \frac{M_l}{\rho_l A} = (1 - S) u_l \ ,$$

where M_l is the mass flowrate of the liquid phase and ρ_l is liquid density. Void fraction α is used in Hadgu's thesis, since he often deals with air/water mixtures. Void fraction is saturation S, that is, volume fraction of vapour phase in place. It is related to the in place dryness or steam quality X by

$$S = \alpha = \frac{X\rho_l}{X\rho_l + (1-X)\rho_v} \ , \tag{3}$$

and to the flowing dryness by

$$S = \alpha = \frac{X_{\text{flow}}\rho_l}{X_{\text{flow}}\rho_l + K(1-X_{\text{flow}})\rho_v} \ . \tag{4}$$

Flowing dryness can be expressed in terms of static dryness X as

$$X_{\text{flow}} = \frac{Xu_v}{Xu_v + (1-X)u_l} \ ,$$

and in terms of saturation S and flow ratio K as

$$X_{\text{flow}} = \frac{S\rho_v K}{S\rho_v K + (1-S)\rho_l} \ ,$$

and flowing enthalpy can be written in the form

$$h_{\text{flow}} = X_{\text{flow}}h_v + (1-X_{\text{flow}})h_l \ .$$

Other useful rearrangements of these equations are, for static dryness X,

$$X = \frac{S\rho_v}{S\rho_v + (1-S)\rho_l} \ ,$$

and

$$X = \frac{X_{\text{flow}}}{X_{\text{flow}} + K(1-X_{\text{flow}})} \ ,$$

and for flowing steam quality

$$X_{\text{flow}} = \frac{S\rho_v u_v}{G} \ .$$

C.2 Mass Conservation of Water and Carbon Dioxide

Note that mass flowrate (input and output) is always the total mass, water plus carbon dioxide. The relative mass of carbon dioxide is always very small though. The equation for conservation of mass of water is simply, in the absence of feedpoints,

$$Q = A(\rho_l(1-S)u_l + \rho_v S u_v) = c$$

where c is some constant. The same equation applies, if M_v is the total mass of water and carbon dioxide in the vapor phase, and M_l is the total mass of liquid water and dissolved carbon dioxide. This is what is coded.

Further details on conservation of carbon dioxide and its consequences for computing flowing steam fraction may be found in appendix H.4. Note for now that $X_{\rm flow}$ is given by conservation of carbon dioxide, once the constant total mass flowrate is known, together with pressure, temperature and mass fraction of carbon dioxide.

The following conservation laws are presented for pure water only.

C.3 Momentum conservation

The momentum conservation equation is

$$\frac{dP}{dz} = -G\frac{d <v>}{dz} + <\rho> g\sin\theta + \phi^2_{\rm FL0}\left[\frac{dP}{dz}\right]_{\rm L0} , \tag{5}$$

where $<v> = (1 - X_{\rm flow})u_l + X_{\rm flow}u_v$ is an average flowing velocity, $<\rho> = (1-\alpha)\rho_l + \alpha\rho_v$ is the usual average density, z is distance down the well, and $G = Q/A$ is taken to be positive for upflow (production). The first term on the RHS is the divergence of momentum flux in the case of constant A, when G can be put inside the derivative; the second is due to gravitational force; and the third is due to friction forces between phases and wall, parameterised as a wall loss term.

The average density $<\rho>$ can be written in terms of flowing steam fraction by using equation (4), to obtain

$$<\rho> = \rho_l\rho_v\frac{X_{\rm flow} + K(1 - X_{\rm flow})}{X_{\rm flow}\rho_l + K(1 - X_{\rm flow})\rho_v} . \tag{6}$$

The original code in GWELL is missing the term K in the denominator of the previous equation, so it does not conserve momentum.

Note that the momentum flux term is not always written correctly for varying wellbore cross-section area A [25]. The term G is often put inside the z derivative, which is only correct for constant A.

Note that using

$$\frac{u_v}{u_l} = \left(\frac{X_{\rm flow}}{1 - X_{\rm flow}}\right)\left(\frac{1-\alpha}{\alpha}\right)\left(\frac{\rho_l}{\rho_v}\right) , \tag{7}$$

it is straightforward to rewrite the momentum flux term in the case of constant A in the alternative forms

$$G < v > = S\rho_v u_v^2 + (1-S)\rho_l u_l^2 = G^2\left(\frac{X^2_{\rm flow}}{S\rho_v} + \frac{(1 - X^2_{\rm flow})}{(1-S)\rho_l}\right) . \tag{8}$$

This is only useful for constant cross-sectional area, since otherwise the term G should not be inside the derivative [25].

The frictional pressure drop is modelled using a two-phase correction factor ϕ^2_{FL0} which is described below. The term $\left[\frac{dP}{dz}\right]_{\mathrm{L0}}$ is computed as in (2.66) and (7.31) in Chisholm:

$$\left[\frac{dP}{dz}\right]_{\mathrm{L0}} = \frac{f_D G|G|}{4r\rho_l}$$

where f_D is the Darcy friction factor given implicitly by the Colebrook equation (see next subsection), and G is computed in the usual way for two-phase flow,

$$G = Q/A = \rho_l(1-S)u_l + \rho_v S u_v \ .$$

C.3.1 Friction Factor

Solutions are needed to the implicit Colebrook-White equation [9], to find for turbulent flow the Darcy friction factor f_D that solves

$$\frac{1}{\sqrt{f_D}} = -2\log_{10}\left(\frac{\epsilon}{3.6D} + \frac{2.512}{\mathrm{Re}\sqrt{f_D}}\right)$$

where D is well diameter, and Re$= (\rho u D)/\mu$, where u is fluid velocity.

Newton iteration can be used to iterate to find a solution, as is done in GWELL. An alternative, adopted in SwelFlo, is to use Serghides' Solution [31], accurate to within 0.0023% and fast since it is explicit. It is given by

$$A = -2\log_{10}\left(\frac{\epsilon}{3.7D} + \frac{12}{\mathrm{Re}_l}\right) , \tag{9}$$

$$B = -2\log_{10}\left(\frac{\epsilon}{3.7D} + \frac{2.51A}{\mathrm{Re}_l}\right) , \tag{10}$$

$$C = -2\log_{10}\left(\frac{\epsilon}{3.7D} + \frac{2.51B}{\mathrm{Re}_l}\right) , \tag{11}$$

$$f_D = \left[A - \frac{(B-A)^2}{C-2B+A}\right]^{-2} , \tag{12}$$

where ϵ is roughness, in the same units as wellbore diameter D.

As suggested in [36], the extended Colebrook equation is used in cases where roughness over diameter exceeds the value 0.05 (as can happen with the Duns and Ros correlation for mist flow), and the friction becomes independent of Reynolds number:

$$f_D = 4\left[\frac{1}{[4\log_{10}(0.27\epsilon/D)]^2} + 0.067\left(\frac{\epsilon}{D}\right)^{1.73}\right] . \tag{13}$$

C.3.2 Two-Phase Correction Factor

The two-phase multiplier $\phi^2_{\rm FLO}$ (friction, liquid only) is taken from Chisholm [10] for the case of a rough casing, with Blasius exponent zero, when it takes the form

$$\phi^2_{\rm FLO} = 1 + (\Gamma^2 - 1)[B_R X_{\rm flow}(1 - X_{\rm flow}) + X^2_{\rm flow}] \ ,$$

where Γ^2 is the ratio of pressure drop if fluid is single-phase vapor to the pressure drop if the fluid is single-phase liquid, and is expressed as

$$\Gamma^2 = \left(\frac{\mu_v}{\mu_l}\right)^n \frac{\rho_l}{\rho_v}$$

with the Blasius exponent n set to the value $1/4$ for smooth flow at this stage, since Γ will be used to determine the smooth parameter B_s. The semi-empirical coefficient B_R for rough well casings is given in terms of the smooth B_s by

$$B_R = 0.5 B_s \left(1 + \left(\frac{\mu_v}{\mu_l}\right)^2 + 10^{-300\epsilon/r}\right) \ .$$

The value of B_s depends on Γ and G, as in Table 3, which is Table 7.7 from Chisholm [10].

Γ	G	B_s
≤ 9.5	< 500	4.8
	$500 \leq G \leq 1900$	$2400/G$
	≥ 1900	$55/\sqrt{G}$
$9.5 < \Gamma < 28$	≤ 600	$520/(\Gamma\sqrt{G})$
	> 600	$21/\Gamma$
≥ 28		$15000/(\Gamma^2\sqrt{G})$

Table 3: Vaues of B_s for smooth pipes

C.4 Energy conservation

Conservation of energy for a producing well takes the form (see for example, Chisholm [10]):

$$\frac{\partial}{\partial z}\left[X_{\rm flow} h_v + (1 - X_{\rm flow}) h_l + \frac{X_{\rm flow}}{2} u_v^2 + \frac{1 - X_{\rm flow}}{2} u_l^2\right] + \frac{Q_t}{Q} - g \sin\theta = 0 \ ,$$

where Q_t is the heat flow rate per metre of casing at depth z from the country to the well. This is the total heat flowing per second through the area of the casing surface contained in one metre of casing length, with units J/s/m. The first two terms are a flowing average enthalpy, and the next two terms are an average kinetic energy of the two-phase flow.

C.5 Heat Flow between country and casing

Following [5], a transient radial heat flow model is used for conductive heat flow between casing and country at depth z,

$$\frac{\partial T}{\partial t} = \frac{D_r}{r}\frac{\partial}{\partial r}\left(r\frac{\partial T}{\partial r}\right) ,$$

where $D_r = \frac{k}{\rho c}$ is the thermal diffusivity of the surrounding rock. Boundary conditions are assumed to be that the wellbore temperature is fixed at T_w, while the temperature far from the well is the reservoir temperature, T_{res}. A transient solution valid for large times $t \gg r_w^2/D_r$ gives [8]

$$Q_t \approx \frac{4k\pi(T_{\text{res}} - T_w)}{\ln\left[\frac{4D_r t}{r_w^2} - 2\eta\right]} ,$$

where $\eta \approx 0.577216$ is Euler's constant. This solution assumes diffusive heat transport between a constant wellbore temperature T_w and surrounding reservoir rock that starts out at the temperature T_{res} at time zero. It does not take into account any changes in wellbore temperature over time.

D Discretisation and numerical method

The wellbore is specified by the user as a number of straight sections with constant geometry, joined end to end, at various angles to the horizontal. A section is subdivided into smaller subsections for numerical accuracy, as illustrated in Fig. (16).

The user provides the length and properties of each section. The first subsection is assumed to start at $z = 0$, and the node at the top is labelled $n = 0$.

If solving from the top downwards, values P_n and T_n for pressure and temperature are known at node n. Note that when carbon dioxide is present, these variables may be used in both single-phase and two-phase regions, since saturation varies with temperature for a gassy two-phase region. Then it is desired to solve for the next values P_{n+1} and T_{n+1}. A nonlinear Newton-Raphson search method, modified by Armijo's Rule, is used for this search, which varies P_{n+1} and T_{n+1} until momentum and energy values at node $n+1$ match those at node n to within absolute errors of 1.0E-08P_n and 1.0E-09E_n respectively, where E_n is the total energy at node n.

Because of the Newton search, the method is implicit. Because simple arithmetic averages of densities and friction values at the two nodes are used for the region between them, the numerical method is equivalent to an implicit method called the trapezoidal rule. This means the method is second order accurate, and is the most accurate of the second-order A-stable linear multistep methods. It also means the direction of iteration (topdown or bottom-up) should not affect stability.

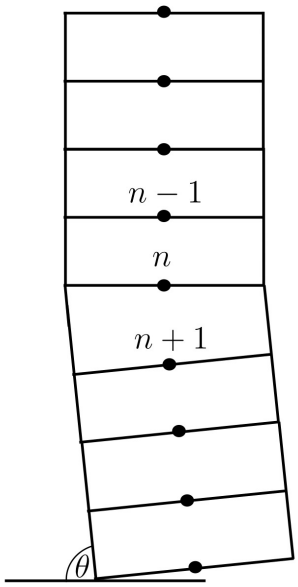

Figure 16: A sketch of two sections of the wellbore set at different angles to the vertical, with subsections.

In particular, integrating equation (5) from node n to node $n+1$, it follows that for constant area A, that is, constant G,

$$\int_{z_n}^{z_{n+1}} \frac{dP}{dz}\, dz = \int_{z_n}^{z_{n+1}} \left(-\frac{d}{dz}[G <v>] + <\rho> g \sin\theta + \phi^2_{\mathrm{FL0}} \left[\frac{dP}{dz}\right]_{\mathrm{L0}} \right) dz \ ,$$

which gives

$$P_{n+1} - P_n = -[G <v>]_{n+1} + [G <v>]_n + \int_{z_n}^{z_{n+1}} \left(<\rho> g \sin\theta + \phi^2_{\mathrm{FL0}} \left[\frac{dP}{dz}\right]_{\mathrm{L0}} \right) dz \ .$$

So far, this is exact for a constant area. Evaluating the integrals of the gravity term and of the friction term is where the approximation is made, and the trapezoidal rule applied to these integrals gives simple averages of the endpoint values. Hence what is implemented in the SwelFlo code is

$$\int_{z_n}^{z_{n+1}} (<\rho> g \sin\theta)\ dz \approx \frac{1}{2} \left([<\rho>]_{n+1} + [<\rho>]_n \right) g \sin\theta\ \Delta z \ .$$

and

$$\int_{z_n}^{z_{n+1}} \left(\phi^2_{\mathrm{FL0}} \left[\frac{dP}{dz}\right]_{\mathrm{L0}} \right) dz \approx \frac{1}{2} \left(\left[\phi^2_{\mathrm{FL0}} \left[\frac{dP}{dz}\right]_{\mathrm{L0}} \right]_{n+1} + \left[\phi^2_{\mathrm{FL0}} \left[\frac{dP}{dz}\right]_{\mathrm{L0}} \right]_{n} \right) \Delta z \ .$$

The momentum flux term needs more careful treatment when area changes. A simple discrete approximation to the momentum flux term is obtained by using the trapezoidal rule on G as

a function of $<v>$:

$$\int_{z_n}^{z_{n+1}} G\frac{d<v>}{dz}\,dz = \int_{z_n}^{z_{n+1}} G\,d<v> = \left(\frac{G_{n+1}+G_n}{2}\right)(<v>_{n+1} - <v>_n)\ .$$

Then the momentum conservation equation becomes, in discrete form, allowing for variable cross sectional area A (and hence variable G):

$$\begin{aligned} P_{n+1} - P_n &= -\left(\frac{G_{n+1}+G_n}{2}\right)(<v>_{n+1} - <v>_n) && (14)\\ &+\frac{1}{2}\left([<\rho>]_{n+1} + [<\rho>]_n\right) g\sin\theta\ \Delta z && (15)\\ &+\frac{1}{2}\left(\left[\phi^2_{\mathrm{FL0}}\left[\frac{dP}{dz}\right]_{\mathrm{L0}}\right]_{n+1} + \left[\phi^2_{\mathrm{FL0}}\left[\frac{dP}{dz}\right]_{\mathrm{L0}}\right]_n\right)\ \Delta z\ . && (16)\end{aligned}$$

Similarly, the energy equation becomes, upon integrating with respect to z,

$$[<h>]_{n+1} - [<h>]_n + [E_k]_{n+1} - [E_k]_n - \frac{1}{2Q}\left([Q_t]_{n+1} + [Q_t]_n\right)\Delta z - g\sin\theta\Delta z = 0\ ,$$

where the flowing enthalpy is

$$<h> \equiv X_{\mathrm{flow}}h_v + (1 - X_{\mathrm{flow}})h_l\ ,$$

and the flowing kinetic energy is

$$E_k \equiv \frac{X_{\mathrm{flow}}}{2}u_v^2 + \frac{1 - X_{\mathrm{flow}}}{2}u_l^2\ .$$

D.1 Newton Step

Given values of pressure and temperature P_n and T_n in node n, the aim is to find values in the next node $n+1$ such that

$$\begin{aligned} F_M(P_{n+1}, T_{n+1}, P_n, T_n) &= 0 && (17)\\ F_E(P_{n+1}, T_{n+1}, P_n, T_n) &= 0 && (18)\end{aligned}$$

where steady-state momentum conservation says

$$\begin{aligned} F_M(P_{n+1}, T_{n+1}, P_n, T_n) \equiv\ & P_{n+1} - P_n + \left(\frac{G_{n+1}+G_n}{2}\right)(<v>_{n+1} - <v>_n)\\ &-\frac{1}{2}\left([<\rho>]_{n+1} + [<\rho>]_n\right) g\sin\theta\ \Delta z\\ &-\frac{1}{2}\left(\left[\phi^2_{\mathrm{FL0}}\left[\frac{dP}{dz}\right]_{\mathrm{L0}}\right]_{n+1} + \left[\phi^2_{\mathrm{FL0}}\left[\frac{dP}{dz}\right]_{\mathrm{L0}}\right]_n\right)\ \Delta z\ , \qquad (19)\end{aligned}$$

and steady-state energy conservation says

$$F_E(P_{n+1}, T_{n+1}, P_n, T_n) \equiv [<h>]_{n+1} - [<h>]_n + [E_k]_{n+1} - [E_k]_n - \frac{1}{2Q}\left([Q_t]_{n+1} + [Q_t]_n\right)\Delta z - g\sin\theta\Delta z \ . \quad (20)$$

In two-phase regions the variables actually used in the Newton step are T and X, although T and P could still be used since there is always carbon dioxide present in the simulated fluid.

The method used is Newton's method in two dimensions, modified by Armijo's Rule. One step of this iterative method is described as follows: an initial guess P^0_{n+1} and T^0_{n+1} at values for P_{n+1} and T_{n+1} is updated to the values

$$\begin{pmatrix} P^1_{n+1} \\ T^1_{n+1} \end{pmatrix} = \begin{pmatrix} P^0_{n+1} \\ T^0_{n+1}) \end{pmatrix} - \lambda J^{-1} \begin{pmatrix} F_M(P^0_{n+1}, T^0_{n+1}, P_n, T_n) \\ F_E(P^0_{n+1}, T^0_{n+1}, P_n, T_n) \end{pmatrix} \quad (21)$$

where the Jacobian matrix J of first partial derivatives is

$$J = \begin{pmatrix} \frac{\partial F_M}{\partial P_{n+1}}(P^0_{n+1}, T^0_{n+1}) \ , & \frac{\partial F_M}{\partial T_{n+1}}(P^0_{n+1}, T^0_{n+1}) \\ \frac{\partial F_E}{\partial P_{n+1}}(P^0_{n+1}, T^0_{n+1}) \ , & \frac{\partial F_E}{\partial T_{n+1}}(P^0_{n+1}, T^0_{n+1}) \end{pmatrix}$$

and where the size of λ, initially one, is halved if the resulting updated values of pressure and temperature do not reduce the values of F_M and F_E to less than their starting values. This reduction by the factor λ is Armijo's Rule, which is described in more detail in the next subsection.

Speed of computation is generally excellent, due in part to initial estimated values of pressure and temperature for the Newton iteration being chosen as linear extrapolations of the previous step, so that often only one or two Newton steps are required. The exception to this is near phase changes. It was found that stepping across a phase change can lead to larger errors than tolerances allow, unless the code automatically reduces subsection size there. So the code reduces step size down to subsections of length just 2cm, at a flash point. The momenta and energies on either side of the flash point are required to match across the flash point, with single-phase values on one side, and two-phase values on the other. For the SwelFlo code, tests show that flash depths are reproducible and are a match, when the same simulation is run topdown and bottom-up, which provides a good test of accuracy and reliability. A good match is also seen between pressures, temperatures and velocities, when comparing topdown and bottomup simulations. Accurate flash-point determination is important for pressure matching, and 2cm gives an accuracy of better than about 200 Pa.

D.2 Modified Newton with Armijo Rule

This is a summary of the modified Newton method that has been developed to solve for T and X_{flow} that satisfy the conservation equations in the next node, for two-phase flow in the

well. The reason for the modification is that occasionally the Newton search for a solution to the conservation equations gets stuck in a two-cycle, stepping over the region where the solution is, especially for the Hadgu correlation at the change from churn flow to transition, where there may be large changes in slope of the curve of vapour phase velocity versus saturation. This behaviour is analogous to the one-dimensional behaviour of Newton's method when trying to find the root of tanh(x)=0, if one starts with too large an x value — it steps further and further away from the solution x=0.

The idea is to use Newton's method to find the direction to step (say in (T, X_{flow}) space for two-phase flow), but then to backtrack: check the size $|f|$ of the error vector (with components being the change in energy and the change in momentum) after stepping and ensure this size reduces from the current value before accepting the Newton step. If the size does not reduce, the length of the step is halved but the Newton direction is retained (we backtrack), and the size $|f|$ checked again. This halving and checking is repeated until a smaller size is achieved. This works for the tanh function, and fixes the issue with rapid changes in the slope of the energy difference [23, pp. 169 ff].

If F_E and F_M are the errors in energy conservation and momentum conservation respectively, and it is desired to have these less than Entol and Momtol respectively, and if x is the vector (T, X_{flow}) in a two-phase region, or the vector (T, P) in a single-phase region, then the method is [23]:

Newton Method with Backtracking and the Armijo Rule:

Set

$$r_0 = |f(x)| \equiv \sqrt{\frac{F_M^2}{\text{Momtol}^2} + \frac{F_E^2}{\text{Entol}^2}} \, .$$

Entol and Momtol are used to normalize or weight the momentum and energy differences so they have equal influence on the size of f. Hence the critical value it is desired to reduce $|f|$ to is $\sqrt{2}$.

§ While $|f(x)| > \tau_r r_0 + \tau_a$, where τ_r is a relative error and τ_a is an absolute error (we will choose $\tau_a = \sqrt{2}$ and $\tau_r = 0$), we do the following to take one modified Newton step, where f' is the gradient of f:

If $|f'(x)| < 10^{-20}$ exit and try reducing subsection size.

Choose search direction $d = -\frac{f(x)}{(f'(x)}$, the Newton step direction.

† Set $\lambda = 1$.

Set $x_t = x + \lambda d$, a trial point in the Newton direction

If $|f(x_t)| < (1 - \alpha\lambda)|f(x)|$ then set $x = x_t$, accepting this step, else set $\lambda = \lambda/2$ and go to † again.

Once the step is accepted, this entire process is repeated from §. Typically α is set to 10^{-4}. The process will stop when $|f|$ is small enough; in practice a limit of 50 is placed on the total

number of § iterations allowed. The process is linear until it steps close enough to the root, then it is quadratic as Newton's method is.

E Conservation equations at Feedzones

The sign convention is for positive flow values for production (hence Q is positive for flow up a wellbore, and for flow into a well from the reservoir at a feed). At a feedpoint, which the code ensures occurs at a node, a virtual node is added at the same depth, in which to mix any incoming fluid with the wellbore fluid. Mixing is assumed to occur at the wellbore pressure, such that flowing enthalpy is conserved, and any inertial effect of influx or efflux of fluid at a feed is not known. Then with regard to the sketch in Fig. (17), conservation of mass of water at a feed at node n takes the form

$$Q_{n+1} = Q_n - Q_f \ .$$

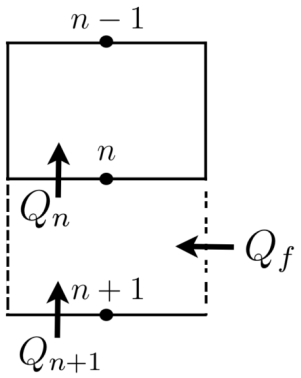

Figure 17: A sketch of a section of the wellbore with a feed at the depth of node n for a topdown simulation. An extra node of zero volume is added between node n and $n+1$, in which to mix any incoming reservoir fluid, at the wellbore pressure P_n.

Details on how the flowrate Q_f is computed, for single and two-phase flow, are to be found in subsection (4.8). Four different types of flow response computations are offered at a feed, productivity index, fixed flowrate, dry steam, and linear or quadratic drawdown.

While the above equation holds no matter what the signs of the flows, the values of XCO2 (carbon dioxide mass fraction) and flowing enthalpy <h> of the fluid in the unknown node $n+1$ do depend (in the same way) on flow directions. There are six different possibilities, illustrated in Fig. (18):

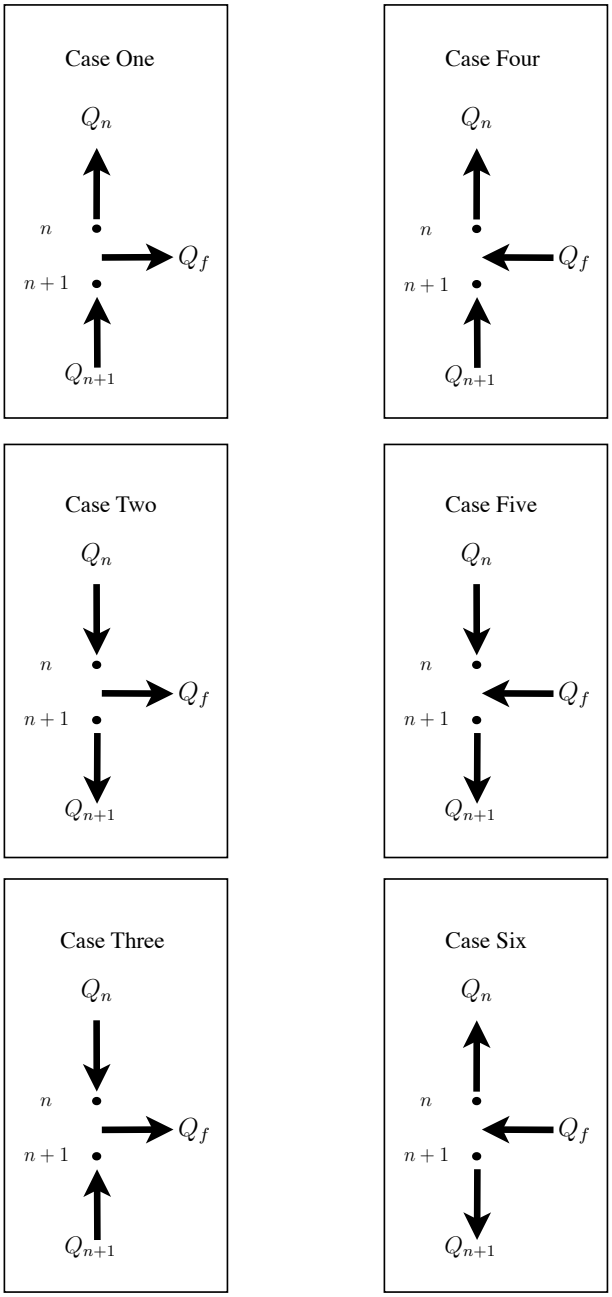

Figure 18: A sketch showing the six different flow situations that are possible at a feed point. The arrows in this figure show the *actual* directions of flow, rather than the conventional directions for positive flow values.

In Cases Three, Four and Five, conservation of carbon dioxide across a feed when the overall mass fraction is XCO2, takes the form

$$Q_{n+1}\mathrm{XCO2}_{n+1} = Q_n\mathrm{XCO2}_n - Q_f\mathrm{XCO2}_f \ ,$$

where the subscript f refers to the properties of fluid flowing between reservoir and wellbore, and the flowing fluid enthalpy takes exactly the same form in these three cases,

$$Q_{n+1} <h>_{n+1} = Q_n <h>_n - Q_f <h>_f \ ,$$

and all enthalpies are flowing enthalpies rather than static enthalpies. No distinction is made between flowing and static enthalpy for any reservoir fluid entering at the feed. The fluid in node $n+1$ is then reverse engineered as necessary to find a new temperature that corresponds to the new values of flowing enthalpy and XCO2.

While no account is taken of the kinetic energy of any incoming reservoir fluid, the kinetic energy of the up-flowing mixture is accounted for, in the next energy balance.

In the other Cases One, Two and Six, the values of $<h>$ and XCO2 must all be the same, before and after the feed. For a topdown or a bottom-up simulation, this makes Case Six problematic, unless the user ensures that the values before the feed match the reservoir values, because there is otherwise a contradiction between the required values from the reservoir and the actual values set. The simulator continues past such a case, by assuming that the fluid entering from the reservoir is consistent with the fluid before the feed, even if it is not set up that way. A warning is issued. Cases One and Two are OK since the feed injects the wellbore fluid into the reservoir, and there is no physical contradiction if the injected fluid properties do not match the reservoir fluid properties.

F Correlations

The algorithms used in SwelFlo, to implement the correlations, are described in more detail in this section. The original correlation publications were consulted, and coded from scratch. The simulator needs values for vapor or liquid phase velocity, given pressure, temperature or enthalpy, gas fraction, and flowing steam quality. Saturation (or equivalently vapour phase velocity) is provided by the correlation. Correlations are a short-cut, accounting for the effect of interfacial terms in the momentum and energy conservation equations when they are written in terms of the individual phases, then added together to get simpler and fewer equations for total amounts.

F.1 Armand correlation

The Armand correlation requires a knowledge of β to compute void fraction α from the Armand coefficient C_A using $\alpha = C_A\beta$, where β is the volumetric gas flow ratio (volume of

vapour per second divided by the total volume flow rate), which can be written as

$$\beta = \left[1 + \left(\frac{1 - X_{\text{flow}}}{X_{\text{flow}}}\right)\frac{\rho_v}{\rho_l}\right]^{-1} . \tag{22}$$

Then the velocity ratio is calculated from

$$K = \left(\frac{X_{\text{flow}}}{1 - X_{\text{flow}}}\right)\left(\frac{1-\alpha}{\alpha}\right)\left(\frac{\rho_l}{\rho_v}\right) . \tag{23}$$

Then

$$u_v = \frac{Q}{A}\left[\frac{X_{\text{flow}}}{\rho_v} + \frac{K(1 - X_{\text{flow}}}{\rho_l}\right] \tag{24}$$

and

$$u_l = u_v/K$$

give the phase velocities required.

There are a number of typos, in GWELL Table 4.3 as well as in Chisholm Table 4.4. A corrected version of these tables is presented in Table 4 for clarity. D is wellbore diameter, and negative signs are chosen for downflow, positive signs for upflow. The terms v_v and v_l represent specific volumes, $v_v = 1/\rho_v$ and $v_l = 1/\rho_l$. The drift velocity is

$$u_{WD} = u_v - u_H = \frac{Q}{A}\left(\frac{1 - X_{\text{flow}}}{\rho_l}\right)(K - 1) .$$

GWELL mistakenly uses the slip velocity in place of the drift velocity in the Fortran code, and replaces the specific velocity U_{SL} in the last line of the table with the liquid viscosity μ_l, in the Fortran code and in the GWELL manual.

Note that if $\beta < 0.9$, we need the drift velocity to apply the correlation, and we need K to find drift velocity, but K depends on saturation S. That is, C_A depends on both S and β. So the formula

$$S = \beta C_A(\beta, S)$$

defines saturation implicitly in terms of β. In this range of β, we want to find saturation, but we need saturation to apply the correlation.

If $\beta > 0.9$, we need the specific velocity $U_{SL} = (1 - X_{\text{flow}})Q/(A\rho_l)$ to compute C_A. This can be done without knowing saturation.

GWELL deals with the implicit nature of the Armand correlation by first estimating saturation by using $C_A = C_{Ah}$, then computing $S_1 = C_A\beta$. Then GWELL calculates a value for $K = K_1$ using this value of saturation. This value for K is then used to compute C_A from the table.

Chisholm deals with the implicit nature of the correlation by using Labuntsov's correlation to find the drift velocity without needing to know saturation. Chisholm summarises it on his p.49,

$$U_{WD} = u_b W_D$$

β	θ	Equations
< 0.9	horiz (0°)	$C_{Ah} = \left[\beta + \frac{1-\beta}{\sqrt{1-\beta(1-v_l/v_v)}}\right]^{-1}$ (Chisholm eqn (4.59) is correct)
	vert (90°)	If $U_H > \frac{U_{WD}\, C_{Ah}}{1-C_{Ah}}$, then $C_{Av} = C_{Ah}$.
		If $U_H < \frac{U_{WD}\, C_{Ah}}{1-C_{Ah}}$, then $w = 1.4\left(\frac{v_v}{v_l}\right)^{0.2}\left(1-\frac{v_l}{v_v}\right)^5$, and: If $D > 19\left(\frac{\sigma v_l}{g(1-v_l/v_v)}\right)^{\frac{1}{2}}$ then $C_{Av} = \left[1 \pm \frac{1.53w}{U_H}\left(\frac{g(v_v-v_l)v_l\sigma}{v_v}\right)^{\frac{1}{4}}\right]^{-1}$, else $C_{Av} = \left[1 \pm \frac{0.35w}{U_H}\left(gD(1-v_l/v_v)v_v\right)^{\frac{1}{2}}\right]^{-1}$.
	All	$C_A = C_{Ah} + (C_{Av} - C_{Ah})\left(\frac{\sin(1.8\theta) - [\sin^3(1.8\theta)]/3}{0.3}\right)$
> 0.9	All	$C_A = \left[1 + \frac{23}{u_H}\left(\frac{\mu_l U_{SL} v_v}{D}\right)^{\frac{1}{2}}\left(1-\frac{v_l}{v_v}\right)\right]^{-1}$

Table 4: Equations for the Armand Coefficient, a corrected version of Table 4.3 in the GWELL manual, and of Table 4.4 in Chisholm [10]. θ is the angle to the horizontal, in degrees, non-negative. Where there is a $\pm$ sign, the negative sign is to be used for downflow.

where

$$W_D \equiv 1.4\left(\frac{\rho_l}{\rho_v}\right)^{0.2}\left(1-\frac{\rho_v}{\rho_l}\right)^5$$

and the bubble velocity is computed as a slug velocity for small enough wellbore diameter, or as the usual bubble velocity for larger diameters:

$$u_b = \begin{cases} 1.53\left(\frac{g\sigma(\rho_l-\rho_v)}{\rho_l^2}\right)^{0.25}, & D \geqslant D_c \\ 0.35\sqrt{gD(1-\rho_v/\rho_l))}\,, & D < D_c \end{cases},$$

where the critical diameter is

$$D_c = 19.10938775\left(\frac{\sigma}{g(\rho_l-\rho_v)}\right)^{0.5}$$

and the value of 19 is refined here to 19.10938775 to give better continuity in u_b when D passes through the value D_c.

Typos in Chisholm include that the first line in his Table 4.4 should have β instead of the value 0.7, and eqn (4.72) should read

$$3.333(\sin(1.8\theta) - 0.333(\sin(1.8\theta))$$

(he has the sign wrong on the second term), and in his Table 4.4, the formula for C_A for all inclinations when $\beta < 0.9$ should read

$$C_A = C_{Ah} + (C_{Av} - C_{Ah})\left(\frac{\sin(1.8\theta) - [\sin^3(1.8\theta)]/3}{0.3}\right)$$

that is, the first minus sign in Chisholm's formula should be a plus sign (or the subscripts on C_A should be reversed in the first set of parentheses).

However, simulations sometimes failed to converge when using the Armand correlation as summarised above, that is, they sometimes failed to find sufficiently accurate approximations to the conservation equations. This is due to the discontinuous nature of the correlation, which is illustrated in Fig (19) obtained by solving the Armand correlation to relate S and β, for a well of radius 0.026m at a pressure of about 1 bara and temperature 100°C, for various total mass flow rates.

It is the jump at $\beta = 0.9$ that gives the trouble. This is where Chisholm suggests switching to the Zuber and Findlay correlation for annular flow, and there is no attempt to ensure this switch is a continuous one. A possible fix would be to smooth the region where $\beta > 0.9$ with a straight line.

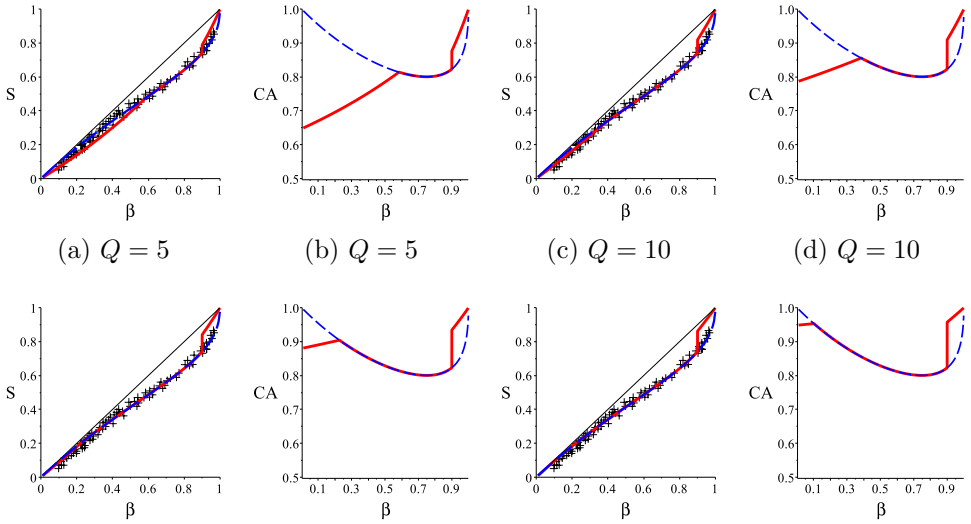

(a) $Q = 5$ (b) $Q = 5$ (c) $Q = 10$ (d) $Q = 10$

(e) $Q = 20$ (f) $Q = 20$ (g) $Q = 50$ (h) $Q = 50$

Figure 19: Plots of saturation $S = \beta C_A(S_0, \beta)$ versus volume flowrate β, and of the Armand coefficient C_A versus β, for Armand's correlations, for various values of Q. The line $S = \beta$ is included for comparison in the S vs β plots. The data points are Armand's experimental data, scanned from Chisholm's book. The solid line is the correlation given in Table 4. The dashed line is the simpler correlation $C_A = C_{Ah}$. Pressure is set to one bar, and wellbore radius to 26 mm, as in Armand's experiments.

However, the most straightforward fix for the jump in the Armand correlation, suggested by the good fits to the Armand data, is to use the simple formula $C_A = C_{Ah}$ given in equation (4.59) in Chisholm, which gives

$$S = \frac{\beta}{\beta + F} \tag{25}$$

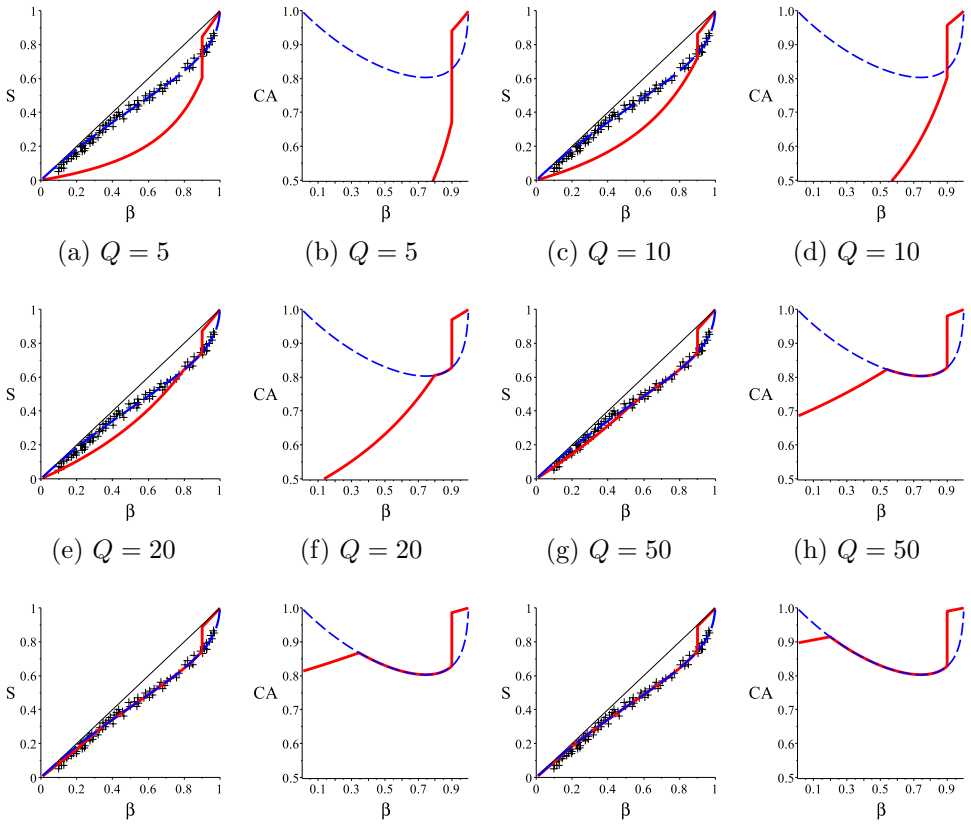

(a) $Q = 5$ (b) $Q = 5$ (c) $Q = 10$ (d) $Q = 10$

(e) $Q = 20$ (f) $Q = 20$ (g) $Q = 50$ (h) $Q = 50$

(i) $Q = 100$ (j) $Q = 100$ (k) $Q = 200$ (l) $Q = 200$

Figure 20: Plots of saturation $S = \beta C_A(S_0, \beta)$ versus volume flowrate β, and of the Armand coefficient C_A versus β, for Armand's correlations, for various values of Q. The line $S = \beta$ is included for comparison in the S vs β plots. The data points are Armand's experimental data, scanned from Chisholm's book. The solid line is the correlation given in Table 4. The dashed line is the simpler correlation $C_A = C_{Ah}$. Pressure is set to 10.4 bar, and wellbore radius to 0.1m.

where

$$F = \frac{1-\beta}{\sqrt{1-\beta\left(1-\frac{\rho_v}{\rho_l}\right)}}$$

which as illustrated in Fig. (19) is a very close match to the detailed Table (4) results over a wide range of flowrates and wellbore conditions, for $\beta < 0.9$. It is also seen to provide a good match to Armand's data. Since this excellent fit also behaves smoothly near $\beta = 0.9$, this is what is adopted in SwelFlo — the simple formula 25.

F.2 Orkiszewski Correlation

The Orkiszewski correlation provides a different way to get saturation S, given β or X_{flow}.

Orkiszewski's correlation [29] starts out assuming that β (and temperature) is known, and from that value it finds liquid and vapour phase velocities. Then saturation can be computed.

$S(\beta)$ is given by the following (Orkiszewski) procedure:

1. start with a value for X_{flow}, and we also know the temperature and pressure;
2. compute

$$\begin{aligned}
\beta &= \frac{X_{\text{flow}} v_G}{X_{\text{flow}} v_G + (1-X_{\text{flow}}) v_L} , && (26)\\
\alpha &= \frac{(1-X_{\text{flow}}) v_L}{X_{\text{flow}} v_G} , && (27)\\
v_{gD} &= \frac{X_{\text{flow}} G}{\rho_v}\left(\frac{\rho_l}{g\sigma}\right)^{0.25} , && (28)\\
v_T &= \frac{G}{\rho_l - \beta(\rho_l - \rho_v)} = G\left(\frac{X_{\text{flow}}}{\rho_v} + \frac{1-X_{\text{flow}}}{\rho_l}\right) , && (29)\\
L_B &= \max(1.071 - \frac{0.7275 v_T^2}{D},\ \ 0.13) , && (30)\\
L_S &= 50.0 + 36.0 v_{gD}\alpha , && (31)\\
L_M &= 75.0 + 84.0(v_{gD}\alpha)^{0.75} , && (32)\\
U_{B1} &= 1.53\left(\frac{g\sigma(\rho_l - \rho_v)}{\rho_l^2}\right)^{0.25} , && (33)\\
U_S &= 0.35\sqrt{gD(1-\rho_v/\rho_l))} , && (34)
\end{aligned}$$

where σ is surface tension, D is wellbore diameter, v_L is specific volume (one over density) of liquid, and v_G is specific volume of the gaseous phase.

3. Then if $\beta < L_B$, the regime is bubble flow; set $u_v = v_T + U_{B1}$, and

$$S = \frac{GX_{\text{flow}}}{u_v \rho_v} \ ,$$

4. Otherwise if $\beta \geq L_B$ and $v_{gD} < L_S$, the regime is slug.

   To get a smooth and monotonic function S of β, there needs to be a transition region between this and the bubble regime, called bubble-slug. It is not enough to simply set the vapour velocity to transit linearly from bubble to slug values, say as β goes from $0.9L_B$ to $1.1L_B$, since although this gives a continuous transition in vapour relative velocity, it does not always give a monotonic $S(\beta)$. This can lead to discontinuous jumps in saturation S, and consequential failure to converge when searching for values of T and X that conserve mass, momentum and energy.

   The resolution of this issue in this regime is to find the value β^* for which the implicit relationship $\beta = L_B$ holds (this relationship is illustrated as the intersection of $y = \beta$ and $y = L_B$ in Fig. (21)), and to use this value β^* to compute X_{flow}, v_T, and $u_v = v_T + U_{B1}$, and use these to calculate $S(\beta^*)$.

   As parameters like flowrate are varied, the piecewise defined curve for L_B changes, keeping the level part at 0.13, but the parabolic part moves back and forth. Hence solutions to $\beta = L_B$ vary between 0.13 and 1.0.

   Then we set a transition region with a slightly positive slope SL, using the equation

$$S_{\text{bu-sl}} = S(\beta^*) + SL(\beta - \beta^*) \ .$$

   S_{slug} in the slug regime is also determined, by $u_v = v_T + U_S$ and $S_{\text{slug}} = \frac{GX_{\text{flow}}}{u_v \rho_v}$. The extent of the transition region is determined by the inequality

$$S_{\text{bu-sl}} > S_{\text{slug}} \ .$$

   That is, while this inequality holds, the value of S output is $S_{\text{bu-sl}}$; otherwise (for β large enough) this inequality ceases to hold, and the regime is slug flow with S output as S_{slug}.

   Note that experience shows that it is best if the slope SL is not too small, as rapid changes in vapour phase velocity can then result at saturations near bubble-slug transition. These cause apparently random convergence issues with the Newton step for solving the conservation equations, depending on whether this transition region is encountered or not. In practice a value of 0.3 is found to give reasonably smooth curves, without the sharp kink seen in Fig. (23) with a value of 0.01.

5. Otherwise if $L_S \leq v_{gD} \leq L_M$, the regime is transition (to mist or annular flow), with relative velocity of vapour changing linearly in v_{gD} from slug value to zero. The

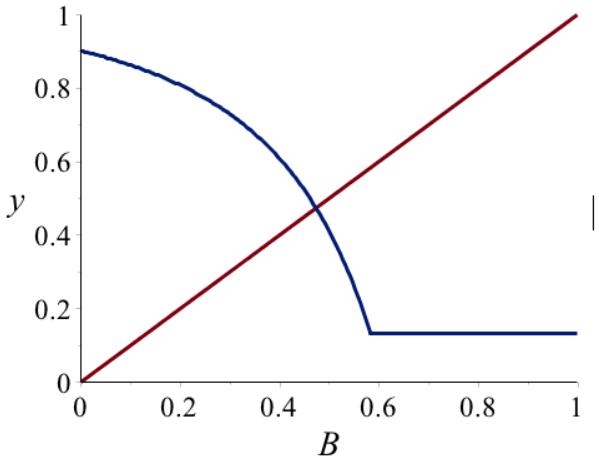

Figure 21: An illustration of finding β^* where $y = \beta$ and $y = L_B$ intersect, plotted against β for particular values of densities and flowrates.

calculations made are:

$$\text{ratio} = \frac{L_M - v_{gD}}{L_M - L_S} , \tag{35}$$

$$u_v = v_T + \text{ratio} \cdot U_S , \tag{36}$$

$$S = \frac{GX_{\text{flow}}}{u_v \rho_v} . \tag{37}$$

6. Otherwise, the regime is mist, with $u_v = v_T$ since both phases move at the same speed, and

$$S = \frac{GX_{\text{flow}}}{u_v \rho_v} .$$

An illustration of how the fluid looks in the four flow regimes (bubble, slug, transition, mist), in a snapshot view of the flow, taken from [29], is presented in Fig. (22).

The result of applying this procedure is illustrated in Fig. (23) — note that the transition regions are small but necessary to ensure a smooth and monotonic dependence of saturation on β.

Note that there is no attempt in the Orkiszewski correlations to account for the deviation of the well from vertical. The correlations are vertical ones. Subsequent studies of inclined flows suggest this is OK for angles up to 20 or 30° from vertical. Further inclination towards horizontal tends in practice to remove the bubble regime, as bubbles tend to hit the upper casing surface and coalesce, and this is not reflected in the Orkiszewski correlation.

Counterflow, where vapour flows upwards and liquid downwards, as in a heatpipe setup, is not accounted for in this formulation either (except in the slug regime), since it would give negative β values, and flowing enthalpy/dryness would depend on which end of the well was being considered.

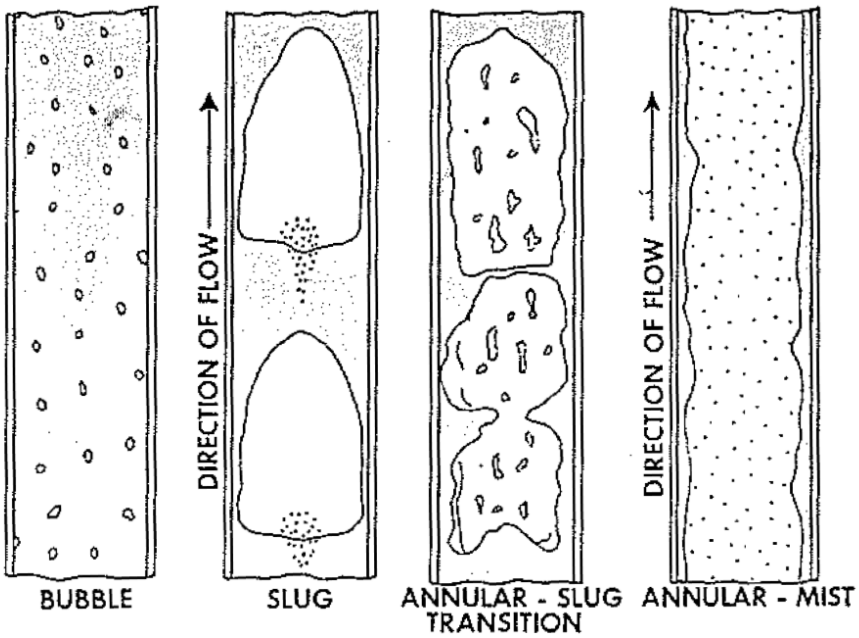

Figure 22: An illustration of the four flow regimes in the Orkiszewski correlation, taken from his paper [29].

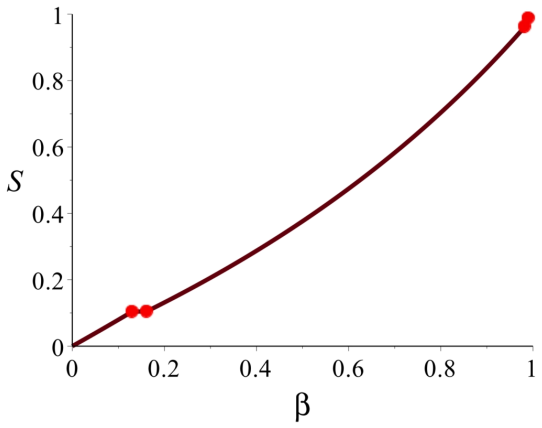

Figure 23: An illustration of the Orkiszewski correlation, showing saturation S as a function of volumetric gas flow β, for a flow of 20 kg/s and fluid properties corresponding to pressure 23 bara and temperature 215°C. The four red disks show the places where bubble changes to bubble-slug, then to slug, then to transition, and finally to mist as β increases. The bubble-slug transition region slope used was $SL = 0.01$.

F.3 Hadgu Correlation

The Hadgu Correlation [20] is described in detail in [19]. It is likely to be the main correlation in WELLSIM. This section summarises the equations comprising the correlation, as coded into SwelFlo. It affects the shapes of the regions describing the nature of the flow in the wellbore (bubble, slug, churn, annular), and the relative velocities of vapour and liquid phases in those regions.

The option "Hadgu v only' means the forward Hadgu correlation is used to calculate the velocities of vapor and liquid phases, depending on the flow regime. This is in contrast to the option "Full Hadgu", where in addition the Hadgu correlations affect the computation of momentum balance or pressure gradient, by using frictional pressure drop formulae from Hadgu's thesis, that differ from Chisholm's modified Martinelli formulae that are used for the Armand and Orkiszewski correlations, and when "v only" options are chosen.

F.3.1 Phase Velocities

The correlations that determine vapor and liquid phase velocities in line with Hadgu's thesis [19] are described here. These correlations are invoked by choosing "Hadgu v only" in the correlation text box in the Input tab. This choice leaves the momentum formulae unchanged from those described in subsection C.3.

First we describe the forward problem, with saturation (a static property) given, and with flowing steam quality to be determined (by using phase velocities). Given the criteria on saturation that Hadgu uses to distinguish flow regimes, the forward problem can be easily set up with no iteration required to solve.

Then since in fact we have flowing steam quality, and we need saturation values, we call the direct problem iteratively to solve the inverse problem of finding saturation given flowing steam quality.

F.3.2 Bubble Flow

Hadgu's equation (7.36) is obtained by using bubble-rise velocities where buoyancy is balanced by a nonlinear drag term, then modified to allow for variations across the radius of the wellbore, and it reads:

$$U_{SL} = -U_{SG}\left(1 - \frac{1}{1.25\alpha}\right) - \frac{1.53}{1.25}(1-\alpha)^{1.5}\left(\frac{g\Delta\rho\sigma}{\rho_l^2}\right)^{0.25}, \tag{38}$$

where σ is surface tension, and $\Delta\rho = \rho_l - \rho_v$.

In the forward problem, we know at each step what the in place dryness or the static saturation is, so from eqn (3) we know what the saturation α is, and we know what Q is

(total mass flowrate, kg/s), so we rearrange eqn (38) using

$$U_{SG} = \frac{G - \rho_l U_{SL}}{\rho_v} \ , \quad \text{where } G \equiv \frac{Q}{A} \tag{39}$$

to obtain an explicit formula for the liquid velocity:

$$U_{SL}\left[1 - \frac{\rho_l}{\rho_v}\left(1 - \frac{1}{1.25\alpha}\right)\right] = -\frac{G}{\rho_v}\left(1 - \frac{1}{1.25\alpha}\right) - \frac{1.53}{1.25}(1-\alpha)^{1.5}\left(\frac{g\Delta\rho\sigma}{\rho_l^2}\right)^{0.25} \ . \tag{40}$$

Transition from (elongated) bubble to slug flow is taken to occur when $\alpha = 0.3$, that is, for smaller void fractions we have bubble flow, transitioning to slug as α increases through the value 0.3. This gives the approximate condition

$$U_{SL} = 1.67U_{SG} - 0.72\left(\frac{g\Delta\rho\sigma}{\rho_l^2}\right)^{0.25} \ , \tag{41}$$

but since we start out by knowing α, it is simpler to check whether it is greater than 0.3 or not.

F.3.3 Slug Flow

Slug flow is considered to hold for S between 0.3 and 0.52. Hadgu considers the rise velocity of a Taylor bubble, with wall drag near the bubble being the dominant factor, and uses the treatment of Fernandes et al [16], developed from a combination of analytical work and experimental data. Many of the variables which appear in this subsection are illustrated in Fig. (24).

In summary, the rise velocity of a Taylor bubble in an infinite medium is calculated as

$$U_\infty = 0.345\left(\frac{Dg\Delta\rho}{\rho_l}\right)^{0.5} \ , \tag{42}$$

where D is the casing inner diameter; the translational velocity U_N of a Taylor bubble is related to the superficial vapour and liquid velocities by

$$U_N = 1.29(U_{SG} + U_{SL}) + U_\infty \ ;$$

the rise velocity of bubbles in the liquid slug is (as was used in the bubble phase also):

$$U_0 = 1.53\left(\frac{g\Delta\rho\sigma}{\rho_l^2}\right)^{0.25}(1-\alpha_{LS})^{0.5} \ ,$$

where $\alpha_{LS} = 0.3$; the velocity of the liquid film around the Taylor bubble is

$$U_{LTB} = 9.916(gD(1-\sqrt{\alpha_{TB}}))^{0.5} = 9.9498\sqrt{r} \ ,$$

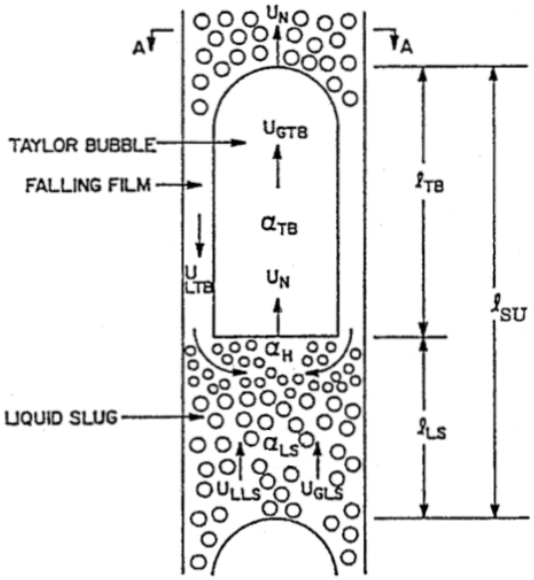

Figure 24: A slug unit, taken from Hadgu's PhD thesis, his Fig. 7.5

where D is wellbore inner diameter; the average velocity of the liquid in the slug is

$$U_{LLS} = U_N - (U_N + U_{LTB}) \left(\frac{1 - \alpha_{TB}}{1 - \alpha_{LS}} \right) \ ;$$

the average velocity of the bubbles in the liquid slug is

$$U_{GLS} = U_{LLS} + U_0 \ ;$$

the average velocity of the gas in Taylor bubbles is

$$U_{GTB} = U_N - (U_N - U_{GLS}) \frac{\alpha_{LS}}{\alpha_{TB}} \ ;$$

the ratio of Taylor bubble length to slug length is

$$\beta = \frac{U_{SG} - \alpha_{LS} U_{GLS}}{\alpha_{TB} U_{GTB}} \tag{43}$$

and the volume average void fraction is

$$\alpha_{SU} = \beta \alpha_{TB} + (1 - \beta) \alpha_{LS} \ . \tag{44}$$

Equation (43), given that $\alpha_{LS} = 0.3$ and $\alpha_{TB} = 0.89$, gives β as a function of the superficial liquid and vapour phase velocities. Then equations (42) through to (44) provide a recipe for going forwards from superficial liquid and vapour phase velocities to saturation $S \equiv \alpha_{SU}$.

The forward problem to be solved is to find the phase velocities, given static dryness X, pressure, temperature and total flowrate. The flow Q may be used as in eqn (39) to eliminate U_{SG}. Then eqn (43), through its dependence on U_N in numerator and denominator, gives β as a ratio of linear functions of the (superficial) liquid phase velocity U_{SL}. The known (in place) dryness X gives an independent value for volume-averaged void fraction (or saturation)

$$\alpha_{SU} = \frac{X\rho_l}{X\rho_l + (1-X)\rho_v} \ . \tag{45}$$

Combining eqns (44) and (45) allows to express β in terms of in place dryness X. Then eqn (43) can be rearranged after some algebra to give an explicit expression for U_{SL}, for slug flow, as a function of dryness X or saturation S. This result is summarised below:

$$\begin{aligned}
U_{SL} &= \frac{\beta A_5 + A_6}{1.29\Delta\rho A_4 - \rho_l} \ , \quad \text{where} && (46)\\
A_6 &= \alpha_{LS}\rho_v(U_0 + U_\infty A_1 - U_{LTB}A_3) - G(1 - 1.29\alpha_{LS}A_1) && (47)\\
A_5 &= 1.29G(\alpha_{TB} - \alpha_{LS}A_3) + \alpha_{TB}U_\infty\rho_v(A_1 + A_2A_3) + && (48)\\
&\quad +U_0\rho_v\alpha_{LS} - U_{LTB}\rho_v\alpha_{LS}A_3 && (49)\\
A_4 &= \beta\alpha_{TB}(A_1 + A_2A_3) + \alpha_{LS}A_1 && (50)\\
A_3 &= \frac{1-\alpha_{TB}}{1-\alpha_{LS}} && (51)\\
A_2 &= 1 - \left(\frac{\alpha_{LS}}{\alpha_{TB}}\right) && (52)\\
A_1 &= 1 - A_3 && (53)\\
\beta &= \left(\frac{\alpha_{SU} - \alpha_{LS}}{\alpha_{TB} - \alpha_{LS}}\right) && (54)\\
\alpha_{SU} &= \frac{X\rho_l}{X\rho_l + (1-X)\rho_v} && (55)\\
G &= \frac{Q}{A} && (56)\\
U_{LTB} &= 9.916[gD(1 - \sqrt{\alpha_{TB}})]^{0.5} && (57)\\
U_0 &= 1.53\left(\frac{g\Delta\rho\sigma}{\rho_l^2}\right)^{0.25}(1-\alpha_{LS})^{0.5} && (58)\\
U_\infty &= 0.345\left(\frac{Dg\Delta\rho}{\rho_l}\right)^{0.5} && (59)\\
\alpha_{TB} &= 0.89 && (60)\\
\alpha_{LS} &= 0.3 && (61)\\
& && (62)
\end{aligned}$$

and then the gas velocity can be calculated from

$$U_{SG} = \frac{G}{\rho_v} - \frac{\rho_l}{\rho_v}U_{SL} \ .$$

F.3.4 Churn flow

The churn flow region is a relatively narrow one, sometimes called transition. The boundary between slug and churn is given by $\alpha = 0.52$, and

$$2\left[\frac{0.4\sigma}{\Delta\rho g}\right]^{0.5}\left(\frac{\rho_l}{\sigma}\right)^{3/5}\left[\frac{0.092}{D}\left(\frac{\rho_l D}{\mu_l}\right)^{-0.2}\right]^{0.4} U_T^{1.12} = 0.725 + 5.15\alpha_H^{0.5} \ ,$$

which can be solved to find a value for U_T, where $U_T = U_{SG} + U_{SL}$. The boundary between dispersed bubble and churn is simply $\alpha = 0.52$. Hadgu has mixed notations here, with α_H being a flowing void fraction which I call β (consistent with [6]), while $\alpha = 0.52$ in [6] is the usual static void fraction. Yet Hadgu sets $\alpha_H = \alpha$ in his criteria for transition.

This does not matter much, since no correlations are given in Hadgu's thesis for churn flow. He uses slug flow parameters for pressure drop calculations, so this is what we use for calculating relative speeds of liquid and vapour — we use the slug flow correlations.

F.3.5 Annular or mist flow

The transition from churn to annular or mist flow is given by $U_{SG}^* > 1.0$, where

$$U_{SG}^* = U_{SG}\left[\frac{\rho_v}{gD\Delta\rho}\right]^{0.5} \ .$$

In the annular flow regime, Hadgu chooses the Baroczy correlation

$$\alpha = \left[1 + \left(\frac{1 - X_{\text{flow}}}{X_{\text{flow}}}\right)^{0.74}\left(\frac{\rho_v}{\rho_l}\right)^{0.65}\left(\frac{\mu_l}{\mu_v}\right)^{0.13}\right]^{-1} \ , \tag{63}$$

which we rearrange to find flowing dryness in terms of saturation α,

$$X_{\text{flow}} = \frac{1}{C+1} \tag{64}$$

$$C = \left(\frac{1-\alpha}{B\alpha}\right)^{1.35} \tag{65}$$

$$B = \left(\frac{\rho_v}{\rho_l}\right)^{0.65}\left(\frac{\mu_l}{\mu_v}\right)^{0.13} \ . \tag{66}$$

The way to implement this is to first compute X_{flow} from the above equations; then combine equations (23) and (24) to get u_v from

$$u_v = \frac{QX_{\text{flow}}}{\alpha A\rho_v} \ . \tag{67}$$

Then use $U_{SG} = \alpha u_v$. Then compute U_{SG}^* and if it is less than or equal to one it is slug flow. If $U_{SG}^* > 1$, it is mist flow, and $U_{SL} = G/\rho_l - U_{SG}\rho_v/\rho_l$. Implementation will run fast since it is explicit in saturation, and does not need iteration to solve.

F.3.6 Implementation of Hadgu Correlation

When the results of the above correlation are plotted in the form of U_{SL} versus S, as in Figs. (25) and (26), a couple of difficulties are apparent. The different regimes do not connect smoothly, and the dependence of U_{SL} on S is not monotonic, so that this function cannot be inverted unless the dependence is forced to be monotonic by introducing transitions between flow regimes.

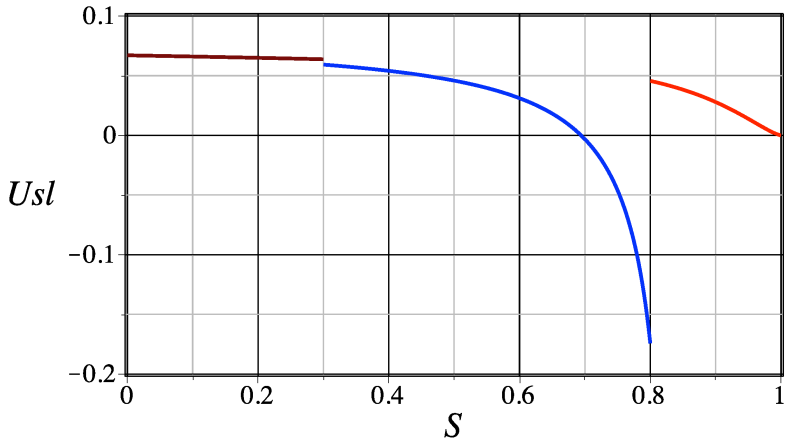

Figure 25: An example of U_{SL} versus saturation for the Hadgu correlation with very small flowrate, when $G = 54$, $T = 246°\text{C}$. The leftmost brown curve is bubble flow, the middle blue curve is slug and churn, and the rightmost red curve is for mist flow.

There is a jump at the transition between bubble and slug flow, which may cause issues when trying to conserve energy and momentum near here. This is smoothed by inserting a bubble-slug transition, in the range $S = (0.28, 0.32)$. U_{SL} is set to a linear function of S between these values, moving smoothly from bubble to slug regions.

The jump from negative U_{SL} values in slug flow to positive values in mist flow is more problematic, and occurs at physical S values for very low flow rates. The condition that the mist value of $U^*_{SG} > 1.0$ is sometimes not met until saturation reaches values where slug values of U_{SL} become negative, or sometimes is not met for any real values of saturation. This, and smaller jumps seen at higher flowrates, are removed by introducing another linear transition region, called *transition*, between slug (churn) and mist flow. The right-hand end of the transition region is given by the mist flow values for which $U^*_{SG} = 1.0$, say S^* and U^c_{SL}. The left-hand end of the transition region we choose to have a slug flow value U_{SL} that is a little greater than U^c_{SL}, that is, that $U_{SL} = U^c_{SL} + \delta$, where $\delta = 0.01$. Then the forward problem is solved to find the corresponding value S^c for S. The transition region is the straight line connecting $(S^c, U^c_{SL} + \delta)$ to (S^*, U^c_{SL}).

For very small flowrates, it is necessary to check that U^c_{SL} is not greater than the maximum possibly value G/ρ_l, and if so, to reset U^c_{SL} to G/ρ_l.

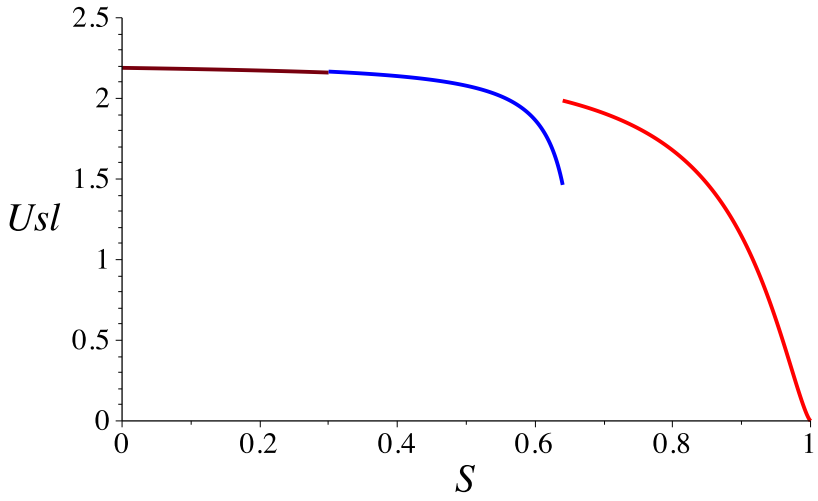

Figure 26: An example of U_{SL} versus saturation for the Hadgu correlation with a larger flowrate, when $G = 1718$, $T = 246$°C. The leftmost brown curve is bubble flow, the middle blue curve is slug and churn, and the rightmost red curve is mist flow.

Note that calculations indicate that the S value where the slug correlation gives zero U_{SL} does not vary much with G, and is about 0.65–0.66.

In the event that the mist value of U^*_{SG} is always less than one in value, there is no mist flow region, and it is necessary to also ensure that no slug flow values are considered with S greater than the value which gives a zero value for U_{SL}, S^{**} say. We do this by using zero for U^c_{SG}, and $S^* = 1$.

If the mist value of U^*_{SG} is always greater than one in value for S in $(0.32, 1)$, there is no slug or transition region, and we use the mist value of U_{SL} for the right-hand end of the bubble-slug transition region (which will now be named the **bubble-mist** transition region, in fact).

F.3.7 Slug to Mist transition

It is possible to compute an explicit value for S^* where $U^*_{SG} = 1.0$ for mist flow, by combining and rearranging eqns (23), (24), and (63)–(66), together with $U_{SG} = \alpha u_v$. This leads (after some algebra) to the following explicit formula,

$$S^* = \frac{1}{1 + C_3} \,, \tag{68}$$

where

$$C_3 = B \left(\frac{1 - C_2}{C_2} \right)^{0.74} \,, \quad C_2 = \sqrt{gD\Delta\rho\rho_v} \,/G \,.$$

The result of using these transition regions to remove jumps in U_{SL} is illustrated in Fig. (27).

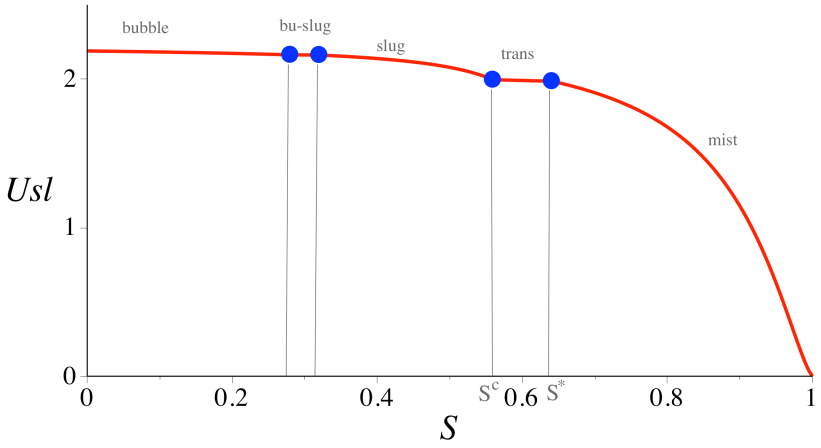

Figure 27: An example of U_{SL} versus saturation for the Hadgu correlation, with transition regions included, when $G = 1718$, $T = 246°C$. The solid circles delineate the bubble-slug (around $S = 0.3$) and transition (near $S = 0.6$) regions.

Note that as G decreases to zero, $C_2 \to \infty$ and C_3 becomes complex valued as C_2 passes through the value one. As this happens, S^* increases to equal the value one, and is not real for values of C_2 greater than one. This signals the situation mentioned earlier, that there is then no mist regime. For a typical wellbore, this occurs as flowrates are reduced through values of about 5 kg/s. As for other correlations, things begin to fail at small flowrates, where counterflow becomes possible. Counterflow (usually vapor flowing upwards and liquid flowing downwards) is not simulated at this stage in SwelFlo.

As G increases, C_2 vanishes, C_3 increases and S^* tends to zero. When S^* reduces below 0.32, this is taken to mean there is no slug or transition region between bubble and mist regions, only the bubble-slug (now bubble-mist) transition.

F.3.8 Implementation logic

Forward Problem:

If $S < 0.28$, bubble flow is used to find U_{SL}. Otherwise:

Compute S^* where mist flow $U^*_{SG} = 1.0$.

If $S < 0.32$, bubble-slug transition flow is used to find U_{SL}. If $S^* < 0.32$, this will be bubble-mist transition. Otherwise:

Compute S^c, where slug flow U_{SL} is a little greater than mist flow at S^*.

If $S < S^c$, slug flow is used to find U_{SL}. Note that this will not arise if $S^c < 0.32$. Otherwise:

If $S < S^*$, transition flow is used to find U_{SL}. Note that this will not arise if $S^* < 0.32$. Otherwise:

Mist flow is used to find U_{SL}.

Inverse Problem:

An iterative method is used to find phase velocities and hence saturation, given flowing steam quality X_{flow}. The Newton method modified by Armijo's Rule was attempted, but the transition regions between regimes can confuse the Newton search, so Brent's method is used. This iteration repeatedly calls the forward problem described above.

Given X_{flow} (and P, T, Q), the iteration actually returns the values of u_v and u_l. Then saturation S is determined by equations 1 and 2 as

$$S = \frac{QX_{\text{flow}}}{u_v A \rho_v} .$$

F.4 Frictional Pressure Drop – Full Hadgu

Hadgu also uses these flow regimes to calculate different forms for the friction term in the momentum equation. These are incorporated into SwelFlo, as detailed here. To use Hadgu's momentum terms as well as Hadgu's phase velocities, it is necessary to choose the "Hadgu full" correlation in the Input Tab options. Hadgu's thesis still has a slightly different treatment to that of SwelFlo, of heat flow between wellbore and surrounding reservoir. Different heat transfer coefficients are allowed for the different regimes. So some small differences might still be expected between SwelFlo with the full Hadgu correlation chosen, and another simulator based on Hadgu's thesis.

F.4.1 Bubble Flow

In this regime, described in the previous subsection,

$$\left(\frac{dP}{dz}\right)_{\text{fri}} = f_H \rho_m u_l^2 / r \ , \tag{69}$$

where r is wellbore radius, and f_H is a (Fanning) friction factor that depends on roughness and on a Reynolds number Re_B, which is given by

$$\text{Re}_B = \frac{\rho_m u_l D}{\mu_l} \ ,$$

where

$$\rho_m = S\rho_v + (1 - S)\rho_l \ .$$

Note that this frictional pressure gradient has been derived from the usual theoretical formula $4\tau_w/D$. There is a slight difference in GWELL and SwelFlo convention, so that $f_D = 4f_H$

where f_D is the (Darcy) friction factor due to White (1974) that has value 64/Re for laminar flow, and f_D is the friction factor used in SwelFlo.

F.4.2 Slug and Churn Flow

In this regime, Hadgu uses the results of Dukler *et al* [13], summarised here as:

$$\left(\frac{dP}{dz}\right)_{\text{fri}} = \frac{f_m \rho_m^{LS} U_{LLS}^2}{r}(1-\beta) \ , \tag{70}$$

where

$$\rho_m^{LS} = \alpha_{LS}\rho_v + (1-\alpha_{LS})\rho_l = 0.3\rho_v + 0.7\rho_l \ ,$$

and f_m depends on the Reynolds number

$$\text{Re}_m = \frac{DU_{LLS}\rho_m^{LS}}{\mu_l} \ .$$

To compute these, we need U_{LLS} and β. Referring to the previous subsection (F.3.3), we compute (given liquid and vapour phase velocities and saturation S):

$$\begin{aligned}
U_{SG} &= Su_v && (71)\\
U_{SL} &= (1-S)u_l && (72)\\
U_\infty &= 0.345\left(\frac{Dg\Delta\rho}{\rho_l}\right)^{0.5} && (73)\\
U_N &= 1.29(U_{SG}+U_{SL}) + U_\infty && (74)\\
U_{LTB} &= 9.916(gD(1-\sqrt{\alpha_{TB}}))^{0.5} = 9.9498\sqrt{r} && (75)\\
U_{LLS} &= U_N - (U_N + U_{LTB})\left(\frac{1-\alpha_{TB}}{1-\alpha_{LS}}\right) = 0.857U_N - 0.143U_{LTB} && (76)
\end{aligned}$$

using $\alpha_{TB} = 0.89$, $\alpha_{LS} = 0.3$. We also have

$$\begin{aligned}
\alpha_{SU} &= \frac{X\rho_l}{X\rho_l + (1-X)\rho_v} && (77)\\
\beta &= \left(\frac{\alpha_{SU}-\alpha_{LS}}{\alpha_{TB}-\alpha_{LS}}\right) = \frac{\alpha_{SU}-0.3}{0.59} && (78)
\end{aligned}$$

F.4.3 Annular or Mist Flow

Hadgu notes that the flow of the liquid phase on the walls dominates frictional losses in this regime. He chooses the correlation

$$\left(\frac{dP}{dz}\right)_{\text{fri}} = f_D \ \rho_l u_l^2/r \ , \tag{79}$$

where the Darcy friction factor f_D is a function of Reynolds number

$$\mathrm{Re}_l = \frac{\rho_l u_l D}{\mu_l} \ ,$$

and is given by the Serghides [31] approximation to the Colebrook equation, accurate to 0.0023% :

$$A = -2\log_{10}\left(\frac{\epsilon}{3.7D} + \frac{12}{\mathrm{Re}_l}\right) \ , \tag{80}$$

$$B = -2\log_{10}\left(\frac{\epsilon}{3.7D} + \frac{2.51A}{\mathrm{Re}_l}\right) \ , \tag{81}$$

$$C = -2\log_{10}\left(\frac{\epsilon}{3.7D} + \frac{2.51B}{\mathrm{Re}_l}\right) \ , \tag{82}$$

$$f_D = \left[A - \frac{(B-A)^2}{C-2B+A}\right]^{-2} \ , \tag{83}$$

where ϵ is roughness, in the same units as wellbore diameter D.

F.4.4 Gravitational Pressure Drop

For bubble flow Hadgu uses the same form as SwelFlo, $<\rho> g\sin\theta$. For slug flow, this is modified slightly to $<\rho> (1-\beta)g\sin\theta$. This is done in SwelFlo by using $\beta = \frac{S-0.28}{0.61}$. For annular flow, the form is $<\rho> g\sin\theta$, and the saturation value used in $<\rho>$ is computed using the Baroczy formulation in eqn. (63).

F.4.5 Momentum Flux Term

The momentum flux term is also called the accelerational pressure drop in Hadgu's thesis. In bubble flow it is the same as SwelFlo usually uses for Armand and Orkiszewski correlations, $G <v>$, in the third form presented in eqn. (8). Hadgu makes the same sign error on the momentum flux term as is made in the GWELL manual. In his PhD thesis, the error originates in the transition from his correct eqn (8.5) to his incorrect eqn (8.6).

In slug flow, Hadgu uses the results of Fernandes *et al* [16] — the pressure gradient required to accelerate downflowing fluid between the slug and the wall to the speed U_{LTB} gives the gradient of momentum flux (rather than the actual momentum flux) as

$$\left(\frac{dP}{dL}\right)_{\mathrm{acc}} = \rho_l U_{LTB}(1-\alpha_{TB})\left(\frac{U_{LTB}+U_{LLS}}{\ell_{SU}}\right) \ . \tag{84}$$

Note that this is already in divergence form — it is not an estimate of momentum flux but rather of the divergence of momentum flux.

The length of a slug unit, ℓ_{SU}, is calculated by using

$$\frac{\ell_{LS}}{\ell_{SU}} = 1 - \beta \ , \quad \text{and} \ \ \ell_{LS} = 20D \ .$$

The RHS of eqn (84) is always positive. Being in divergence form means that it should change sign as the direction of iteration changes between topdown and bottomup.

In his thesis, Hadgu appears to ignore (set to zero) the momentum flux term in the annular flow region. Since our experience with simulations is that momentum flux can be very significant in the upper parts of a geothermal well, we use the Baroczy correlation he favours for annular flow, inverted in equations (64) to (66), to evaluate the usual momentum flux $G <v>$.

F.5 Duns and Ros Correlation

The Duns and Ros correlation [14, 36] is based on the Ros correlation, developed from tests on a vertical pipe rigged in the laboratory, and using air-water and air-liquid hydrocarbon mixtures.

As for the Orkiszewski correlation, the Duns and Ros (1963) correlation [14, 36] starts with known values for the superficial velocities $U_{SG} = Su_v = QX_{\text{flow}}/(\rho_v A)$ and $U_{SL} = (1-S)u_l = Q(1-X_{\text{flow}})/(\rho_l A)$, and with wellbore diameter and liquid viscosity, values for dimensionless liquid velocity, dimensionless gas velocity, dimensionless pipe diameter and dimensionless liquid viscosity may be written down:

$$N_{lv} = U_{SL}\left(\frac{\rho_l}{g\sigma}\right)^{0.25} , \tag{85}$$

$$N_{gv} = U_{SG}\left(\frac{\rho_l}{g\sigma}\right)^{0.25} , \tag{86}$$

$$N_d = D_h\sqrt{\frac{\rho_l g}{\sigma}} , \tag{87}$$

$$N_l = \mu_l\left(\frac{g}{\rho_l\sigma^3}\right)^{0.25} , \tag{88}$$

where $D_h = 4A/P$ is hydraulic pipe diameter which matches the actual diameter for a circular cross-section, A is cross-section area, and P is the length of the pipe perimeter. Note that a variety of sources [29, 19, 36, 11, 7] confirm that the density in N_{gv} (and in the other dimensionless numbers) is indeed liquid density ρ_l.

Then the flow regime is determined, as bubble, slug, mist, or transition, according to the values of the variables L_b, L_s, L_m:

$$L_b = L_1 + L_2 N_{lv} \ , \tag{89}$$

$$L_s = 50 + 36N_{lv} \ , \tag{90}$$
$$L_m = 75 + 84N_{lv}^{0.75} \ . \tag{91}$$

The numbers L_1 and L_2 are correlated to the nondimensional pipe diameter as illustrated in Fig. (28), and this correlation is evaluated in SwelFlo by using interpolation on a digitized version of this figure, as given in Table (5).

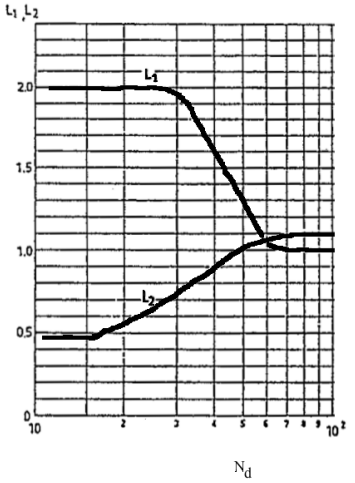

Figure 28: The values of L_1 and L_2 and their dependency on diameter number N_d, according to Duns and Ros.

The flow regions — bubble, where the liquid phase is continuous; slug, where neither phase is continuous with churn flow at low liquid flow rates and dispersed bubble flow at high liquid flow rates; transition, which is where there is a transition to mist flow; and mist, where the gas phase is continuous and annular liquid flow occurs — are delineated by the values of L_b, L_s and L_m as listed in Table (6). The correlations for these different regions are discussed further, below.

In each of these regions, as detailed in the next subsection, Duns and Ros offer a correlation that gives a value for the dimensionless slip velocity

$$V_{SD} = V_s \left(\frac{\rho_l}{g\sigma} \right)^{0.25} \ , \tag{92}$$

where the slip velocity is

$$V_s = u_v - u_l \ .$$

To summarise then, given the Duns and Ros correlation, and given values for the superficial velocities U_{SG} and U_{SL}, we are given a way to calculate a value for the slip velocity V_s.

L_1	L_2	N_d	F_1	F_2	F_3	F_4	N_l	F_5	F_6	F_7	$\frac{f_1 U_{SG} N_d^{2/3}}{4U_{SL}}$	f_2
2.0	0.5	10.0	1.25	0.24	0.83	-5.0	0.003	0.218	0.48	0.125	0.001	1.0
2.0	0.55	20.0	1.25	0.24	0.86	9.0	0.005	0.205	0.2	0.11	0.01	1.02
1.97	0.74	30.0	1.25	0.24	0.98	16.0	0.007	0.195	0.01	0.098	0.1	1.05
1.6	0.9	40.0	1.25	0.24	1.25	22.0	0.01	0.18	-0.1	0.088	0.3	1.07
1.3	1.0	50.0	1.26	0.24	1.64	32.0	0.015	0.177	-0.12	0.078	0.5	1.0
1.05	1.06	60.0	1.3	0.27	1.9	36.0	0.02	0.17	-0.1	0.07	1.0	0.78
1.0	1.1	70.0	1.36	0.38	2.3	43.0	0.03	0.158	0.34	0.062	3.0	0.51
1.0	1.1	80.0	1.64	0.59	2.8	51.0	0.05	0.13	0.96	0.051	10.0	0.34
1.0	1.1	90.0	1.9	0.83	3.1	55.0	0.08	0.08	1.7	0.043	70.0	0.22
1.0	1.1	100.0	2.1	0.95	3.25	55.0	0.1	0.058	2.14	0.039	200.0	0.208
1.0	1.1	150.0	2.05	1.03	3.4	55.0	0.15	0.045	2.16	0.034	500.0	0.208
1.0	1.1	200.0	1.9	0.98	3.7	55.0	0.3	0.053	1.86	0.03		
			1.65	0.93	3.8	55.0	0.5	0.067	1.76	0.027		
			1.3	0.85	4.0	55.0	0.8	0.085	1.74	0.026		
			0.95	0.75	4.1	55.0	1.5	0.105	1.74	0.024		

Table 5: Digitized versions of numbers used in the Duns and Ros correlation

Flow Region	Limits
bubble	$0 \leq N_{gv} < L_b$
slug	$L_b \leq N_{gv} < L_s$
transition	$L_s \leq N_{gv} < L_m$
mist	$N_{gv} \geq L_m$

Table 6: Duns and Ros flow regions

After doing this, we can find saturation S as follows: using the definition of slip velocity in the form

$$V_s = \frac{U_{SG}}{S} - \frac{U_{SL}}{1-S} \,, \tag{93}$$

we rearrange this to obtain a quadratic equation for the static vapour saturation S (in terms of known values U_{SG}, U_{SL}, and V_s):

$$V_s S^2 - (V_s + U_{SG} + U_{SL})\, S + U_{SG} = 0 \,. \tag{94}$$

The solution of this that lies in the range $(0, 1)$ is given explicitly by

$$S = \frac{(U_{SG} + U_{SL} + V_s)\left[1 - \sqrt{1 - \frac{4V_s U_{SG}}{(U_{SG}+U_{SL}+V_s)^2}}\ \right]}{2V_s} \,. \tag{95}$$

When V_s is zero, this takes the limiting value

$$S = \frac{U_{SG}}{U_{SG} + U_{SL}} \,. \tag{96}$$

That is, given U_{SG} and U_{SL}, we can use the Duns and Ros correlation to calculate a value for the slip velocity V_s, and we substitute these three values into eqn. (95) to find saturation S. This defines the forward problem.

Finally we obtain liquid and vapour phase velocities by using

$$u_v = U_{SG}/S \;;\;\; u_l = U_{SL}/(1-S) \,.$$

F.5.1 Bubble Flow Region

Dimensionless slip velocity is given by

$$V_{SD} = F_1 + F_2 N_{lv} + F_3' \left(\frac{N_{gv}}{1 + N_{lv}}\right)^2 \,, \tag{97}$$

where

$$F_3' = F_3 - \frac{F_4}{N_d} \,,$$

and the parameters F_1, F_2, F_3 and F_4 depend on the dimensionless liquid viscosity as determined by Duns and Ros, and as illustrated in Fig. (29). Digitisations of these graphs are given in Table (5).

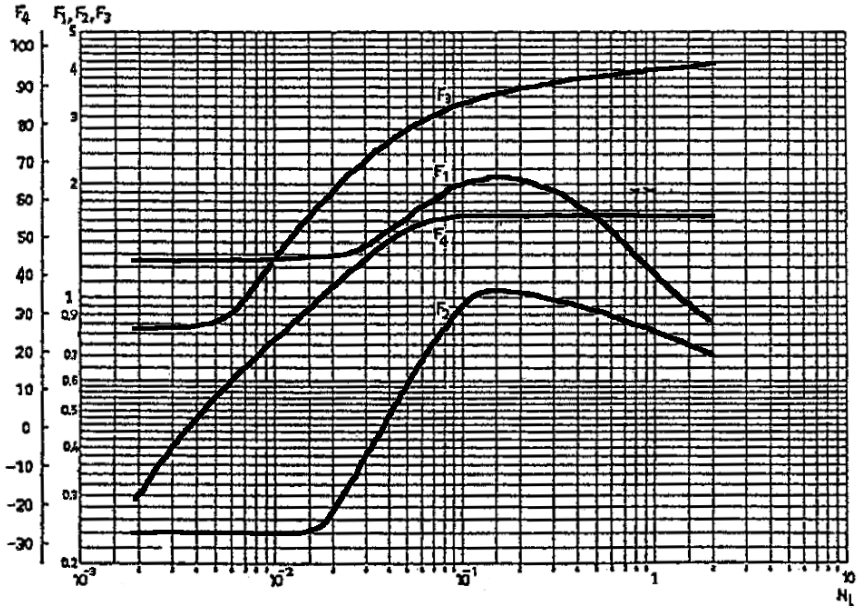

Figure 29: The values of F_1, F_2, F_3, and F_4 used in the bubble region, and their dependency on dimensionless liquid viscosity N_l, according to Duns and Ros. From the uppermost curve downwards, they are F_3, F_1, F_4 and F_2.

F.5.2 Slug Flow Region

The dimensionless slip velocity for slug flow under the Duns and Ros correlation is given by the relationship

$$V_{SD} = (1 + F_5)\frac{N_{gv}^{0.982} + F_6'}{(1 + F_7 N_{lv})^2} \ , \tag{98}$$

where

$$F_6' = 0.029 N_d + F_6 \ ,$$

and where the parameters F_5, F_6, and F_7 depend on dimensionless liquid viscosity as illustrated in Fig. (30) and listed in Table (5).

F.5.3 Mist Flow Region

Slip velocity is assumed negligible in mist flow, so that $V_{SD} = 0$, and as in eqn (96),

$$S = U_{SG}/(U_{SG} + U_{SL}) \ .$$

Note that zero slip flow implies that

$$u_v = u_l = \frac{Q}{A\rho_m} \ .$$

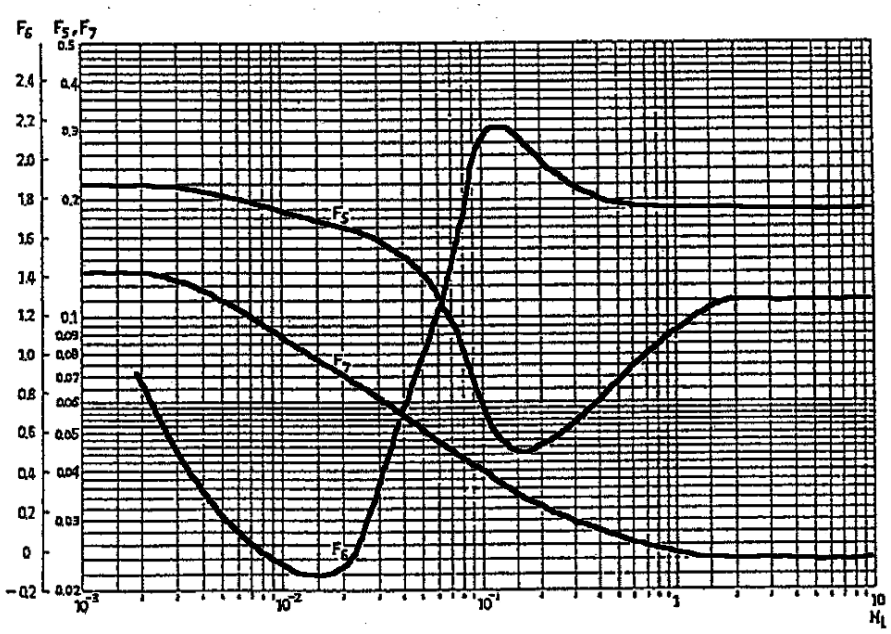

Figure 30: The values of F_5, F_6, and F_7 used in the slug region, and their dependency on dimensionless liquid viscosity N_l, according to Duns and Ros.

F.5.4 Transition Region

In the transition region between slug and mist flow regions, Duns and Ros calculate a total pressure gradient that is the linearly weighted average of the mist and slug total pressure gradients, using N_{gv} as the measure of distance. Since our focus is on computing slip V_{SD}, and since transition is relatively small and not often encountered, we will instead use a linear transition from the slug flow value of V_{SD} to zero.

F.5.5 Bubble-Slug Transition

Numerical results indicate that the saturation S typically increases monotonically as U_{SG} increases, but not when there is a transition from bubble to slug regions, where S can decrease temporarily when going from bubble to slug, especially at low flowrates. This makes the correlation non-invertible (S as a function of N_{gv} or U_{SG} then has no inverse function). In initial versions of the simulator, we started out knowing saturation and wanted to find U_{SG} ,and we cannot solve uniquely for U_{SG} as a function of S when the correlation is noninvertible. This issue is further complicated by the fact that the dependence of S on V_s is not simple, as N_{gv} increases. It is observed numerically that V_s increases monotonically with N_{gv} through the non-invertible S region, but with a jump in value there.

It is not clear that the dependence should be monotonic, given that we start out knowing U_{SG} and we want a saturation value. But jumps in saturation prevent the Newton method from

solving the conservation equations, so in SwelFlo we choose to avoid such jumps by making an invertible transition region between the bubble and slug regions.

To make the correlation invertible and smooth we introduce a Bubble-Slug transition region as follows.

If in the slug region, we check the value of S against the value S^* obtained by using the bubble correlation with maximal value $N_{gv} = L_b$, plus a small amount Δ. Then if S is less than $S^* + \Delta$, we need to correct it to linearly interpolate between S^* and $S^* + \Delta$, based on the current value of U_{SG}.

Note that L_b actually depends on N_{gv}. They are equal when

$$U_{SG}\left(\frac{\rho_l}{g\sigma}\right)^{0.25} = L_1 + L_2\left(\frac{Q/A - \rho_v U_{SG}}{\rho_l}\right)\left(\frac{\rho_l}{g\sigma}\right)^{0.25} ,$$

that is, when

$$U_{SG} = U^*_{SG} = \frac{\rho_l L_1\left(\frac{g\sigma}{\rho_l}\right)^{0.25} + \frac{L_2 Q}{A}}{\rho_l + L_2\rho_v} .$$

We then need an explicit value U^{**}_{SG} for U_{SG} that corresponds to the saturation value $S^* + \Delta$ in the slug flow region by solving simultaneously (setting $V_s\left(\frac{\rho_l}{g\sigma}\right)^{0.25} = V_{SD}$, and using eqn (**??**) in) the equations

$$\begin{aligned} V_s &= \frac{U_{SG}}{S^* + \Delta} - \frac{U_{SL}}{1 - S^* - \Delta} \\ V_{SD} &= (1 + F_5)\frac{N_{gv}^{0.982} + F'_6}{(1 + F_7 N_{lv})^2} . \end{aligned}$$

Since U_{SL} varies with U_{SG} (keeping G fixed) and since also N_{lv} depends on U_{SL}, this is a nonlinear relationship that needs to be solved using a Newton method, to find the value U^{**}_{SG}.

Then the interpolated value for S in the bubble-slug transition range lies in the range S^* to $S^* + \Delta$, and is calculated for the current value of U_{SG} as

$$S = S^* + \left(\frac{U_{SG} - U^*_{SG}}{U^{**}_{SG} - U^*_{SG}}\right)\Delta .$$

F.5.6 Low Flowrates

Note that for low flowrates (Q less than 15 kg/s for a well of radius 0.1m), even with the bubble-slug transition region introduced here, a plot of S against U_{SG} reveals that the Duns and Ros correlation is not invertible (there are S values with more than one U_{SG} value

generating them), and that some S values cannot be realized at very low flowrates. This is illustrated in Fig. (31), where flowrates of 1, 5, 10 and 15 kg/s are used with a wellbore radius of 0.1m, a pressure of 70 bara, and a static steam fraction of 0.5. The regions (for $Q = 5, 10$ kg/s) where the correlation becomes multivalued are at the upper end of the slug region, and the lower end of the transition region. When $Q = 15$kg/s and higher, the correlation is single-valued and invertible and covers the entire S range of $(0, 1)$. When Q is less than 5kg/s, the correlation is single-valued but does not reach to $S = 1$.

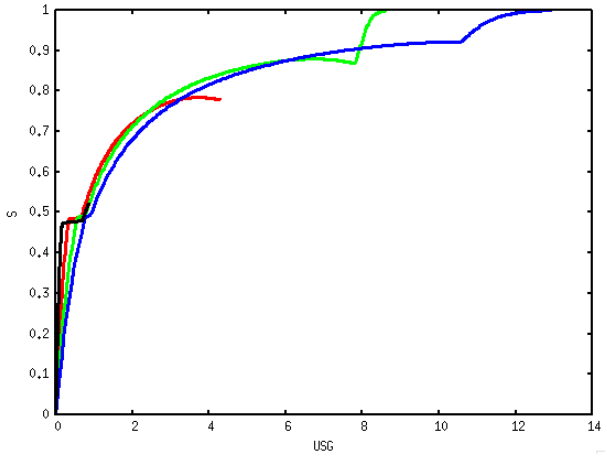

Figure 31: An illustration of issues with the Duns and Ros correlation at low flowrates (1 (black), 5 (red), 10 (green) and 15 kg/s (blue)), a wellbore radius of 0.1m, a pressure of 70 bara, and a static steam fraction of 0.5. U_{SG} values are input from zero to maximum for the given flowrate, and S is computed according to the Duns and Ros correlation as discussed in the text. We observe that higher saturation values are not realizable at low flowrates, and that sometimes several U_{SG} values correspond to one saturation value, making the correlation noninvertible there.

F.5.7 Duns and Ros Momentum Equation

If the full Duns and Ros correlation is chosen, the treatment of momentum terms is different to the usual SwelFlo treatment, and is as detailed here.

F.5.8 Friction Pressure Changes

The usual SwelFlo treatment is to use a two-phase multiplier based on Martinelli and Nelson, and modified by Chisholm [10]. Duns and Ros take a slightly different approach, depending on the flow region.

Bubble Flow and Slug Flow

For bubble flow and for slug flow, Duns and Ros assume the continuous liquid phase is the main contributor, and they correct the single phase pressure drop with their own two-phase multiplier f_m to obtain

$$\left(\frac{dp}{dz}\right)_f = f_m \rho_l U_{SL} \frac{V_m}{2D_h}$$

where

$$V_m = U_{SG} + U_{SL}$$

and their two-phase multiplier takes the form

$$f_m = f_1 \frac{f_2}{f_3}$$

where f_1 is the usual liquid-phase Darcy friction factor that solves the Colebrook equation, using the Reynolds number

$$\mathrm{Re} = \frac{\rho_l U_{SL} D_h}{\mu_l} \ ,$$

and where f_2 corrects for two-phase effects, and is a function of $f_1 U_{SG} N_d^{2/3}/(4U_{SL})$ (plotted as the "vertical" correlation in Fig. (32), and listed in Table (5)). The parameter f_3 is a further correction term for saturation and viscosity effects, and is given by

$$f_3 = 1 + \frac{f_1}{4}\sqrt{\frac{U_{SG}}{50 U_{SL}}} \ .$$

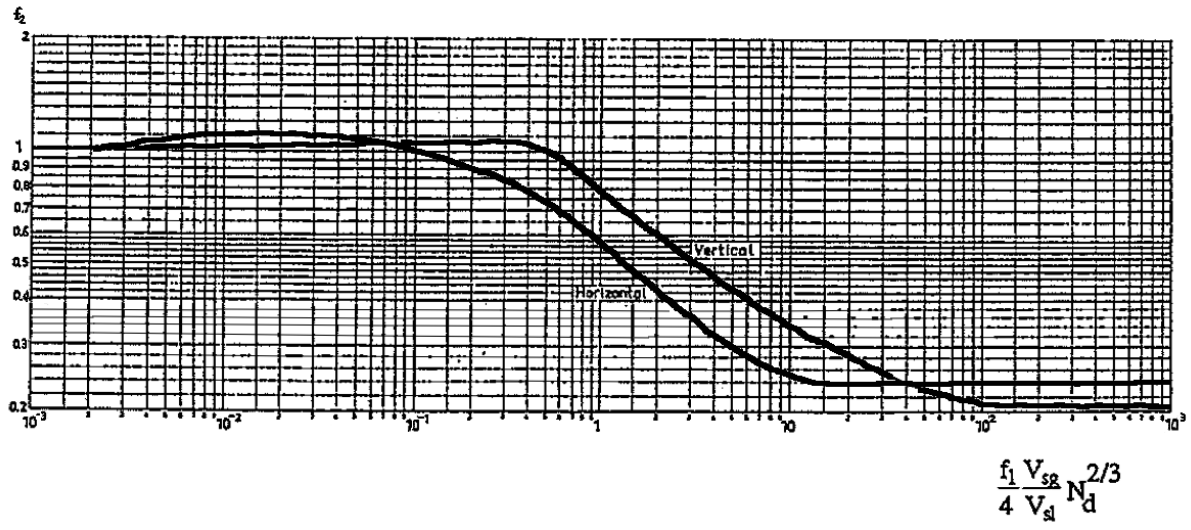

Figure 32: The value of f_2 versus $f_1 U_{SG} N_d^{2/3}/(4U_{SL})$ used in computing frictional pressure changes in the bubble region, according to the Duns and Ros correlation

Note that even their liquid phase pressure drop term,

$$\rho_l U_{SL} \frac{V_m}{2D_h} = \rho_l U_{SL} \frac{U_{SG} + U_{SL}}{2D_h}$$

takes a different form to the usual SwelFlo term based on [10], which emphasizes the liquid velocity by weighting it with density:

$$\frac{G^2}{2D_h \rho_m} = \frac{(\rho_v U_{SG} + \rho_l U_{SL})(\rho_v U_{SG} + \rho_l U_{SL})}{2D_h(S\rho_v + (1-S)\rho_l)} \ .$$

Transition Regime

A weighted average (depending on the value of N_{gv}) of the slug and mist flow values for frictional pressure drop is used here. That is, if DP_s is the slug term, and DP_m the mist term, then

$$\left(\frac{dp}{dz}\right)_f = DP_s + \left(\frac{N_{gv} - L_s}{L_m - L_s}\right) DP_m \ .$$

Mist Flow Regime

Friction in the Duns and Ros mist flow regime is assumed to be due to the drag of the vapour on the wavy liquid flow that clings to the walls of the wellbore, so that

$$\left(\frac{dp}{dz}\right)_f = f_1 \rho_g \frac{U_{SG}^2}{2D_h} \ , \tag{99}$$

where the Darcy friction factor f_1 depends on the vapour phase Reynolds number

$$\mathrm{Re} = \frac{\rho_g U_{SG} D_h}{\mu_v} \ .$$

The roughness this flow experiences is associated with ripples on the liquid film on the walls. They are correlated to the number N_w, defined as

$$N_w = \left(\frac{U_{SG}\mu_l}{\sigma}\right)^2 \frac{\rho_g}{\rho_l} \ ,$$

so that

$$\frac{\epsilon}{D_h} = \begin{cases} 34\frac{\sigma}{\rho_g U_{SG}^2 D_h} & N_w < 0.005 \\ 174.8\frac{\sigma N_w^{0.302}}{\rho_g U_{SG}^2 D_h} & N_w \geq 0.005 \end{cases} \ . \tag{100}$$

If these relative roughness values are found to be greater than 0.05, the friction factor is found using the extended Colebrook equation

$$f_1 = 4\left[\frac{1}{[4\log_{10}(0.27\epsilon/D_h)]^2} + 0.067\left(\frac{\epsilon}{D_h}\right)^{1.73}\right] \ . \tag{101}$$

F.5.9 Momentum Flux Terms

Duns and Ros take the pressure drop due to changes in momentum flux to be zero, unless the flow region is mist flow. SwelFlo adopts this approach if the user selects the full Duns and Ros correlation option. However, our experience with other correlations suggests that momentum flux changes can be significant in accelerating slug flow regions.

Then (in the mist regime) the pressure gradient due to divergence of momentum flux in the mist flow region is taken to be a given fraction of the total pressure derivative,

$$\left(\frac{dp}{dz}\right)_{acc} = \frac{(U_{SG}+U_{SL})U_{SG}\rho_m}{P}\left(\frac{dp}{dz}\right)_t = \mathrm{MF}\left(\frac{dp}{dz}\right)_t \quad \text{say} , \tag{102}$$

where P is pressure (Pa), and $\left(\frac{dp}{dz}\right)_t$ is the total pressure divergence.

This leads to

$$\left(\frac{dp}{dz}\right)_t = \left(\frac{dp}{dz}\right)_{acc} + \left(\frac{dp}{dz}\right)_f + \left(\frac{dp}{dz}\right)_{grav} = \mathrm{MF}\left(\frac{dp}{dz}\right)_t + \left(\frac{dp}{dz}\right)_f + \left(\frac{dp}{dz}\right)_{grav} ,$$

where the subscript *acc* means momentum flux or acclerational pressure drop, f means friction, and *grav* means gravitational pressure drop. so that

$$\left(\frac{dp}{dz}\right)_t = \left[\left(\frac{dp}{dz}\right)_f + \left(\frac{dp}{dz}\right)_{grav}\right]/(1-\mathrm{MF}) .$$

F.5.10 Gravitational Pressure Drop

Duns and Ros use the same form as SwelFlo, $<\rho> g \sin\theta$.

F.6 Hagedorn and Brown Correlation

Hagedorn and Brown made pressure measurements on a 457m test well, for nearly 3,000 pressure points and a range of gas-liquid flow rates, viscosities and tubing diameters. The key idea is to use a homogeneous (equal phase velocity) model to compute frictional and acceleration pressure changes, and then to match the measured total pressure drop by choosing a value for the pseudo-liquid holdup (or equivalently a pseudo-saturation) that make the gravitational pressure change correct. The dimensionless numbers listed in the Duns and Ros correlation are used to correlate the pseudo-holdup. Hence pseudo-saturation is used as a parameter to correlate the equations with the measured pressure drop, and saturation itself is never computed in this correlation.

It is noted in [11] that this correlation is generally adequate for vapour saturations less than 0.99–0.95, but may not be accurate for mist flow.

A major difference here to most other correlations is that there are no flow regimes, and no true value is computed for saturation S. The emphasis of Hagedorn and Brown is on matching observed pressure changes, for a water-air mixture where presumably energy conservation is not required to be considered. This makes the Hagedorn and Brown correlation of limited interest in the geothermal context, where temperature changes are also important.

Futhermore, implementation is challenging for a geothermal wellbore simulator, as the primary output of the correlation is the pressure gradient in a situation where temperature is irrelevant. The output that is needed is saturation, given flowing steam quality (that is, given U_{SG} and U_{SL}).

It is not possible to use pressure gradient to obtain saturation, since as noted below the relationship is not invertible — one pressure gradient corresponds to two different saturations.

The way forward is to use the pseudo-saturation that the Hagedorn and Brown correlation gives, as a measure of steam saturation. In fact, since the pseudo-saturation is sometimes larger than the physically realisable maximum saturation obtained for homogeneous flow, the minimum of pseudo-saturation and homogeneous saturation is used as actual saturation S.

Some of the following discussion relates to the computation of pressure gradient, which is how the Hagedorn and Brown correlation was originally set up. However, the saturation we extract from the correlation does not require any computation of pressure gradients within the correlation. Such computation is left to the numerical computation of conservation equations elsewhere in the code.

F.7 The Forwards Hagedorn & Brown Correlation

The Brill and Beggs 1991 [7] interpretation of the Hagedorn and Brown correlation is considered, as described in [7, 36, 11], together with the original publication [21]. A homogeneous flow model is used to compute frictional and acceleration (divergence of momentum) terms, and the pseudo-holdup or saturation value to be used in these terms and in the gravitational term is determined by the correlation itself. This pseudo-holdup is essentially a correlation parameter, that Hagedorn and Brown have fitted to their data, that gives a match to experimental pressure gradients for a given pair of values of steam and liquid flow, U_{SG} and U_{SL}.

The conservation of momentum equation is written in the following form, in terms of the total pressure gradient:

$$\left(\frac{dp}{dz}\right)_t = \left(\frac{dp}{dz}\right)_{acc} + \left(\frac{dp}{dz}\right)_f + \left(\frac{dp}{dz}\right)_{grav}, \tag{103}$$

where subscript acc means accelerational (pressure gradient associated with the momentum flux divergence), subscript f means pressure gradient due to friction, and subscript $grav$

means gravitational pressure gradient.

The friction pressure gradient is

$$\left(\frac{dp}{dz}\right)_f = f_D \rho_f \left(\frac{V_m^2}{2D_h}\right) = \frac{fG^2}{2\rho_s D_h} \,, \tag{104}$$

where

$$\rho_f = \frac{\rho_n^2}{\rho_s} \,, \quad \rho_n = \frac{\rho_l U_{SL} + \rho_v U_{SG}}{U_{SL} + U_{SG}} = \frac{G}{V_m} \,, \quad \rho_s = S'\rho_v + (1 - S')\rho_l \,, \quad V_m = U_{SL} + U_{SG} \,,$$

and S' is a pseudo-saturation, chosen to give a match to total pressure gradient as observed in the Hagedorn and Brown experiments and as detailed here.

The Darcy friction factor f_D depends on the Reynolds number

$$\mathrm{Re} = \frac{\rho_n V_m D_h}{\mu_s} = \frac{G D_h}{\mu_s}$$

where the two-phase viscosity is defined in terms of the pseudo-saturation as

$$\mu_s = \mu_l^{(1-S')} \mu_v^{S'} \,.$$

The acceleration pressure gradient term used by Hagedorn and Brown is based on homogeneous flow:

$$\left(\frac{dp}{dz}\right)_{acc} = -\frac{\rho_s}{2} \frac{d(V_m^2)}{dz} \,.$$

Note that the minus sign is unclear in [36] section 5.3 due to the use of a Δ symbol, but is correctly present in his coding ([36] Appendix 8. p.149).

Determination of the derivative of V_m^2 in the above equation is tackled in different ways in different interpretations of the correlation. One approach is that of Torrens. A look at the coding in Torrens' thesis [36] reveals that there the derivative term above is evaluated by using

$$U_{SG}^{(2)} = U_{SG}^{(1)} \left(\frac{\rho_v^{(1)}}{\rho_v^{(2)}}\right) \,, \quad U_{SL}^{(2)} = U_{SL}^{(1)} \,,$$

where the superscript (1) means to use P_1 to evaluate, and the superscript (2) means to use P_2 to evaluate. Then the new value of V_m is given by $V_m^{(2)} = U_{SG}^{(2)} + U_{SL}^{(2)}$, and the derivative is approximated as

$$\frac{\rho_s}{2} \frac{d(V_m^2)}{dz} \approx \rho_s V_m^{(1)} \left(\frac{V_m^{(2)} - V_m^{(1)}}{P_2 - P_1}\right) = \rho_s V_m^{(1)} \left(\frac{\Delta V_m}{\Delta P}\right) \,.$$

Rearranging the Torrens calculation gives

$$\Delta V_m = \frac{M_g}{A}\left(\frac{1}{\rho_v^{(2)}} - \frac{1}{\rho_v^{(1)}}\right) = -\frac{U_{SG}}{\rho_v}\Delta\rho_v \ . \tag{105}$$

That is, the Torrens approach is to consider that changes in vapour phase density dominate changes in V_m as pressure changes. However, U_{SG} will also change, and this is ignored.

A different approach is used by Brill and Beggs [7], who use the Duns and Ros mist flow correlation to compute the acceleration term, rather than the Hagedorn and Brown correlation. This will make the pseudo-holdup value incorrect when the acceleration term is significant, since it was set by Hagedorn and Brown by fitting to data and using a different acceleration calculation.

Since Hagedorn and Brown essentially fit a pseudo-holdup to measured pressure changes, it is important to use the same method as the one they have used, to compute the derivative of V_m^2, irrespective of what actually happens. Any deviation from the formulae used by Hagedorn and Brown will invalidate the fitted correlation for pseudo-holdup.

A close examination of their original paper gives a hint of what has been done to compute the difference of V_m^2 from one point to another point that is a pressure (and temperature) increment away. Hagedorn and Brown comment ([21], p. 481, item 4) that they determine ρ_v at an average pressure and temperature, and "calculate the velocity of the mixture" (here presumed to mean V_m) "at both ends of the increment using the pressures at those two points and the ratio of the flow rates as measured at the out-flow end of the tube" — presumably the ratio referred to is of U_{SG} and U_{SL}.

This suggests that the ratio U_{SL}/U_{SG} is taken to be fixed at a value, say R_u, over the increment, so that since

$$\rho_l U_{SL} + \rho_v U_{SG} = G \ ,$$

and then using the ratio we have

$$U_{SG} = \frac{G}{\rho_v + \rho_l R_u} \ .$$

At node 1, specific gas velocity is given by

$$U_{SG}^{(1)} = \frac{G}{\rho_v^{(1)} + \rho_l^{(1)} R_u} \ ,$$

and at node 2, since G is the constant mass flowrate per unit area, and R_u is *assumed* constant,

$$U_{SG}^{(2)} = \frac{G}{\rho_v^{(2)} + \rho_l^{(2)} R_u} \ .$$

These can be rearranged to get

$$U_{SG}^{(2)} = U_{SG}^{(1)}\left(\frac{\rho_v^{(1)} + \rho_l^{(1)} R_u}{\rho_v^{(2)} + \rho_l^{(2)} R_u}\right) \ , \tag{106}$$

which tends to Torrens' formula in the limit that $\rho_l R_u$ is much less than ρ_v.

Since this is the original formulation in [21], it provides the best way to calculate dV_m/dP. The change in V_m is then given by

$$\Delta V_m = -V_m \left(\frac{\Delta\rho_v + R_u \Delta\rho_l}{\rho_v + R_u \rho_l} \right) = -\frac{1}{\rho_n}(U_{SG}\Delta\rho_v + U_{SL}\Delta\rho_l) \ , \tag{107}$$

where Δ means the value in node 2 minus the value in node 1.

Since pressure gradient is not known a priori in the forwards correlation, the implicit nature of the accelerational pressure derivative is accommodated by using

$$\left(\frac{dp}{dz}\right)_{acc} = -\rho_s V_m \frac{dV_m}{dz} = -\rho_s V_m \frac{dV_m}{dP}\left(\frac{dP}{dz}\right)_t \approx -\rho_s V_m \frac{\Delta V_m}{\Delta P}\left(\frac{dP}{dz}\right)_t = \epsilon \left(\frac{dP}{dz}\right)_t \ ,$$

where ΔV_m is as given in the previous equation, so that computation of ϵ in SwelFlo is given by

$$\epsilon = -\rho_s V_m \frac{\Delta V_m}{\Delta P} = \frac{\rho_s V_m}{\rho_n}\left(U_{SG}\frac{d\rho_v}{dP} + U_{SL}\frac{d\rho_l}{dP} \right) > 0 \ .$$

The acceleration pressure gradient is taken across to the left side of eqn (103) and the equation is made explicit in total pressure gradient to get:

$$\left(\frac{dp}{dz}\right)_t = \frac{\left(\frac{dp}{dz}\right)_f + \left(\frac{dp}{dz}\right)_{grav}}{1-\epsilon} \ . \tag{108}$$

Note that a comparison between this and Torrens' approach is possible if one considers the physically reasonable limit that $\frac{d\rho_l}{dP}$ is relatively small, so that equation (107) becomes

$$\Delta V_m \approx -U_{SG}\frac{\Delta\rho_v}{\rho_n} \ ,$$

which looks the same as Torrens' equation (105) with the exception that ρ_n replaces ρ_v. Both this comparison and the one made just after equation (106) indicate that Torrens' computation and the one used in Hagedorn and Brown's original paper become very close to each other when vapour flow dominates, since then $R_u \to 0$ and $\rho_n \to \rho_v$. This is when the acceleration terms are significant.

The gravitation pressure gradient in the Hagedorn and Brown correlation uses pseudo-saturation S' in place of saturation, in the usual form

$$\left(\frac{dp}{dz}\right)_{grav} = [S'\rho_v + (1-S')\rho_l] g \sin\theta \ .$$

F.7.1 Pseudo-saturation Correlation

Hagedorn and Brown [21] originally presented graphical correlations for pseudo liquid holdup $(1 - S')$. We use our own slightly adjusted versions of the DeGance and Atherton [11] fits:

$$\begin{aligned} S' &= 1 - \psi \exp\left[-3.6372 + 0.8813 \ln(N_{\text{hold}}) - 0.1335(\ln(N_{\text{hold}}))^2 \right. \\ &\quad \left. +0.018534(\ln(N_{\text{hold}}))^3 - 0.001066(\ln(N_{\text{hold}}))^4\right] \end{aligned}$$

provided that if N_{hold} is outside certain bounds,

$$S' = \begin{cases} 1 - \psi(1 - \frac{211.5480647974693}{N_{\text{hold}}}) & , \quad N_{\text{hold}} > 1000 \\ 1 - 0.00131950127\psi & , \quad N_{\text{hold}} < 0.1 \end{cases} .$$

I have slightly altered these conditions from those in [11], to ensure that a smooth transition is seen at the bounds, to more than eight decimal places, as N_{hold} is varied. The resulting graph of the ratio of liquid holdup to ψ, $R_l/\psi = (1 - S')/\psi$, is plotted against N_{hold} in Fig (33), and looks the same as the equivalent plot in [11].

Also, it was found necessary to be very careful about the rate at which the ratio of liquid holdup to ψ approaches the value 1, as $U_{SG} \to 0$ (that is, as $N_{\text{hold}} \to \infty$), since a too-rapid approach to zero can lead to negative saturations at very low vapour content. This can affect simulations particularly near the flash point, when saturations are very small.

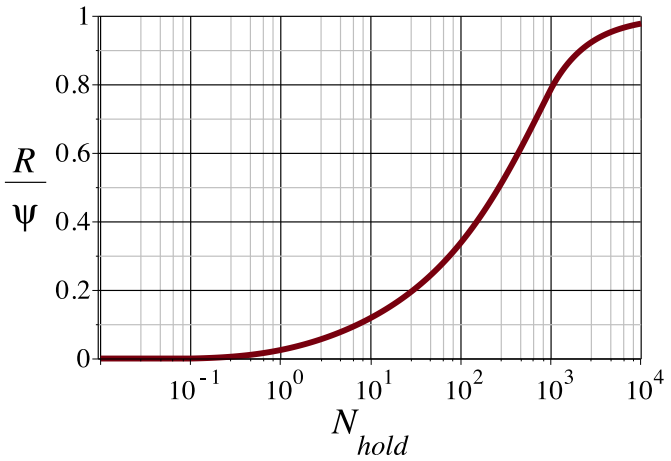

Figure 33: A graph of the correlation presented here, of R_l/ψ against N_{hold}, a slight modification of the Hagedorn and Brown correlation.

Furthermore,

$$N_{\text{hold}} = C_n \left(\frac{N_{lv}}{N_{gv}^{0.575}}\right) \left(\frac{P}{1.01325 \times 10^5}\right)^{0.1} \left(\frac{10^6}{N_d}\right) ,$$

where

$$C_n = \exp[-4.895 - 1.0775 \ln N_l - 0.80822(\ln N_l)^2 - 0.1597(\ln N_l)^3 - 0.01019(\ln N_l)^4] \ ,$$

provided that also

$$C_n = \begin{cases} 0.011440529 & N_l > 0.4 \\ 0.0018693617 & N_l < 0.002 \end{cases} \ ,$$

and where

$$\psi = 1 + \exp[6.6598 + 8.8173 \ln N_{sec} + 3.7693(\ln N_{sec})^2 + 0.5359(\ln N_{sec})^3] \ ,$$

with the limits

$$\psi = \begin{cases} 1.0 + 0.17536897977 N_{sec} & N_{sec} < 0.01 \\ 1.8200679697 & N_{sec} > 0.0857938 \end{cases} \ ,$$

where the limits on ψ and C_n have been refined to make them monotonic, and smoother (to seven decimal places) at the limits. The decay of ψ to 1.0 for small N_{sec} (rather than setting ψ exactly to 1.0 for small N_{sec}) is set so that small values of saturation can be explored near the flash point. The formulae presented above for C_n and ψ are graphed in figs. (34) and (35), and look the same as the graphs used by [11] to deduce their formulae for the Hagedorn and Brown correlation.

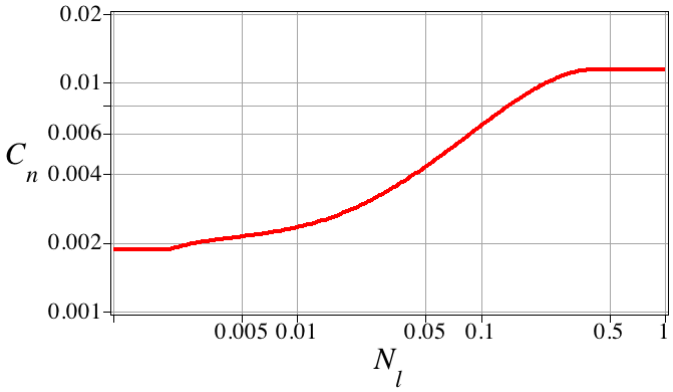

Figure 34: A graph of the function C_n versus N_l used in the Hagedorn and Brown correlation.

Finally, we have

$$N_{sec} = \frac{N_{gv} N_l^{0.38}}{N_d^{2.14}} \ ,$$

and the dimensionless numbers N_{lv}, N_{gv}, N_l, N_d are as defined in eqns (85) to (88) in the previous section on the Duns and Ros correlation.

Note that in [11, 7] the definitions of these numbers appear at first sight to be missing the gravitational terms — these are absorbed into the coefficients used there. The different conversion factors used in [11, 7] arise because surface tension is in different units to the other parameters (petroleum engineering units have been used), and because gravity has been absorbed into these factors also.

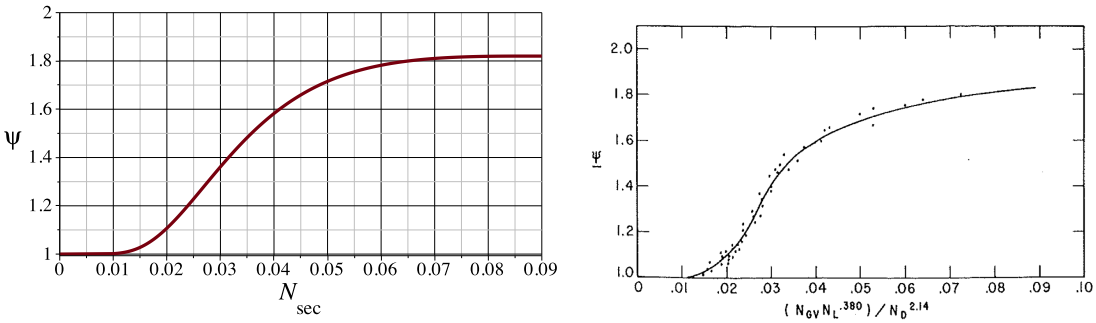

Figure 35: A graph of the function ψ versus N_{sec} used in the Hagedorn and Brown correlation. Plotted alongside of this for comparison is the corresponding figure from the original publication of Hagedorn and Brown.

F.7.2 Implementing the Hagedorn and Brown correlation

Fig. (36) shows a graph of the pressure gradients typically obtained versus a range of values of U_{SG} as input to the forwards Hagedorn and Brown correlation as described in the previous section and coded into Fortran. Note that there are ranges of pressure gradient, especially for lower pressure values and higher flowrates, where there are two values of U_{SG} for one value of pressure gradient. That is, the correlation is sometimes noninvertible — given a pressure gradient, there may be two values of U_{SG} matching it. This corresponds to the observation made by Hagedorn and Brown ([21], p.480) that sometimes there is a reversal in the curvature of the pressure-depth traverses near the top of the well, and that the correlation for ψ matches this reversal with a high degree of accuracy.

Figure (38) shows more detail near zero U_{SG} (and for a slightly different value of S), and illustrates that S' does go to zero as U_{SG} goes to zero, and that the pressure gradient goes closer to liquid static, which dominates the friction gradient, in contrast to what happens near pure vapour, where friction gradient dominates. Figure (37) shows computed total pressure gradient versus U_{SG}, together with the values of friction pressure gradient, gravitational pressure gradient, pseudo-saturation S', and homogeneous saturation. It is clear from the figure that the pseudo-saturation is in a one-to-one relationship with U_{SG}. It also clear from this figure that the interaction between an increasing friction pressure gradient (with increasing U_{SG}) and a decreasing gravitational pressure gradient, is the cause of the noninvertibility of the overall pressure gradient.

The way forward is to use saturation as a measure of pseudo-saturation. This is uniquely given by the value of U_{SG}. While Hagedorn and Brown acknowledge that pseudo-saturation is not necessarily the same as actual saturation, they also note that they take some trouble to use realistic values for the contribution of friction to pressure drop, and this leads to pseudo-saturation values that should be close to the true saturation.

The pseudo-saturation S' is seen in fig. (37) to be sometimes greater than the homogeneous

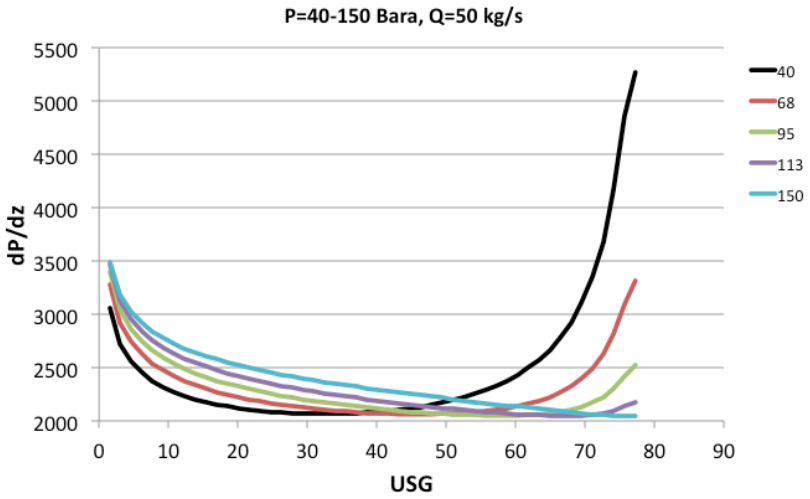

Figure 36: A plot of the pressure gradient obtained (Pa/m), versus U_{SG} value input to the Hagedorn and Brown correlation, for each of five different pressure values. Parameter values set are $S = 0.44$, pressure range is 40–150 bars, $Q = 50$ kg/s.

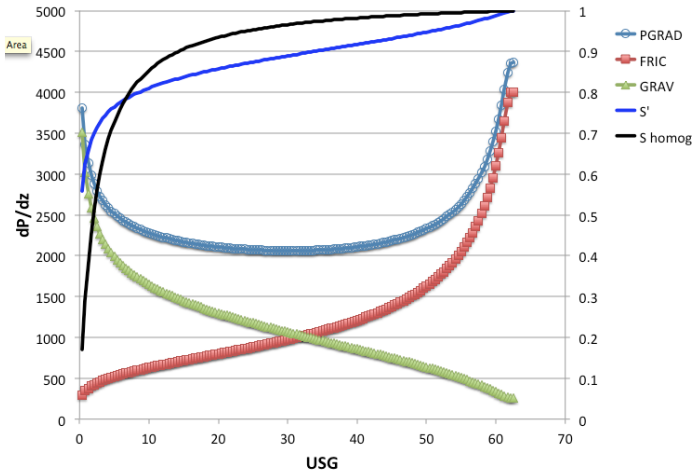

Figure 37: A plot of the pressure gradient obtained (Pa/m), versus U_{SG} value input to the Hagedorn and Brown correlation, for $P = 40$ bara, $S = 0.8$, $Q = 50$ kg/s. Also shown are the contributions from friction and gravity, as pressure gradients. Also plotted are the pseudo-saturation S' and the homogeneous saturation, which forms an upper limit on what the value of true saturation can be.

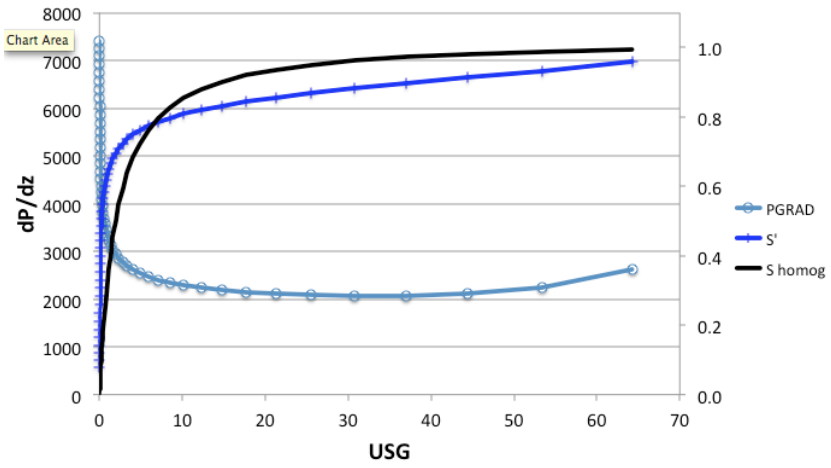

Figure 38: A plot of the pressure gradient obtained (Pa/m), versus U_{SG} value input to the Hagedorn and Brown correlation, for $P = 40$ bara, $S = 0.44$, $Q = 50$ kg/s, showing more detail near zero U_{SG} values. Also shown are the pseudo-saturation S' and the homogeneous saturation, which forms an upper limit on what the value of true saturation can be.

value from eqn (96) ,

$$S_H = U_{SG}/(U_{SG} + U_{SL}) \; .$$

This is unphysical if S' is interpreted as actual saturation, since the homogeneous saturation corresponds to equal gas and liquid phase velocities, and for upflow vapor can not flow slower than the liquid phase since the vapour phase is more buoyant.

Hence it is necessary to set S equal to the smaller of S' and S_H, as illustrated in figure (39). In this figure, we see a shortcoming of the correlation — it has S' values greater than the maximum possible (homogeneous flow) value; that is, at a given saturation, the gas flow velocity is less than the liquid phase flow velocity there, which is unphysical. So in SwelFlo, if this happens, homogeneous flow is used. In homogeneous flow, there is no slip between gas and liquid, which is also not very realistic for bubble flow. Steam fractions are very small here which may help reduce the impact of the homogeneous assumption on downhole profiles.

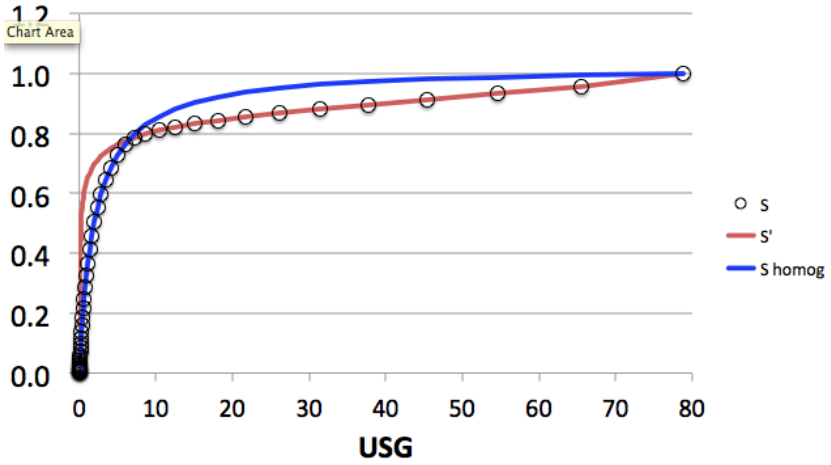

Figure 39: A plot of the saturation obtained, versus U_{SG} value input to the Hagedorn and Brown correlation, for $P = 40$ bara, $S = 0.9$, $Q = 50$ kg/s, showing more detail near zero U_{SG} values. Also shown are the pseudo-saturation S' and the homogeneous saturation, which forms an upper limit on what the value of true saturation can be.

G Choking

As noted in, for example, [3, 4], when the speed of a fluid flow in a pipe reaches the speed of sound, any further increase in the pressure difference driving that flow has no observed effect on the flow rate, and the flow is called choked.

Choking corresponds mathematically to a steady solution to the conservation equations ceasing to exist, if one begins at bottomhole and integrates upwards to a depth where the speed of sound is exceeded by the velocity of a component.

Physically the cause is that in a time-varying flow, pressure differences propagate at the speed of sound, so that if a flow is going at the speed of sound then any information about a change in pressure downstream cannot propagate upstream, so cannot change the flow upstream.

Another view is that explained in Chisholm [10], that choking occurs when the entire pressure gradient is accounted for by the momentum flux term, leaving no possibility of accounting for friction or gravitational terms.

The method used in SwelFlo is the same as in GWELL, and is based on the lecture notes by Kjaran and Eliasson [22]. The choke velocity is estimated as

$$u_{CH} = \sqrt{\frac{k_m}{\rho_m}}$$

where k_m is a two-phase fluid bulk modulus defined by

$$\frac{1}{k_m} = \frac{S}{k_v} + \frac{1-S}{k_l}$$

where each individual phase bulk modulus, for subscripts v for vapor and l for liquid, is given by

$$k = \rho \frac{dP}{d\rho} \ .$$

If the two-phase mean velocity $Su_v + (1-S)u_l$ exceeds the choke velocity u_{CH}, the user is warned in the last column of the main output file, with the word CHOKED at the depths that choking occurs. If the two-phase mean velocity exceeds twice the choke velocity, the simulation is stopped and the user is warned that choking occurred. Choking is more commonly observed in bottom-up simulations.

The subroutine that checks for choking is a separate calculation, included as an extra check on the solution obtained. I expect that solving the conservation equations becomes difficult when choking is encountered, giving non-convergence of the Newton method, separately to the choking check being discussed here.

H Non-condensable Gases

The effect of non-condensable gas in geothermal fluid is to alter the saturation curve for pure water, due to the effects of partial pressure of the non-condensable gases. The most prevalent such gas is carbon dioxide, which is used in SwelFlo as a proxy for all such gases.

In particular, if the temperature of liquid-phase liquid is raised, it begins to boil at a temperature (the bubble point) that is below the pure water saturation value. On the other hand, if the temperature of vapor-phase is lowered, it begins to form liquid droplets at almost the same temperature as the pure water saturation value. Hence the single line that is a saturation curve for pure water, opens out into a two-phase region when carbon dioxide is present. The more carbon dioxide, the wider the two-phase region opens out. An illustration for a percentage by mass of carbon dioxide, XCO2=0.01% is in Fig. (40).

The conservation equations for pure water still hold, provided the liquid water phase is replaced with the liquid phase (water and dissolved carbon dioxide) and the steam phase is replaced with the vapor phase, with partial pressures of the water (steam) component and of the carbon dioxide component adding to produce the total vapor pressure.

The presence of even just a little carbon dioxide then means that the two-phase line is replaced by a two-phase region, so that in principle, the static steam dryness X is now dependent on pressure and temperature and XCO2. Given any three values in the set X, P, T, XCO_2, the other value is then determined, for a two-phase fluid. Usually XCO_2 is given or known, and P is retained as a primary variable. SwelFlo retains T as the third primary variable, and determines X and other secondary variables like enthalpy as a consequence.

H.1 Phase states

A sequence of checks provides the state of the fluid, liquid (water plus carbon dioxide in solution), two-phase (liquid water with carbon dioxide in solution, steam, and carbon dioxide in gas form), and vapor (water and carbon dioxide both purely in vapor phase).

H.1.1 Liquid

The mixture is all liquid if the total pressure is greater than the saturation pressure of pure water at the given temperature, and the solubility of CO_2 in water is greater than the given value of XCO_2.

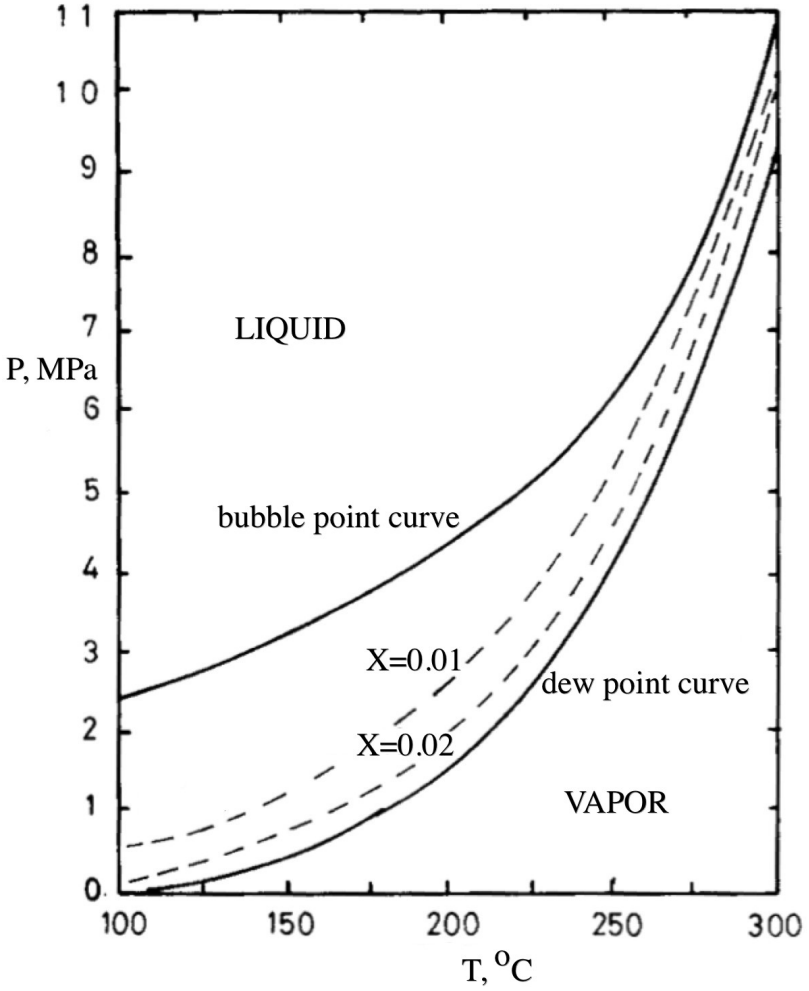

Figure 40: Phase diagram for water with 0.01% XCO2. The solid curves show bubble point (boiling point) and dew point (condensation point), while the dashed curves are contours of constant static steam mass fraction, inside the two-phase region between bubble point and dew point. The dew point curve is only slightly higher than the saturation curve for pure water.

H.1.2 Two-phase

If the total pressure is greater than the saturation pressure of pure water at the given temperature, but the solubility of carbon dioxide in pure water is less than the given value of XCO_2, then a gas phase will also exist, and the fluid is two-phase.

H.1.3 Vapor

If the total pressure is less than or equal to the saturation pressure of pure water at the given temperature $P_S(T)$, the fluid is all in the gas state.

H.2 Solubility of Carbon Dioxide

The relative amounts of carbon dioxide dissolved in the liquid phase and present in the gas phase is determined by solubility. Work by Takenouchi and Kennedy [33] and by Ellis and Golding [15] is used. Pritchett et al [30] fitted the following relationship to the data gathered by [33]:

$$\mathrm{XC}_l = \frac{P_{\mathrm{CO2}}}{A + BP_{\mathrm{CO2}}}$$

where XC_l is the mass fraction of carbon dioxide dissolved in liquid water, and $P_{\mathrm{CO2}} = P - P_S(T)$ is the partial pressure of carbon dioxide in the coexisting gas phase. The values of A and B depend on temperature as

$$A = a_1 + a_1 T + a_2 T^2 \,, \quad B = b_1 + b_1 T + b_2 T^2$$

where the values of a_i and b_i are given in Table 7.

i	a_i	b_i
1	1.03549E+03	2.04465E+01
2	1.60369E+01	-1.07449E-01
3	-4.83594E-02	1.44701E-04

Table 7: The coefficients in the quadratic dependence of A and B on temperature, for calculation of the solubility of carbon dioxide in water.

H.3 Mass Fraction of Carbon Dioxide in Gas

The mass fraction of carbon dioxide in the vapor phase which is in equilibrium with the liquid phase can be calculated in different ways. One way is described by the following fit to the

results of Takenouchi and Kennedy [33]:

$$\mathrm{XC}_v = \frac{P_{\mathrm{CO2}}}{P} \ ,$$

where XC_v is the mass fraction of carbon dioxide in the vapor phase. This is used in GWELL with a statement that it is better than Dalton's law for matching downhole data. A reference is also made to Pritchett et al [30], and in this manuscript a very detailed set of instructions for determining the state of geothermal fluid in the presence of carbon dioxide is presented. In particular, Pritchett et al note that for states of geothermal interest, the above expression is a good fit to the experimental data of Takenouchi & Kennedy [33].

Furthermore, Sutton [32] notes that the above expression, relating the masses of carbon dioxide and water in the vapor phase rather than the mole fractions (Daltons Law says the mole fraction should be used), gives a better fit to the data of Malanin [24], Todheide & Franck [35], and Takenouchi & Kennedy [33], for pressures between 100 and 300 bars. The fit is within 5% for temperatures in the range 110–280°C and within 25% for temperatures in the range 300–330°C.

An alternative approach for ideal gases is based on Dalton's law. Dalton's law states that the sum of the partial pressures of carbon dioxide and of water is the total pressure. Combining Dalton's law with the ideal gas law gives

$$P = P_s + P_{\mathrm{CO2}} = n_w RT/V + n_c RT/V$$

where P_s is the partial pressure of water component or saturation pressure, P is total pressure, and n_w is the number of moles of water present in the vapor phase, and n_c is the number of moles of carbon dioxide present in the vapor phase, both in the same volume V of vapor, and at the same temperature T.

Then it follows that

$$\frac{P_{\mathrm{CO2}}}{P} = \frac{n_c}{n_c + n_w} = \mathrm{YC}_v$$

where $\mathrm{YC}_v = n_c/(n_c + n_w)$ is the mole fraction of carbon dioxide in the vapor phase. Since the molar mass of carbon dioxide is 44, and of water is 18, the mass fraction of CO_2 in the vapor phase can be written as

$$\mathrm{XC}_v = \frac{44\,\mathrm{YC}_v}{44\,\mathrm{YC}_v + 18(1 - \mathrm{YC}_v)} \ .$$

so that mole fraction can be written in terms of mass fraction by rearranging this to give

$$\mathrm{YC}_v = \frac{18\mathrm{XC}_v}{18\mathrm{XC}_v + 44(1 - \mathrm{XC}_v)} \ .$$

A plot of XC_v against YC_v (Fig. 41) reveals that XC_v is larger, so that switching from the GWELL mass fraction formulation to Dalton's law will lead to smaller partial pressures of carbon dioxide, given XC_v, or to larger values of XC_v, given a value for P_{CO2}.

Note that Battistelli et al [2] describe a modified Equation of State module for the geothermal reservoir simulator TOUGH2, designed to handle three-component mixtures of water, sodium chloride and a non-condensible gas. Their algorithm for linking the partial pressure of the gas with the mass fraction of gas in the vapor phase, is to assume densities combine as for an ideal gas, so that total vapor phase density is the sum of the water vapor density at saturation pressure for the brine, and the density of the non-condensible gas at the partial pressure of that gas. Then the mass fraction of the vapor that is non-condensible gas is the ratio of the density of the gas to the total density of the vapor phase. This leads to exactly the same expression for mass fraction as that derived above using Dalton's Law.

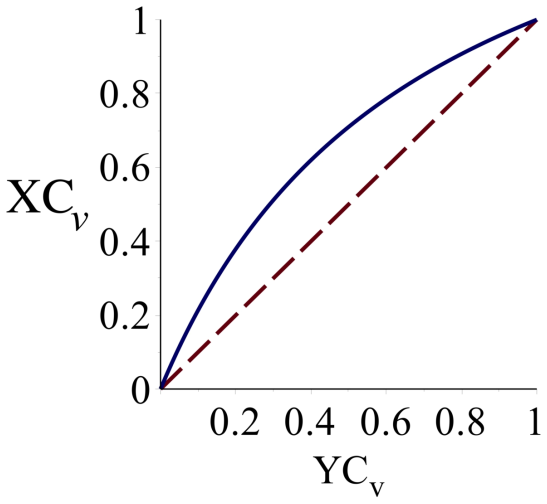

Figure 41: Mass fraction of CO_2 in the vapor phase XC_v, versus the mole fraction in the vapor phase YC_v.

SwelFlo allows the user to choose to use the GWELL mass fraction formulation

$$\mathrm{XC}_v = \mathrm{XC}_v^M = \frac{P_{\mathrm{CO2}}}{P} \ ,$$

or the Dalton's Law formulation

$$\mathrm{XC}_v = \mathrm{XC}_v^D = \frac{44\,\mathrm{YC}_v}{44\,\mathrm{YC}_v + 18(1-\mathrm{YC}_v)} \ ,$$

where

$$\mathrm{YC}_v = \frac{P_{\mathrm{CO2}}}{P} \ ,$$

or the user can choose a combination that lies between these two options,

$$\mathrm{XC}_v = r\mathrm{XC}_v^D + (1-r)\mathrm{XC}_v^G$$

by setting the parameter r to a value between zero and one on a slider control.

For pure vapor, both choices have

$$\mathrm{XC}_v = XCO_2 \ .$$

Then for the GWELL mass fraction, the partial pressure of carbon dioxide is given by $P_c = \mathrm{XC}_v P$. For the Dalton's Law formulation, the partial pressure of carbon dioxide is given by $P_c = \mathrm{YC}_v P$. The combination option uses

$$P_c = (r\mathrm{YC}_v + (1-r)\mathrm{XC}_v)P \ .$$

Given the careful comparisons made by Pritchett et al and by Sutton, we recommend using the mass fraction option, not the Dalton's Law or the combination option.

H.4 Computation of the Phase State

The logic used to decide the phase state is the same as that used by Pritchett et al [30] and in GWELL. The approach is first to check if $P \leq P_S$, in which case everything is in the vapor phase. Otherwise, solubility XC_l is checked at the partial pressure of carbon dioxide $P_{\mathrm{CO2}} = P - P_S$.

If solubility exceeds the total mass fraction of carbon dioxide present, the phase is all liquid. Otherwise, the mass fraction XC_v in the vapor phase is computed as in the previous subsection, and the formula

$$X = \frac{XCO_2 - \mathrm{XC}_l}{\mathrm{XC}_v - \mathrm{XC}_l} \tag{109}$$

is used to determine a steam dryness X. This dryness is in turn used to check again finally that the state really is two-phase, or if X is effectively zero or one.

If fluid is not moving, the dryness X determined by the above equation is the static steam fraction, since the mass of carbon dioxide in M_{water} kg of water-gas mixture consisting of M_{liquid} of liquid phase and M_{vapor} of vapour phase, is given by

$$XCO_2 \ M_{\mathrm{water}} = \mathrm{XC}_l M_{\mathrm{liquid}} + \mathrm{XC}_v M_{\mathrm{vapor}}$$

which on dividing through by M_{water} gives

$$XCO_2 = \mathrm{XC}_l(1-X) + \mathrm{XC}_v X \ .$$

In the above equation, $X = M_{\mathrm{vapor}}/M_{\mathrm{water}}$ is the static steam fraction. It rearranges to give eqn (109).

If fluid is moving, as in a producing well, conservation of carbon dioxide gives

$$XCO_2 \ Q = \mathrm{XC}_l M_l + \mathrm{XC}_v M_v$$

which on dividing through by Q gives

$$XCO_2 = \mathrm{XC}_l(1-X_{\mathrm{flo}}) + \mathrm{XC}_v X_{\mathrm{flo}} \ ,$$

since $X_{\rm flo} = M_v/Q$. This rearranges to give eqn (109) with flowing steam quality, that is,

$$X_{\rm flo} = \frac{XCO_2 - {\rm XC}_l}{{\rm XC}_v - {\rm XC}_l} \ . \tag{110}$$

Hence flowing steam quality is determined by mass conservation, P, T, and gas fraction XCO_2, when the two-phase mixture is flowing in a wellbore.

H.5 Finding Pressure

The equation (110) may be rearranged, together with the law ${\rm XC}_v = \frac{P_{\rm CO2}}{P}$, to obtain an equation that gives a quadratic equation for pressure in terms of $X_{\rm flo}$, T, and gas fraction XCO_2, as follows.

$$XCO_2 = X_{\rm flo}\left(\frac{P - P_s}{P}\right) + (1 - X_{\rm flo})\left(\frac{P - P_s}{A + B(P - P_s)}\right) \ ,$$

where P_s is the saturation pressure for pure water in bars absolute at temperature T. This rearranges to give the quadratic in P (in bars, not Pa):

$$aP^2 + bP + c = 0 \ ,$$

where

$$\begin{aligned} a &= B(XCO_2 - X_{\rm flo}) - 1 + X_{\rm flo} \\ b &= A(XCO_2 - X_{\rm flo}) + BP_s(2X_{\rm flo} - XCO_2) + P_s(1 - X_{\rm flo}) \\ c &= P_s X_{\rm flo}(A - BP_s) \end{aligned}$$

where A, B and C are the temperature-dependent coefficients given above in subsection (H.2).

The above rearrangement is only valid if the mass based empirical law ${\rm XC}_v = \frac{P_{\rm CO2}}{P}$ is used to relate steam mass fraction to partial pressure. If Dalton's Law is used, the quadratic to be solved for the partial pressure $P_{\rm CO2}$ in bars is

$$a_d P_{\rm CO2}^2 + b_d P_{\rm CO2} + c_d = 0 \ ,$$

where

$$\begin{aligned} a_d &= 44(B(XCO_2 - X_{\rm flo}) - 1 + X_{\rm flo}) \\ b_d &= 44A(XCO_2 - X_{\rm flo}) + 18P_s(B\ XCO_2 + X_{\rm flo} - 1) \\ c_d &= 18A\ P_s X_{\rm flo} \end{aligned}$$

If a combination of the mass and Dalton's laws, is chosen by the user, then an iterative method is used to find pressure given flowing steam fraction and temperature, from the method in subsection (H.4).

H.6 Density, Viscosity, Enthalpy, Surface Tension of Carbon Dioxide

The next six pages are lifted from the GWELL manual, as the code is taken directly from GWELL code.

where,

α_{vCO2} = mass fraction CO_2 in gas phase
P_{CO2} = partial pressure of CO_2 as expressed by Equation (5.2)
P = the total pressure

For cases of dry gas (all gas state), the above relation becomes,

$$\alpha_{CO2} = \frac{P_{CO2}}{P} \qquad (5.6)$$

where,

α_{CO2} = total mass fraction of CO_2

Equations 5.5 and 5.6 above fit the experimental data better than Dalton's Law, which states that the mole fraction of the component gas is proportional to its partial pressure.

5.1.3 DENSITY

5.1.3.1 Carbon Dioxide (CO_2)

The density of CO_2 is calculated from the expression obtained from Pritchett et al. (1981).

$$\rho_{CO2} = \frac{P_b}{z(P_b, T_K)\ R\ T_K} \times 10^9 \qquad (5.7)$$

where,

ρ_{CO2} = density of CO_2 in kg/m^3
R = the gas constant, 1.88919E6 erg/g-°K
T_K = temperature in °K
P_b = pressure in bars
$z(P_b, T_K)$ = gas compressibility factor evaluated using an analytical fit of the data by Vargaftik (1975).

For pressures less than 300 bars,

$$z(P_b,T_K) = A + B(P_b - 300) + C(P_b - 300)^2 + D(P_b - 300)^3 + E(P_b - 300)^4 \qquad (5.8)$$

For pressures greater than 300 bars,

$$z(P_b,T_K) = A + B(P_b-300) + F(P_b-300)^2 \qquad (5.9)$$

where,

P_b = the pressure in bars

T_K = the temperature in °K

The temperature dependent coefficients are evaluated from,

$$A = A_0 + A_1T_K + A_2T_K^2 + A_3T_K^3 + A_4T_K^4 \qquad (5.10)$$

$$B = B_0 + B_1T_K + B_2T_K^2 + B_3T_K^3 + B_4T_K^4 \qquad (5.11)$$

$$C = C_0 + C_1T_K + C_2T_K^2 + C_3T_K^3 + C_4T_K^4 \qquad (5.12)$$

$$D = D_0 + D_1T_K + D_2T_K^2 + D_3T_K^3 + D_4T_K^4 \qquad (5.13)$$

$$E = \frac{1 - A + 300B - 300^2C + 300^3D}{300^4} \qquad (5.14)$$

$$F = F_0 + F_1T_K + F_2T_K^2 + F_3T_K^3 + F_4T_K^4 \qquad (5.15)$$

The values of the coefficients given in Table 5.2 give a satisfactory fit to the experimental data between 77 to 350°C.

TABLE 5.2

VALUES OF COEFFICIENTS FOR CALCULATION OF CO_2 DENSITY

	A	B	C	D	F
0	8.09759	-3.62183E-02	-3.43992E-03	-2.10949E-05	6.82528E-05
1	-7.10670E-02	3.73836E-04	2.77555E-05	1.66021E-07	-6.70714E-07
2	2.38501E-04	-1.32285E-06	-8.30370E-08	-4.86891E-10	2.37181E-09
3	-3.36774E-07	1.97631E-09	1.09429E-10	6.31079E-13	-3.57746E-12
4	1.72976E-10	-1.06781E-12	-5.36712E-14	-3.05175E-16	1.95665E-15

5.1.3.2 Mixtures

5.1.3.2.1 Liquid

Since the amount of CO_2 dissolved in the liquid phase is small (low solubility of CO_2 in water), it is assumed that the density of the liquid is equal to the density of pure water at the same temperature. So,

$$\rho_l \approx \rho_{H2O} \qquad (5.16)$$

where,

ρ_l = the density of mixture
ρ_{H2O} = the density of pure water

5.1.3.2.2 Gas

For the gas mixture, the same expression used by Sutton (1976) and Pritchett et al. (1981) is used.

$$\rho_g = \rho_s + \rho_{CO2} \qquad (5.17)$$

where,

ρ_s = the density of steam
ρ_{CO2} = the density of CO_2

Both values of density are evaluated at the given temperature and corresponding partial pressures.

5.1.4 ENTHALPY

5.1.4.1 Carbon Dioxide (CO_2)

The enthalpy of CO_2 is evaluated using the formula given by Sweigert et al. (1946).

$$H_{CO2} = 1688 + 1.542T_K - 794.8LOG_{10}(T_K) - \frac{4.135E+04}{T_K} - \frac{3.571E-04\ P_{CO2}}{(T_K/100)^{10/3}}\ (1 + 7.576E-08P_{CO2}) \qquad (5.18)$$

where,

H_{CO2} = the enthalpy of CO_2 in kJ/kg
P_{CO2} = the partial pressure of CO_2 in Pa
T_K = the temperature in °K

5.1.4.2 Heat of Solution

The heat of solution of a gas is the change in enthalpy brought about by the dissolution of the gas in water. The equation of the heat of solution is calculated using a polynomial fit to the experimental data obtained by Ellis and Golding (1963) and is valid for temperatures in the range 100-300°C.

$$H_{soln} = -71.33 - 6.0198T + 0.07438T^2 - 2.9244E\text{-}04T^3 + 4.4522E\text{-}07T^4 \quad (5.19)$$

where,

H_{soln} = the heat of solution in kJ/kg
T = temperature in °C

5.1.4.3 Enthalpy of the Mixture

The enthalpy of the mixture is evaluated using,

$$H_m = xH_v + (1 - x)H_l \quad (5.20)$$

where,

x = mass fraction of gas phase
H_v = enthalpy of the gas phase in kJ/kg
H_l = enthalpy of the liquid phase in kJ/kg

The liquid and gas phase enthalpies are evaluated as average enthalpies of the different components weighted by their individual mass fractions.

$$H_l = (1 - \alpha_{lCO2})H_w + \alpha_{vCO2}(H_{CO2} + H_{soln}) \quad (5.21)$$

and,

$$H_v = (1 - \alpha_{vCO2})H_s + \alpha_{vCO2} H_{CO2} \quad (5.22)$$

where,

α = mass fraction CO_2
H = enthalpy, kJ/kg

The subscripts l, v, w, s, lCO2, vCO2 and soln stand for liquid phase, gas phase, water, steam, CO_2 in liquid phase, CO_2 in gas phase and solution respectively.

The total mass fraction of the gas phase, x, is calculated using a mass balance on CO_2.

$$x = \frac{\alpha_{CO2} - \alpha_{lCO2}}{\alpha_{vCO2} - \alpha_{lCO2}} \qquad (5.23)$$

5.1.5 VISCOSITY

5.1.5.1 Carbon Dioxide (CO_2)

Fits to the viscosity of CO_2 as a function of pressure and temperature are based on the data tabulated by Vargaftik (1975). For the viscosity, μ_{CO2}, in poise,

$$\mu_{CO2} = (A + BT + CT^2 + DT^3 + ET^4) \times 10^{-8} \qquad (5.24)$$

where,

T = temperature in °C

The pressure dependent coefficients are found from the linear interpolation between the tabulated values in Table 5.3.

5.1.5.2 Mixture

The viscosity of the liquid phase is assumed to be approximately equal to the viscosity of pure water since the amount of dissolved CO_2 is small. For the gas phase, a weighted average is used.

$$\mu_l \approx \mu_{H2O} \qquad (5.25)$$

$$\mu_v = \alpha_{vCO2}\,\mu_{CO2} + (1 - \alpha_{vCO2})\,\mu_s \qquad (5.26)$$

5.1.6 SURFACE TENSION

The effect of CO_2 on the surface tension of water has been studied by Heuer (1957) as part of his Ph.D. dissertation. He measured the interfacial tension of H_2O-CO_2 at different temperatures and partial pressures of CO_2 (P_{CO2}). The results are shown in Figure 5.3.

TABLE 5.3

VALUES OF COEFFICIENTS FOR CALCULATION OF CO_2 VISCOSITY

P (bars)	A	B	C	D	E
0	1357.8	4.9227	-2.96610E-03	2.85290E-06	-2.18290E-09
100	3918.9	-35.984	2.58250E-01	-7.11780E-04	6.95780E-07
150	9660.7	-135.479	9.00870E-01	-2.47270E-03	2.41560E-06
200	13156.6	-179.352	1.12474	-2.98864E-03	2.85911E-06
300	14796.8	-160.731	8.50257E-01	-1.99076E-03	1.73423E-06
400	15758.3	-144.887	6.73731E-01	-1.41990E-03	1.13548E-06
500	16171.6	-125.341	5.00750E-01	-9.04721E-04	6.19087E-07
600	16839.4	-115.700	4.08927E-01	-6.35032E-04	3.53981E-07

Although the results showed that interfacial tension decreases with increasing P_{CO2}, partial pressures greater than 10 bars at the wellhead rarely occur in geothermal well discharge fluids. At P_{CO2} lower than 10 bars, the decrease in surface tension is less than 15%. Therefore in this study, the interfacial tension of H_2O-CO_2 is assumed to be approximately the same as that for pure water.

$$\sigma_m \approx \sigma_{H2O} \qquad (5.27)$$

where,

σ_m = surface tension of mixture

σ_{H2O} = surface tension of water

5.2 WATER-SODIUM CHLORIDE SYSTEM (H_2O-NACL)

The total dissolved solids in geothermal brines varies from that of ordinary well water up to concentrated solutions as high as 40% by weight. Sodium chloride (NaCl) is typically 70 to 80% of the total dissolved solids. The other most abundant components are potassium chloride (KCl), calcium chloride ($CaCl_2$) and silica (SiO_2). The silica concentration in geothermal brines is usually between 200 and 600 ppm (Wahl, 1977). Since NaCl is the major component of the total dissolved solids, the geothermal brine can be treated as a solution of NaCl in water to evaluate its fluid properties. The principal effects of dissolved solids are boiling point elevation, increased viscosity, increased density, increased surface tension and decreased specific heat.

I Corrected Area Treatment

A careful derivation of the equations for conservation of momentum reveals that the usual form taken for the acceleration term (that is, the momentum flux term) is only correct for constant area, and is incorrect at places where the casing size changes. Correct versions can be found in [25, 34, 37], and are reviewed briefly here.

The momentum conservation equation, after careful averaging of the three-dimensional form across the wellbore cross-sectional area, is usually written as

$$\frac{\partial p}{\partial z} = -\frac{1}{A}\frac{\partial}{\partial z}(AC_{vv}S\rho_v u_v^2 + AC_{vl}(1-S)\rho_l u_l^2) - \frac{2f}{D} < \rho v|v| > +\rho_m g\sin\theta \ , \tag{111}$$

where $< \rho v|v| >$ is an appropriate average value, $\rho_m \equiv S\rho_v + (1-S)\rho_l$ is the usual two-phase average fluid density, and f takes account of two-phase correlations but is related to the Fanning friction factor, which is equal to the Darcy or Moody friction factor divided by four. The correlation coefficients C_{vv} and C_{vl} are less than but of the order of one, and account for the fact that the average of the square of velocity is not the square of the average velocity, over the cross-section of the well.

The first term on the right-hand side, the momentum flux term, is often rewritten in a number of ways. We note here some alternative forms for the momentum flux, based on rewriting

$$C_{vv}S\rho_v u_v^2 + C_{vl}(1-S)\rho_l u_l^2 = Gu_m = G^2 v_e$$

where u_m is a flowing average velocity

$$u_m = C_{vv}Xu_v + C_{vl}(1-X)u_l$$

and X is the flowing steam quality, the steam mass flow rate divided by the total mass flowrate

$$X = \frac{M_v}{Q} = \frac{AS\rho_v u_v}{Q} \ .$$

The second form uses the effective specific volume

$$v_e = \left[\frac{C_{vv}X}{\rho_v} + \frac{KC_{vl}(1-X)}{\rho_l}\right]\left[X + \frac{1-X}{K}\right]$$

where $K \equiv \frac{u_v}{u_l}$ is the slip.

It is useful to note that

$$\frac{u_v}{u_l} = \left(\frac{X}{1-X}\right)\left(\frac{1-S}{S}\right)\left(\frac{\rho_l}{\rho_v}\right)$$

when deriving the above alternative forms for part of the momentum flux.

Then the momentum flux term can also be written in the forms

$$-\frac{1}{A}\frac{\partial}{\partial z}(Qu_m)$$

since $AG = Q$ is a constant, or using the second form above (see also [37, eqn. 14]),

$$-\frac{1}{A}\frac{\partial}{\partial z}(AG^2 v_e) \ ,$$

or

$$-\frac{1}{A}\frac{\partial}{\partial z}(QGv_e) \ ,$$

or, bringing the constant Q outside the derivative,

$$-G\frac{\partial}{\partial z}(Gv_e) \ .$$

Then conservation of momentum is often written as an expression for the pressure gradient down a geothermal well, as the sum of the divergence of the momentum flux, the frictional losses, and the gravitational or static pressure gradient,

$$\frac{\partial p}{\partial z} = -\frac{1}{A}\frac{\partial}{\partial z}(Qu_m) - \frac{2f}{D} < \rho v|v| > +\rho_m g \sin\theta \ , \tag{112}$$

and since $AG = Q$ is the steady mass flowrate, Q can be brought outside the derivative in the momentum flux term, so that momentum conservation can be written as

$$\frac{\partial p}{\partial z} = -G\frac{\partial}{\partial z}(u_m) - \frac{2f}{D} < \rho v|v| > +\rho_m g \sin\theta \ , \tag{113}$$

Chisholm's version of the momentum flux term relies on A being constant, since he writes

$$-G^2\frac{\partial v_e}{\partial z} \ ,$$

which relies on A (or equivalently G) being independent of z to bring it outside the derivative.

The momentum flux term in GWELL also is only correct if A is constant with depth, since GWELL uses the term $-\frac{\partial}{\partial z}(Gu_m)$ instead of $-G\frac{\partial}{\partial z}(u_m)$.

Both GWELL and Chisholm's versions, valid for constant area, are incorrect by about a factor of two at places where wellbore radius changes. Such places are also where the momentum flux term can dominate the pressure gradient, so the effect on pressure gradient there is significant. However, the effect of using the incorrect form, on overall pressure profile down a well, is typically still small [25].

The **Hagedorn and Brown correlation** uses a momentum flux term of the form

$$\left(\frac{dP}{dz}\right)_{\text{acc}} = -\frac{\rho_s}{2}\frac{d}{dz}(V_m^2) \ ,$$

where

$$V_m = U_{SG} + U_{SL} = Su_v + (1-S)u_l \ , \ \ \rho_s \equiv S'\rho_v + (1-S')\rho_l \ .$$

This assumes a constant area. It is not obvious how to include the effect of area depending on z, since the correlation uses homogeneous flow to compute V_m, then corrects using S'. Note that the correlation is not used to compute momentum conservation directly, only to calculate vapor and liquid phase velocities given temperature and saturation. Hence no changes have been made to it.

The **full Duns and Ros correlation** assumes zero momentum flux, except in the mist regime, where flow is taken to be homogeneous (so that liquid and vapor phase velocities are the same), and the momentum flux term is related to total pressure gradient as

$$\left(\frac{dp}{dz}\right)_{acc} = \frac{(U_{SG}+U_{SL})U_{SG}\rho_m}{P}\left(\frac{dp}{dz}\right)_t = \text{MF}\left(\frac{dp}{dz}\right)_t \quad \text{say} \ , \tag{114}$$

where P is pressure (Pa), and $\left(\frac{dp}{dz}\right)_t$ is the total pressure gradient.

Since the total pressure gradient term in the momentum conservation equation does not depend explicitly on $A(z)$, this method used to relate momentum flux gradient only to overall gradient cannot be used when area depends on z, since then momentum flux depends on z through both pressure and area. That is, the full Duns and Ros correlation cannot be upgraded in any obvious way to allow for area varying with depth, for mist flow.

The **Hadgu correlation** takes the usual form

$$-\frac{\partial}{\partial z}(Gu_m)$$

for bubble and mist regimes in the original constant area formulation, so I have modified it in the same way as above, that is, I have altered it to read

$$-G\frac{\partial}{\partial z}(u_m) \ .$$

However, in the slug and churn regimes a special correlation is used to correlate directly the gradient of the momentum flux, which depends on the velocity of the down-flowing fluid around the Taylor bubble, following the Fernandes *et al* [16] development. The correlation depends on the wellbore diameter, and does not adapt to conform to the variable $A(z)$ derivation here. Hence no attempt is made to do so for these two regimes under the Hadgu correlation.

It is uncommon to see area A included as a variable function of depth in the geothermal wellbore simulation literature — A is usually assumed to be independent of depth. An exception is that Taitel's horizontal flow modelling development [34] has variable area correctly included. The work by Yadigaroglu *et al* [37, eqn. 11] has the same form of momentum conservation equation as presented here in equation (111), and also presents the AG^2v_e form of the momentum flux [37, eqn. 14] .

The sign convention used above, that the velocity terms G, u_m, and v, are positive for flow in the direction of increasing z, that is, downwards in the well, is the opposite of the usual geothermal convention of positive velocities for upflow. Then the geothermal convention if used would reverse the sign on the friction term (only).

J Productivity Index at Feedpoints

The development in this section is explained more fully in [26].

The usual definition of feedpoint productivity P_1 is in t/hr/bar,

$$P_1 = \frac{\tilde{Q}}{\left(\tilde{P}_{\text{res}} - \tilde{P}_{\text{well}}\right)}$$

where $\tilde{Q}$ is the flowrate at the feed (t/hr), $\tilde{P}_{\text{res}}$ is reservoir pressure in bars, and $\tilde{P}_{\text{well}}$ is wellbore pressure in bars. This applies at a fixed downhole pressure and drawdown, and hence at given wellbore and reservoir viscosities. When increased production rates are simulated for an output curve, the wellbore viscosity can reduce appreciably, especially if the flashpoint reaches the feedpoint. To account for this change in viscosity, the above equation is usually rewritten guided by Darcy's law for flow, as

$$Q = \frac{\Sigma}{\nu}\left(P_{\text{res}} - P_{\text{well}}\right) \tag{115}$$

where the number Σ is called a *productivity index* (units m^3), ν is the kinematic viscosity ($\text{m}^2.\text{s}^{-1}$), and flowrate and pressures are now in kg/s and Pa. This productivity index is related to the more usual productivity P_1 by (after converting P_1 to SI units):

$$\Sigma = \frac{P_1\,\nu}{3.6 \times 10^5}\ .$$

The best way to calculate an output curve is to use equation (115) to calculate the flow Q at a feedpoint, given the pressure in the wellbore, since this properly accounts for the effects of changes in viscosity on feed flowrate — the productivity index Σ is independent of these, while the usual productivity does depend on the current value of viscosity.

The simulator will calculate a value for productivity index at bottomhole, for all feedpoint cases except that of dry steam drawdown. If an output curve is requested, this computed value will be used, unless a value has been provided explicitly in the input file and the type of feedpoint is type one (see the later section on input file setup).

This formulation is straightforward to apply when ν is roughly the same in the reservoir and in the wellbore. When ν depends strongly on pressure, as it does when flow becomes two-phase, some care is needed in calculating an effective value of ν, as it may vary considerably between reservoir and wellbore, due particularly to changes in fluid density. Carelessly calculated viscosity values can show up as anomalous drops in the flowrate, as pressure at bottomhole is decreased through the flashpoint, giving unusual looking output curves.

Equation (115) still holds for varying $\nu(P)$, with a pressure gradient dP/dr across a narrow region of practically constant pressure, in the form of Darcy's law,

$$W = -\frac{kA}{\nu(P)}\frac{dP}{dr} \ , \tag{116}$$

where k is an effective permeability to flow, W is the mass flow (positive if flowing outwards from the well), and A is the cross-sectional area the flow is passing through. Rearranging this, and using $Q = -W$ so that positive Q corresponds to production, and integrating from undisturbed reservoir to wellbore gives

$$\int \frac{dP}{\nu(P)} = \int \frac{Q}{kA} dr \ . \tag{117}$$

In a linear one-dimensional geometry, equation (117) becomes

$$\int_{P_{\rm well}}^{P_{\rm res}} \frac{dP}{\nu(P)} = \frac{QR}{kA} \ , \tag{118}$$

and putting $\Sigma = \frac{kA}{R}$ gives

$$Q = \Sigma \int_{P_{\rm well}}^{P_{\rm res}} \frac{dP}{\nu(P)} \ , \tag{119}$$

and comparison with (115) indicates that the effective viscosity should be written as

$$\frac{1}{\nu_{\rm eff}} = \frac{1}{P_{\rm res} - P_{\rm well}} \int_{P_{\rm well}}^{P_{\rm res}} \frac{dP}{\nu(P)} \ . \tag{120}$$

This is in the integrated sense the average value of $1/\nu$ when plotted against pressure. The same integral average formula for productivity index arises if a radially symmetric cylindrical or spherical geometry is used instead of linear. The simplest approximation to this would be the usual arithmetic average of $1/\nu$, using reservoir and wellbore values. This is however not very accurate in some situations — it can give non-monotonic flow dependence on the pressure difference $P_{\rm res} - P_{\rm well}$.

In particular, the form of equation (119) makes it clear that flowrate Q should be monotonic in the pressure difference $P_{\rm res} - P_{\rm well}$, since ν is always positive, so the area under the curve $1/\nu$ increases monotonically as the range of integration increases.

What is currently implemented in SwelFlo is to approximate the integral by using a twenty-one point trapezoidal rule, that gives good results and monotonic behaviour for flowrate versus pressure drop across the feedpoint.

Note that when flow is single phase, and/or the kinematic viscosity is practically constant, this formulation drops back to the simple case (115). The pseudopressure approach provides a smooth combination of both single and two-phase flow conditions.

The left-hand side of this equation may be understood by considering the concept of pseudopressure. The quasi-steady equation for isenthalpic flow in a porous medium is ([18], p.292)

$$\nabla \left(\frac{k}{\nu} \nabla P \right) = 0 \, , \tag{121}$$

where ν is in general the two-phase kinematic viscosity,

$$\frac{1}{\nu} = \frac{k_{rl}}{\nu_l} + \frac{k_{rv}}{\nu_v} \, ,$$

where k_{rl} and k_{rv} are relative permeabilities for liquid and steam, respectively, and ν_l and ν_v are kinematic viscosities for liquid and steam respectively.

Equation (121) can be rewritten as

$$\nabla^2 m = 0 \tag{122}$$

where the pseudopressure $m(P)$ is defined to be

$$m \equiv \int \frac{1}{\nu} \, dP \, .$$

Equation (122) then says that in general pseudopressure varies linearly with r in the steady state (while pressure does not, unless kinematic viscosity is constant), so that

$$\int_{P_{\text{well}}}^{P_{\text{res}}} \frac{dP}{\nu(P)} = CR \, , \tag{123}$$

where C is some constant, and R is the distance from the wellbore to the location that reservoir pressure is taken from.

K A Sample Input File

This is an example of the file SWFinput.txt, that is used by the program to save the simulation input setup between simulations. It is kept in the project directory, and is read by the simulator on startup, and whenever the project directory is changed. It is saved to whenever a simulation is run. It is not intended to be edited directly by the user, but indirectly by SwelFlo. However, it is just a text file and can be edited by the user if desired.

```
A template, used in absence of an input file. Prodn, flash in well.
One feed, topdown flow, Orkiszewski correlation. No output file asked for.
No reservoir T profile, one casing section 1000m vertical. Ready to run.
   1  1  0  0  0.000000  0 T F T T F  0.00  0.00  0  50
   0  (No data files)
   2  wellhead conditions
   800000.0  20.0  169.75  837557.42  920000.0 5.955E-002  0.10  1.0E-03
   0.0  0.0  0.0  0.00  0.00  0.00  0.0  0.0
   1.00000000E-003  0.0  0.0
   1000.000
   2.00
   2800.00
   1000.00
   604800.0
   1    casing section
  1000.000  0.100E+00  0.00E+00 0.200E+02   90.0    0.00    1
   0   (no reservoir profile)
   1    feed point
   1000.0  1  5500000.1  216.916  929860.0  0.0  1.0E-003  4.5052E-012  0.0
```

L GWELL coding errors

This is just a short note on some issues with the existing coding of the Armand and Orkiszewski correlations in GWELL, which also affect the computation of energy conservation in GWELL and in codes based on GWELL.

These issues arise around the meaning and use of dryness. In the GWELL code, dryness X is used interchangeably in

1. thermodynamic calculations where it reflects the void fraction [10] and is dryness for a static fluid or for a homogeneous flow with equal velocities for vapour and liquid phases, and
2. in correlations and in the energy conservation equation where it must be the flowing steam quality, or the ratio of the mass flow rate of vapour to the total mass flow rate

[10].

The correct dryness to use in the correlations (and in the Orkiszewski correlation, as noted explicitly in the GWELL manual) is X_{flow}, the ratio of steam mass flow rate to total mass flow rate, the flowing steam quality. This mass fraction is a flowing mass fraction, different to the in place mass fraction whenever vapour is flowing at a different velocity to liquid. Dryness (and enthalpy) measured at wellhead will in fact reflect this flowing mass fraction. But the thermodynamics of vapour/liquid/carbon dioxide equilibrium depend on saturation or mass fraction in place. GWELL's correlations and energy balance assume that the flowing dryness is the same as the dryness in place, which is generally incorrect. This manual describes corrected Orkiszewski and Armand correlations, as well as a more careful energy balance that reflects the flux of energy into and out of a computational element, rather than the existing GWELL energy conservation equation, which uses energy in place multiplied by total mass flow.

In GWELL, the variable X is used to denote both the static steam mass fraction solved for along with temperature in two-phase regions, and the flowing steam quality that appears in correlations, momentum conservation, energy conservation, friction calculations, and choking computations. The following GWELL subroutines are affected by the confusion between flowing steam quality and static steam fraction: ARMAND, CHOKED, ENERGY, FEED1, FEED2, FEED3, FRIC1, MOMENTUM, REGIME, RESMOM, and RESMOM2 (which also has the wrong sign on the momentum flux divergence term A1).

The change required to correct can be nontrivial. For example, in ARMAND, the correlation essentially gives saturation in terms of flowing steam quality, which when written correctly has to be iterated to get flowing properties given the current static properties. In GWELL this subroutine is written in a contradictory and confused way, by starting as if X is flowing not static steam mass fraction, then computing saturation from that through the correlation (but not properly iterating, just repeating twice and taking an average if necessary), and calculating a slip velocity where it should compute a drift velocity. So correction of this subroutine involves a complete rewrite.

More details on this issue with GWELL and any code that is based on GWELL, are to be found in [27].

M Version Notes

Version 2.01 has a minor fix to correct the output of flowing wellhead enthalpies to the file SWFoutcrv***.csv that contains output curve simulated results, if any.

Version 2.00 corrects the interpretation of the steam mass fraction that is returned by the subroutine CO2 (based on the one in GWELL). It is in fact a flowing steam quality that is returned, when there is two-phase flow in the wellbore, not the static steam fraction. Previous versions of SwelFlo which used the incorrect interpretation of a static steam mass fraction led

to enthalpies that were higher by up to about 5% than they should be. Now the simulator works with flowing steam quality as a fundamental variable, alongside pressure and temperature, allowing correlations to be more simply computed then previously, by starting with flowing steam quality and using the correlation to find static steam volume fraction (saturation S).

Version 1.11 corrects a coding error in Version 1.10 that led to all feeds being treated as dry steam during output curve computation, if any feed was set to dry steam type.

Version 1.10 adds a facility to invoke SwelFlo from the command line, and to provide optional argument that cause it to run silently (no windows are put up, so an input file must then be provided), that give an input file, and that give a path to a folder that will accept output.

Version 1.00 is the first released version of SwelFlo. It used some parts of routines originally from the Fortran 77 programme called GWELL, converted to Fortran 90, but is also substantially improved and corrected and augmented.

Various errors in the coding of GWELL have been corrected in SwelFlo. Feedpoint viscosity is computed as an integral average over inverse values viscosity from wellbore to reservoir pressures, as described in [26].